DESIGNING ENERGY EFFICIENT GREENHOUSES INCORPORATING RENEWABLE ENERGY SYSTEMS FOR YEAR-ROUND FOOD SECURITY IN NORTH AMERICAN WINTER CLIMATES

SHIMA JAVAHERI
Master of Science, College of Environment, 2016

A thesis submitted
in partial fulfilment of the requirements for the degree of

DOCTOR OF PHILOSOPHY

in

EARTH, SPACE, AND PHYSICAL SCIENCE

Department of Geography
University of Lethbridge
LETHBRIDGE, ALBERTA, CANADA

© Shima Javaheri, 2023

DESIGNING ENERGY EFFICIENT GREENHOUSES INCORPORATING RENEWABLE ENERGY SYSTEMS FOR YEAR-ROUND FOOD SECURITY IN NORTH AMERICAN WINTER CLIMATES

SHIMA JAVAHERI

Date of Defense: November 16, 2023

Dr. James Byrne	Professor	Ph.D.
Dr. Paul Hazendonk Thesis Co-Supervisors	Associate Professor	Ph.D.
Dr. Dan Johnson Thesis Examination Committee Member	Professor	Ph.D.
Dr. Roland Kroebel Thesis Examination Committee Member	Research Scientist	Ph.D.
Dr. Rupp Carriveau External Examiner University of Windsor	Professor	Ph.D.
Dr. Kent A. Peacock Chair, Thesis Examination Committee	Professor	Ph.D.

Dedication

This study is earnestly dedicated to my parents, as well as my husband Jon, for all their patience, support, and friendship.

Abstract

Local food production may not meet food market needs because of population growth and urbanization. Greenhouse cultivation has been used as an effective technique for providing an environment isolated from outside conditions to grow a wide variety of high-quality products with secure and sustainable harvesting in all seasons, especially in northern climates. The main problem with greenhouse cultivation is energy consumption required to maintain the indoor environment desirable for plant growth. Energy efficiency and conservation have become important issues around the world due to the cost increase, disruptions in availability, and the growing significance of environmental problems. Developing efficient greenhouses can be one of the most important actions to support food security and climate resilience. One objective of designing an energy-efficient greenhouse is to reduce CO_2 emissions caused by burning fossil fuels to operate a greenhouse or generate electricity to be used in greenhouses so, increasing the investment in renewable energy for greenhouses is an energy-saving action. Therefore, the main goal of this study was to investigate energy-efficient designs of greenhouses for year-round food security in the harsh and changing climate of Southern Alberta, Canada. Using EnergyPlus™, a well-known building energy simulation tool, the most energy efficient greenhouse has been determined through modelling, simulation, and comparison of greenhouses different in parameters such as shape, dimension, orientation and covering material. In the first part of the study, the optimum design between 6 types of conventional greenhouses was investigated considering different variables for mentioned parameters. In the second part, the thermal performance and energy consumption of Conventional Greenhouses (CGs), Chinese Style Greenhouses (CSGs) and Plant Factories (PF) were compared and the most energy-efficient one was selected. After finding the greenhouse with the minimum energy requirement in the first two

parts, the hybrid renewable energy systems have been selected for the optimized greenhouse structure using Hybrid Optimization of Multiple Electric Renewables (HOMER), to minimize the use of fossil fuels and reduce CO_2 emissions. Economic criteria were considered as a substantial part of optimizing greenhouse design and hybrid energy system components. The results of the study showed the most energy-efficient design is a Chinese Style Greenhouse when it is built using affordable and thermal resistance materials. Using PV panels in a checkerboard layout along with a wind turbine on the roof of the greenhouse combined with the grid, was the most optimal on-grid power system.

Acknowledgements

I would like to express my great appreciation to my family and my husband's family, professors, laboratory colleagues, and friends for their support throughout my PhD. I am grateful for all my father's assistance through the ups and downs of the doctorate program and my mother's enthusiastic encouragement. I would like to extend a very special thanks to the love of my life, Jon Kenwood, who went above and beyond to help me with my work. I want to express my gratitude to my supervisor Dr. James Byrne, my advisor Dr. Paul Hazendonk, and my thesis committee members Dr. Dan Johnson and Dr. Roland Kroebel for all their advice, guidance, constructive recommendations, and invaluable patience throughout my study.

I would also like to offer my grateful thanks to Dr. Rupp Carriveau, Dr. Greg Pyle, and Dr. Kent Peacock for their invaluable contribution to my PhD comprehensive examination and final thesis defense. My appreciative thanks are furthermore extended to the Department of Geography and Environment, the School of Graduate Studies, the International Student Center, the Solutions Centre, and the Library of the University of Lethbridge for all their support and assistance.

I wish to express my deep gratitude for financial and other support from the University of Lethbridge, Siksika SRDL Business Group, Old Sun Community College, the Alberta Real Estate Foundation, Lethbridge County, Canadian Agricultural Partnership (weather data development), and the MITACS National R&D Consortium.

Table of Contents

List of Tables

List of Figures

Chapter 1: Introduction

Significant population growth, urbanization, dietary change, and other consequences of economic development are increasing the demand for energy, food, and water by 30-50% in the next two decades (Esmaeili and Roshandel 2020). Field production cannot meet the growing food demand as there is no efficient way to distribute the products. As well, poor distribution can lead to a massive waste of the products. Also, this method is dependent on regional climate which can result in uncertainty in production. There is a need for a fast, reliable, and high-yield agriculture method that occupies a smaller area (Figueiroa and Torres 2022). Greenhouse technology can be an effective way to provide food even when energy and water are scarce. Food can be supplied locally, with a shorter growing period, and in larger volumes, by using greenhouses. The yield per unit of cultivated area in greenhouses is around 10 times more than field crop production methods (Vox *et al*. 2010). Also, growing in a greenhouse will result in a prolonged production period for seasonal plants, better quality, and less use of protective chemicals such as pesticides (Manonmani *et al.* 2016). In general, it is possible to have a clean, secure, and safe production of food in greenhouses by controlling all the elements of what is growing in them, controlling greenhouse climate conditions to set the desired factors for the indoor environment, and protecting the plants by making an isolated environment from the outside conditions.

Developing a controlled environment in a greenhouse and adapting its microclimate according to the needs of plants by maintaining factors such as temperature, relative humidity, CO_2 concentrations, and illumination result in a large amount of energy usage. This can result in an unsustainable production performance which means there is no natural resources preservation in producing food and farming (Vox *et al*. 2010). One of the challenging issues in the greenhouse industry and energy demand field is sustainable horticulture. After labour costs, energy

consumption can be accounted as the second-largest overhead cost in greenhouse crop production (Iddio *et al*. 2020). In cold climates, most of the energy is consumed to heat the greenhouse while in hot climates, this energy is used for ventilation purposes. Ahmed *et al*. (2019) reported that the heating costs in Canadian greenhouses are 15–20% of total production costs. In another report, it was shown that greenhouse heating costs could go as high as 30–40% of total production costs (Yang *et al.* 2012). Energy saving has become one of the most controversial and important issues around the world due to the shortage of energy reserves, increasing energy prices, and the environmental problems, such as climate change, arising from the production and consumption of energy. According to the Government of Canada, about 82% of Greenhouse Gas (GHG) emissions come from the combustion of fossil fuels in order to make energy including heating and electricity. Considering the fact that most of the energy demand of the greenhouse sector is directly or indirectly provided by fossil fuels, a significant amount of CO_2 is emitted, which contributes to the greenhouse effect (Wang *et al.* 2023).

During recent decades, one of the most significant challenges for both researchers and producers has been the reduction of energy consumption in greenhouse operation as well as finding ways to manage, save, produce, and store the energy of this sector (Rasheed *et al*. 2018). Energy-saving techniques such as energy-efficient structural design, and the use of renewable energy systems are the most common ways to manage the energy load (Ahamed *et al*. 2018). The structural design of a greenhouse optimizes the effects of different structural parameters and architecture of a greenhouse on its microclimate, resulting in energy savings due to the reduction of heating, cooling, and lighting requirements. Using an optimal hybrid renewable energy system to supply the greenhouse energy demand can lower the usage of fossil fuels and lessen the environmental impacts of greenhouse cultivation by reducing the emission of greenhouse gases to a large extent.

Parameters and variables such as climate conditions, shape, size, structure, construction materials, operating schedule, etc. are involved in designing a greenhouse. As these parameters have a strong, non-linear, and complex interactions with each other, optimizing greenhouse design is beyond human calculation capabilities (Dahlan *et al*. 2018). Building energy simulation tools such as EnergyPlus™, which is based on the energy balance method, can be used to predict the thermal performance as well as energy consumption of greenhouses (Pakari and Ghani 2022). There are a number of technology options and the variation in technology costs and availability of energy resources that should be considered in designing energy systems. Through using simulation-optimization tools such as HOMER, it is possible to evaluate the many possible system configurations and find the optimal one (Nayanatara *et al*. 2019).

The main goal of this study is to find the most energy-efficient design for a year-round greenhouse located in the harsh and changing climate of Southern Alberta by optimizing the structural parameters of the greenhouse using EnergyPlus™ and finding an optimum hybrid renewable energy system to supply its energy demand using HOMER.

1.1. Thesis objectives

This project has three main objectives to better investigate the feasibility of developing a year-round energy-efficient greenhouse in the continental climate[1] of Southern Alberta, in particular at the Old Sun Community College in Siksika First Nation of the Blackfoot Confederacy (east of Calgary, AB, Canada). The simulation time is during the year 2020. The objectives of the study are as follows:

[1] Continental climates often have a significant annual variation in temperature (warm summers and cold winters).

- Optimizing the physical characteristics of conventional greenhouses by minimizing the interior average temperature deviation from the optimum temperature range suitable for growing plants using EnergyPlus™,
- Comparing the thermal performance and energy requirement of the most energy-efficient conventional greenhouse design in the first step of the study with Chinese Style Greenhouses, and Plant Factories using EnergyPlus™ which considers energy and initial investment cost analysis as well as the profit from sale of the products,
- Determining the optimum hybrid renewable energy system (wind turbine and solar panels) which generate electricity in combination with greenhouse cultivation within the same building through using HOMER and by considering economic, technical, and environmental criteria as well as performing a sensitivity analysis on grid power price and sellback rate for the most optimum hybrid renewable energy system.

1.2. Thesis structure

This is a journal article format thesis. The first chapter is the introduction of the thesis. The objectives stated above are presented in the three following chapters. In the second chapter, a parametric study was conducted to find the most optimum structural parameters of conventional greenhouses. A total of 1408 scenarios were developed to better investigate the effect of shape, height, orientation, and covering materials on the thermal performance of the greenhouse. EnergyPlus™ was used to predict the average temperature. In the third chapter, the energy demand and thermal performance of three different greenhouse facilities (Conventional Greenhouses, Chinese Style Greenhouses, and Plant Factories) were assessed using EnergyPlus™. Scenarios were defined to investigate the effect of increasing volume (increasing height) and two different opaque wall construction materials on the energy efficiency of each

facility. An economic analysis of the energy cost and upfront costs of greenhouse construction was conducted to better compare the facilities with each other. In the fourth chapter, different combinations of the energy system components including the grid, generator, PV panels, wind turbine, and battery were compared to determine the optimum hybrid renewable energy system. In developing the systems, it was assumed that greenhouse crop production is integrated with solar and wind electricity generation within the same building. Economic, technical, and environmental criteria are used to find the optimum system. The fifth chapter is the summary and conclusion of the thesis and outlines the main findings of the research.

References

Ahamed, M. S., Guo, H., & Tanino, K. (2018). Energy-efficient design of greenhouse for Canadian Prairies using a heating simulation model. *International Journal of Energy Research, 42*(6), 2263-2272. doi:10.1002/er.4019

Ahamed, M. S., Guo, H., & Tanino, K. (2019). Energy saving techniques for reducing the heating cost of conventional greenhouses. *Biosystems Engineering, 178*, 9-33. doi:10.1016/j.biosystemseng.2018.10.017

Alinejad, T., Yaghoubi, M., & Vadiee, A. (2020). Thermo-environomic assessment of an integrated greenhouse with an adjustable solar photovoltaic blind system. *Renewable Energy, 156*, 1-13. doi:https://doi.org/10.1016/j.renene.2020.04.070

Dahlan, N. Y., Z. Sakimin, S., Faizwan, M., Ajmain, N., & A. Aris, A. (2018). Automated calibration of greenhouse energy model using hybrid evolutionary programming (EP)-EnergyPlus. *Indonesian Journal of Electrical Engineering and Computer Science, 12*(2). doi:10.11591/ijeecs.v12.i2.pp648-654

Esmaeli, H., & Roshandel, R. (2020). Optimal design for solar greenhouses based on climate conditions. *Renewable Energy, 145*, 1255-1265.

Figueiroa, V., & Torres, J. P. N. (2022). Simulation of a small smart greenhouse. *Designs, 6*(6). doi:10.3390/designs6060106

Hoarcă, I. C., Bizon, N., Șorlei, I. S., & Thounthong, P. (2023). Sizing design for a hybrid renewable power system using HOMER and iHOGA simulators. *Energies, 16*(4). doi:10.3390/en16041926

Iddio, E., Wang, L., Thomas, Y., McMorrow, G., & Denzer, A. (2020). Energy efficient operation and modeling for greenhouses: A literature review. *Renewable and Sustainable Energy Reviews, 117*. doi:10.1016/j.rser.2019.109480

Manonmani, A., Thyagarajan, T., Elango, M., & Sutha, S. (2016). Modelling and control of greenhouse system using neural networks. *Transactions of the Institute of Measurement and C0000ontrol, 40*(3), 918-929. doi:10.1177/0142331216670235

Nayanatara, C., Baskaran, J., Dharani, S., Sri, V. K., & Kanmani, E. (2019, 27-28 March 2019). *Optimization of hybrid energy resources using Homer software.* Paper presented at the 2019 International Conference on Computation of Power, Energy, Information and Communication (ICCPEIC).

Pakari, A., & Ghani, S. (2022). Regression equation for estimating the maximum cooling load of a greenhouse. *Solar Energy, 237*, 231-238. doi:10.1016/j.solener.2022.04.006

Rasheed, A., Lee, J., & Lee, H. (2018). Development and optimization of a building energy simulat0000ion model to study the effect of greenhouse design parameters. *Energies, 11*(8). doi:10.3390/en11082001

Vox, G., Teitel, M., Pardossi, A., Minuto, A., Tinivella, F., & Schettini, E. (2010). Sustainable greenhouse systems. *Sustainable Agriculture: Technology, Planning and Management*; Nova Science Publishers, Inc.: New York, NY, USA.

Wang, L., Li, X., Xu, M., Guo, Z., & Wang, B. (2023). Study on optimization model control method of light and temperature coordination of greenhouse crops with benefit priority. *Computers and Electronics in Agriculture, 210*, 107892. doi:https://doi.org/10.1016/j.compag.2023.107892

Yang, S. H., Lee, C. G., Lee, W. K., Ashtiani, A. A., Kim, J. Y., Lee, S. D., & Rhee, J. Y. (2012). Heating and cooling system for utilization of surplus air thermal energy in greenhouse and its control logic. *Journal of Biosystems Engineering*, *37*, 19–27

Chapter 2: Effect of Changing Structural Parameters of a Greenhouse on its Energy Consumption: A Case Study in a Cold Climate of Southern Alberta, Canada

2.1. Introduction and background

In the near future, conventional local food production may not meet food market needs because of population growth and climate change. Greenhouse cultivation has been used as an appropriate technique to allow an environment isolated from outside conditions to grow a variety of high-quality products. In this way, secure and sustainable harvesting is achievable in all seasons. This is especially true outside low latitude locations where, because of the harsh climate, year-round production is challenging. Through the use of greenhouses, local production is feasible in all regions, leading to low transport energy overhead as well as economic benefits for the region. The main problem with greenhouse cultivation is energy consumption. These structures use energy to heat during the cold season, cool during the warm season, and use electricity for light, ventilation, and irrigation. Energy saving has become one of the most pressing issues around the world due to the shortage of energy reserves, increasing conventional energy prices, and the growing significance of environmental problems including climate change. Climate change can be the result of Greenhouse Gas (GHG) emissions resulting from the use of fossil fuels. According to the Government of Canada (2020), about 82% of GHG emissions in Canada come from the production and consumption of energy. In this regard, improving the agriculture sector's energy efficiency will help reduce emissions and support climate resilience. There are three steps toward greenhouse energy efficiency: the reduction of the energy demand, the system efficiency optimization, and the exploitation of renewable energy sources (Fabrizio 2012).

Designing energy-efficient greenhouses by optimizing structural design parameters to minimize annual energy requirements using energy simulation models are of paramount

importance to researchers, manufacturers, and greenhouse growers. For example, Choab *et al*. (2019) carried out an extensive literature review on greenhouse systems and analyzed key design parameters characterizing greenhouse systems' overall performance and its indoor microclimate. The parameters discussed were covering material, greenhouse shape, greenhouse orientation and natural ventilation. They also reviewed the thermal models and the computational fluid dynamics existing in the literature related to designing greenhouses. In general, factors affecting the energy efficiency of greenhouses are as follows:

- the outside climate (e.g., solar radiation, wind, humidity),
- dimension of the greenhouse,
- shape,
- orientation,
- the angle of the roof,
- the number and width of spans,
- covering materials (e.g., single, double glazing, plastic sheets, and films, or combinations of these materials (Choab *et al*. 2019)),
- the plants growing in the greenhouse,
- the desired temperature inside the greenhouse.

Among these factors, the shape and orientation of greenhouses represent the critical criteria for solar energy collection as they strongly influence the incidence angle between solar radiation and the sunlit surface. This angle determines the transmission and reflection of solar radiation through the glazed surface (Deian *et al*. 2014). Consequently, the shape and orientation influence greenhouses' indoor environment, heating energy requirements, and in general, determines energy efficiency. Hence, it is important to find the optimal orientation and form

wherever practical. Cover material is also an essential factor that determines the energy efficiency of greenhouses, as it affects internal environmental conditions such as temperature, relative humidity, and vapor pressure deficit. The selection of the appropriate materials must be compatible with the structural and functional aspects of the greenhouse (Choab *et al*. 2019). By having a well-designed greenhouse, a large amount of energy can be collected and stored while the indoor climate can be kept acceptable and thermal losses minimized. Ahamed *et al.* (2018c) studied the effect of design parameters including shape (even-span gable roof, uneven-span gable roof, modified arch, vinery, and Quonset), orientation, the angle of the roof, and width of the span separately on the energy demand of conventional-style greenhouses for the Canadian Prairies using GREENHEAT as a greenhouse heating simulation model. The result of their study showed the East-West oriented multi-span gable roof greenhouse would be energy efficient for a large commercial greenhouse at high northern latitudes, whereas an E-W oriented (wider span) Quonset shape would be energy-efficient for the single-span greenhouse. Esmaeli and Roshandel (2020) used a validated thermal model linked with an optimization algorithm to achieve an optimal greenhouse design for year-round or seasonal production in varied climates by minimizing the greenhouse temperature deviation from a suitable temperature range. Design structural parameters were roof angles, width, and height of a semi-passive solar greenhouse. The result of their study indicated that for each climate condition, the optimal greenhouse will have different sizing. Chen *et al.* (2018) sought to maximize solar energy collection utilizing the law of the solar trajectory and the theory of heat balance. An optional model was developed to determine the best opening and closing time of the thermal insulation curtain for the south-pitched roof of a solar greenhouse in nine different latitudes. Furthermore, they determined the optimal orientation for solar greenhouses according to heat transfer and Extreme Value Theory including the impact from geographical latitude. They showed that with increased latitude, the

opening time of the thermal insulation curtain should be delayed and that the closing time of the thermal insulation does not change. Also, with higher latitude, larger displacement is needed from the true south to the west to find the optimal orientation. Chen *et al.* (2020) developed a greenhouse solar radiation mathematical model, coded in the MATLAB platform, to optimize the orientation and shape of a greenhouse design at different latitudes in China to maximize the global solar radiation collected to save energy for heating the greenhouse in winter. They concluded that the sawtooth greenhouse with the East-West orientation was optimal for capturing the maximum global solar radiation in winter and the minimum global solar radiation in summer. Çakır and Sahin (2015) developed a model in the MATLAB platform to optimize design parameters such as: orientation, roof shape, floor area, and the ratio of the greenhouse's length to width (K number) to obtain maximum energy input from the sun. They found that the dominant parameter on solar energy gaining rates is roof shape, for which in this particular region the elliptic was the best option. Also, this model is able to optimize the K number and orientation for any greenhouse type. Ma *et al.* (2019) used EnergyPlus™ to evaluate the thermal performance and energy consumption of a double-slope greenhouse. The objective of their study was to design a new roof for the shade room of the greenhouse by selecting the best inner surface, insulation, and outer surface materials and calculating the minimum required insulation thickness for the designed roof. It concluded that the new roof construction increased the indoor temperature and a reduction in the energy consumption in the double-slope greenhouse. Ahamed *et al*. (2020) used TRNSYS, a commercial building energy simulation package, to model a conceptual Chinese Style Greenhouse (CSG) in a region with a similar climate to northern Canada. The TRNSYS model was compared with the CSGHEAT model to find its deficiencies in the microclimate modelling of greenhouses. They observed that the CSGs had the potential for year-round production by minimizing the high heating costs for northern greenhouse production. Rasheed *et*

al. (2018) studied the influence of different greenhouse design parameters separately on the thermal environment of a greenhouse using the Transient System Simulation Tool (TRNSYS). The work design parameters considered include: greenhouse shape, orientation, glazing, natural ventilation, covering materials, and the thickness of the covering material of a single-span greenhouse. They concluded that a naturally ventilated greenhouse with a gothic-shaped roof, an East-West orientation, and with double-glazed PMMA covering was sufficient to meet the minimum heat energy requirement.

Greenhouse designing is a complicated task. As demonstrated above, different factors should be considered in the design procedure. The important thing about these factors is that they have non-linear and complex relations with each other. In this regard, changing one of these factors can change the way the other factor is influencing the greenhouse microclimate so their effect on greenhouse energy efficiency must be taken into account together (Belkadi *et al*. 2019). The importance of this fact has been underrated in previous studies that sought the most energy-efficient greenhouse design by optimizing the greenhouse design parameter. Furthermore, studies on designing efficient greenhouses located in the Northern American climate are still rare. Few assessments of greenhouse energy efficiency have been undertaken for challenging climates such as in southern Alberta, which is dry, sunny, and windy with hot summers and harsh cold winters.

This study endeavours to find suitable conditions for a highly energy-efficient greenhouse installation to be used for educational purposes and to provide year-round food security in the harsh climate of Southern Alberta. Through working with Old Sun Community College in Siksika First Nation of the Blackfoot Confederacy (east of Calgary, Alberta, Canada), greenhouse structures for year-round food production have been developed. Thus, the optimum structural parameters will be sought via a comparative analysis to achieve high energy efficiency while maintaining the greenhouse's suitability for educational purposes. In other words, this work will

investigate the influence of different structural parameters on the internal temperature of a greenhouse using EnergyPlus™, a dynamic simulation model, which amounts to a ‘‘parametric study” into building thermal performance.

2.1.1. Objective

The objective of the study is to model an energy-efficient greenhouse that has minimum interior average temperature deviation from the optimum temperature range throughout the year, 2020. This has been done by optimizing the physical characteristics of the greenhouse.

2.2. Methodology

2.2.1. Site description

Figure 2-1 shows the location of Old Sun Community College (OSCC) (starred location) in Siksika Indian Reserve, Calgary Region, Alberta, Canada.

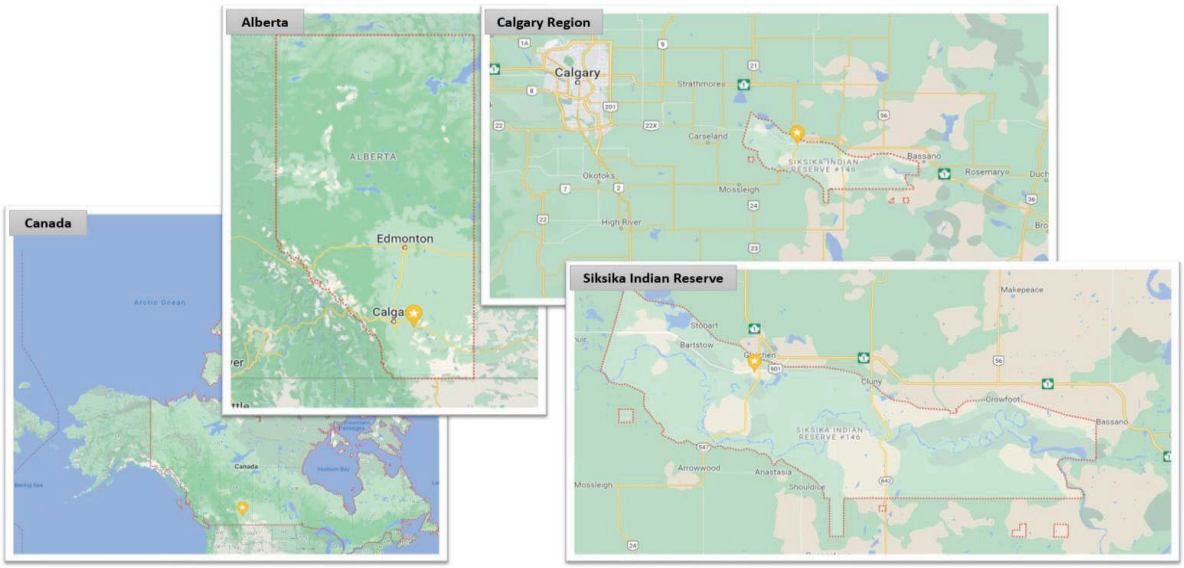

Figure 2- 1: Case study location in Siksika Indian Reserve, Calgary Region, Alberta, Canada

Land located in the South of OSCC has been considered as the location of an educational greenhouse. The land is 55 meters long and 15 meters wide. The location of this land can be seen in Figure 2-2. A climate graph, as well as a graph of sunshine values and sunset hours for the

location of study in 2020 are shown in Figures 2-3 and 2-4.

Figure 2- 2: Old Sun Community College land

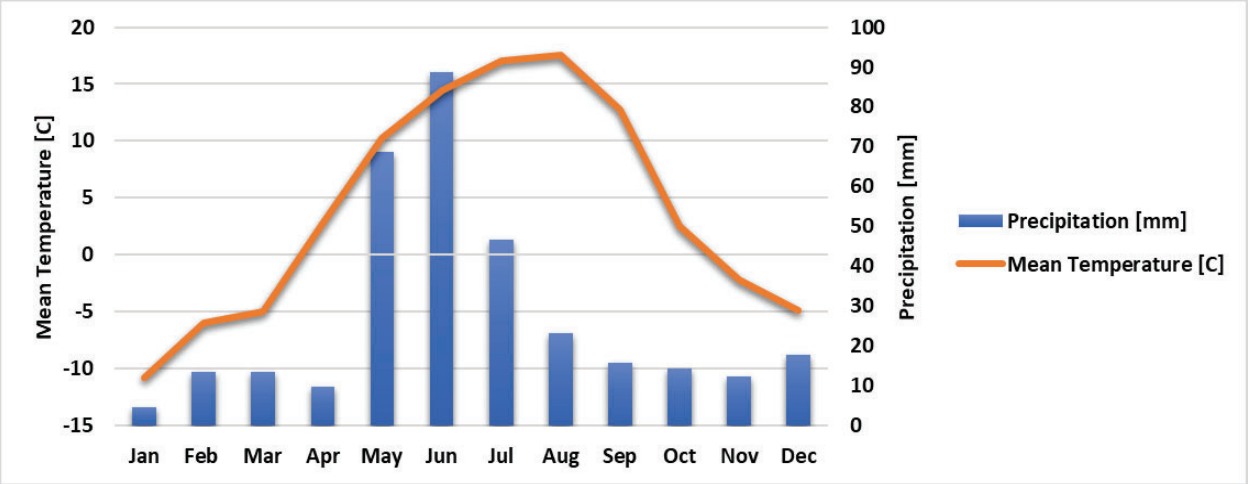

Figure 2- 3: Climate graph for Old Sun Community College in 2020

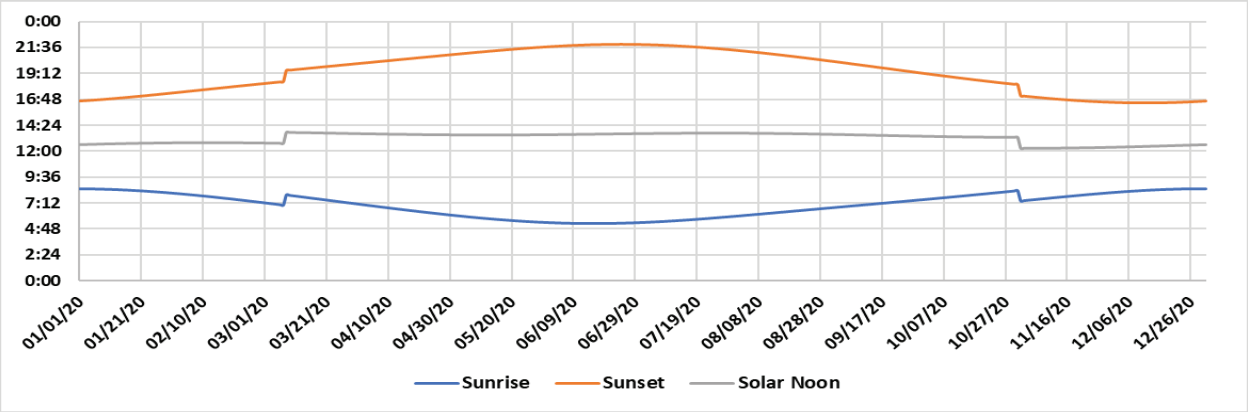

Figure 2- 4: Daily variation values of sunshine and sunset hours in 2020

2.2.2. Energy simulation tools

Building Performance Simulation (BPS)/Energy Simulation/Building Information

Molding (BIM) tools are a key instrument in the evaluation of the building energy demand and thermal comfort (Mazzeo *et al.* 2019). Energy modelling software applications help in designing efficient energy systems in green buildings, in terms of efficient usage of energy resources, lowering energy costs, increasing the usage of natural energy resources (e.g., solar energy), and reducing the negative impacts of fossil fuel use on the surrounding environment (Al Ka'bi 2020; Azhar *et al*. 2009; Liao and Teo 2018).

EnergyPlus™ , a simulation tool that has shown an acceptable level of accuracy in estimating the greenhouse thermal performance and energy requirement in previous studies (Figueiroa and Torres 2022; Ma *et al*. 2022; Arenghi *et al*. 2021; Lebre *et al.* 2021; Alinejad *et al.* 2020; Ma *et al*. 2019; Chen *et al.* 2018; Deiana *et al*. 2014), was used in this study.

2.2.2.1. EnergyPlus™ - Energy simulation tool

EnergyPlus™, developed by the U.S. Department of Energy, is a whole-building energy analysis and thermal load simulation program that has shown a continuous enhancement in the possibility of adding and validating new models (Mazzeo *et al.* 2019).

EnergyPlus™ contains different modules that can simulate a building exposed to different environmental and operating conditions to calculate the building's indoor microclimate and the energy required for heating and cooling it (NREL 2015). The simulation is based on the fundamental heat balance principles. Equation 2-1 demonstrates the general heat balance used in EnergyPlus™.

$$m_z C_z \frac{dT_z}{dt} = \sum_{i=1}^{N_{sl}} \dot{Q}_\iota + \sum_{i=1}^{N_{Surfaces}} h_i\, A_i (T_{si} - T_z) + \sum_{i=1}^{N_{Zones}} \dot{m}_i\, C_p (T_{zi} - T_z) + \dot{m}_{inf} C_p (T_\infty - T_z) + \dot{Q}_{sys} \tag{2-1}$$

Where, $\sum_{i=1}^{N_{sl}} \dot{Q}_\iota$ is the sum of the convective internal loads, $\sum_{i=1}^{N_{Surfaces}} h_i\, A_i (T_{si} - T_z)$ is

convective heat transfer from the zone surfaces, $\sum_{i=1}^{N_{Zones}} \dot{m}_i\, C_p(T_{zi} - T_z)$ is the heat transfer due to interzone air mixing, $\dot{m}_{inf} C_p(T_\infty - T_z)$ is the heat transfer due to infiltration of outside air, $\dot{Q}_{sys}$ is air systems output, and $C_z \frac{dT_z}{dt}$ is energy stored in zone air. This is the main equation used by EnergyPlus™ to estimate zone air temperatures.

The heat balance equation for this study has been defined as follows (Ahamed *et al*. 2018a,b; Esmaeili and Roshandel 2020; Shen *et al*. 2018; Alinejad *et al*. 2020; Van Beveren *et al*. 2015):

$$m_{air} C_{p,air} \frac{dT_{in}}{dt} = Q_{sun} + Q_{people} - Q_{long} - Q_{loss} - Q_{vent} - Q_{crop} \pm Q_{store} \pm Q_{soil} \pm Q_{inf} \quad (2\text{-}2)$$

In Equation 2-2 Q_{sun}, Q_{people}, Q_{long}, Q_{loss}, Q_{vent}, Q_{crop}, Q_{store}, Q_{soil}, and Q_{inf} are heat gains due to absorbed solar radiation through greenhouse cover (Shortwave), heat gain due to existence of people working in or visiting the greenhouse, heat loss due to transferring thermal radiation (Longwave), heat loss due to conduction and convection, heat loss due to natural ventilation, heat loss due to crop evapotranspiration, heat exchange via convection between the heat storage wall and inside air, heat exchange via conduction between indoor air and soil, and heat exchange between outdoor and indoor air due to infiltration, respectively.

The amount of crop evapotranspiration is related to the net radiation at the crop surface and the crop's adjacent air temperature. The effect of crop evapotranspiration has not been included as a variable in this study. Also, no storage wall has been defined in the greenhouses models, and the value related to heat exchange between the greenhouse environment and the storage wall is zero as well.

A general structure of data flow in this program as used in this study is as follows:

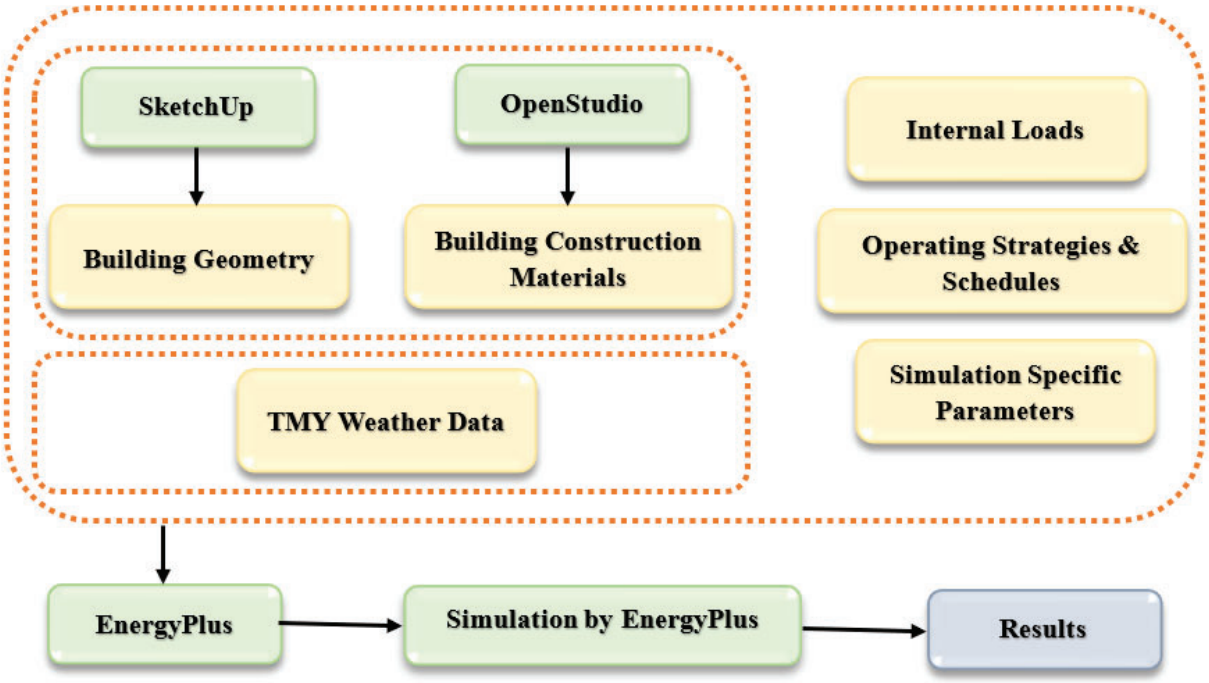

Figure 2- 5: A general structure of EnergyPlus™ data entry used in the study

2.2.3. Parametric study

The parametric study was used to understand the effect of changing each structural parameter input on the design objective function, while all other building parameters are kept fixed. This technique can be repeated iteratively with other variables. As exploring alternative design options is too time-consuming and practically impossible due to a large number of combinations, an appropriate parametric tool, named JEPlus, has been coupled with EnergyPlus™ to define different scenarios in less time. Python code has also been developed to call and run all defined EnergyPlus™ files.

2.2.4. Simulation outline

The summation of the hourly temperature differences above the maximum temperature of the optimum range and below the minimum temperature of the optimum range, which represents the overheating degree hours and overcooling degree hours, were chosen as the thermal

performance index of the greenhouse and defined in Equation 2-3 as the objective function (Deiana *et al*. 2014; Esmaeli and Roshandel 2020).

$$\begin{cases} f_{Maximum} = \sum_{T}^{TotalSimulationControlHours} (Zone\ Air\ Temperature - Optimum\ Temperature_{Maximum}), & Zone\ Air\ Temperature > Optimum\ Temperature_{Maximum} \\ f_{Minimum} = \sum_{T}^{TotalSimulationControlHours} (Optimum\ Temperature_{Minimum} - Zone\ Air\ Temperature), & Zone\ Air\ Temperature < Optimum\ Temperature_{Minimum} \\ f_{BetweenMaximum\&Minimum} = 0 & Optimum\ Temperature_{Minimum} < Zone\ Air\ Temperature < Optimum\ Temperature_{Maximum} \end{cases} \quad (2\text{-}3)$$

$$f = \sum (f_{Maximum} + f_{Minimum}) \quad (2\text{-}4)$$

By using Equation 2-4, the sum of temperature deviations inside the greenhouse from the optimum temperature range defined for the growing plants throughout the simulation time has been found for each of the models. EnergyPlus™ has been used to estimate zone air temperature for each of the scenarios defined.

2.2.5. Development of the greenhouse models (scenarios)

2.2.5.1. Structural design parameters description

In this study, 6 different shapes of Gothic, Even-Span, Uneven-Span, Modified Arch, Vinery, and Quonset and 4 orientations[1] of 0 (East-West), 30, 60, and 90 (North-South) degrees have been investigated regarding their effect on energy demand. Two different ridge heights of 5.5 and 7.5 meters have been considered. The gutter height for the greenhouses with a span of 7.5 meters is 2 meters and for the span of 10 meters is 3 meters. Several common cover materials including Ethylene tetrafluoroethylene (ETFE), Horticulture Glass (HG), Polycarbonate (PC),

[1] It should be noted that the orientation of the greenhouses is in the same direction as the greenhouse longer dimension except for 2500 m^2 and 4500 m^2 which the orientation is in greenhouse's gutter direction. Because of the dimension of the OSCC land, orientation 0 is the only greenhouse that can be considered.

Polyethylene (PE), Polymethylmethacrylate (PMMA), Polyolefin (PO) film, Polyvinyl chloride (PVC) and Woven film have been used in this study to conduct the simulation. Table 2-1 shows the characteristics and properties of these greenhouse covers.

Table 2- 1: The characteristics and properties of different greenhouse covers (Part *et al.* 2021; Rasheed *et al.* 2020)

Cover Characteristics	Greenhouse Covers							
	PE[a]	PVC[b]	HG[c]	PMMA[d]	PC[e]	PO[f] film	ETFE[g]	Woven film
Solar transmittance	0.86	0.91	0.89	0.82	0.78	-	-	-
Solar reflectance	0.1	0.07	0.08	0.12	0.14	-	-	-
Visible radiation transmittance	0.89	0.92	0.91	0.92	0.75	0.89	0.923	0.747
Visible radiation reflectance	0.08	0.08	0.08	0.07	0.15	-	-	-
Thermal radiation transmittance	0.18	0.06	0	0	0.02	-	-	-
Thermal radiation emission	0.79	0.62	0.9	0.98	0.89	-	-	-
Conductivity ($W\ m^{-1}\ K^{-1}$)	0.33	0.13	0.76	0.19	0.19	-	-	-
Thickness (mm)	0.1	0.1	4	10	10	0.146	0.097	0.212
Solar Heat Gain Coefficient						0.9	0.93	0.54
Coefficient of Heat Transmission ($W/m^2 \cdot K$)						6.03	6.03	5.91

[a]Polyethylene
[b]Polyvinyl Chloride
[c]Horticulture Glass
[d]Polymethylmethacrylate
[e]Polyolefin
[f]Ethylene Tetrafluoroethylene

The result of a survey about the size of greenhouse operations in Alberta in 2019 (Laate and Dr. Mirza Consultants 2020) shows the most common greenhouse area in Alberta is between 930 m^2 to 3700 m^2. This survey can be evidence of the optimum area for greenhouse cultivation in Alberta. In this study, because of the limited dimension of OSCC land, the maximum area of the greenhouse that can be built on this land is 825 m^2. Scenarios have been defined in a way that they lead to the maximum area. Scenarios with an area of 2500 m^2 and 4500 m^2 have also been defined for the four shapes of Gothic, Even-Span, Uneven-Span, and Modified Arch. This has been done to show the influence of area on thermal performance.

Values and options of the mentioned parameters above are demonstrated in Table 2-2. In general, 1408 scenarios have been investigated in this study. Table 2-3 shows how the number of scenarios has been calculated.

Table 2- 2: Different scenarios definitions

Number of Shape	**1**	**2**	**3**	**4**	**5**	**6**	**7**	**8**	**9**	**10**	**11**	**12**	**13**	**14**	**15**	**16**	**17**	**18**	**19**	**20**	**21**	**22**
Greenhouse Type	**Gothic**					**Even-Span**					**Uneven-Span**					**Modified Arch**					**Vinery**	**Quonset**
Span	2	5	7	5	12	2	5	7	5	12	2	5	7	5	12	2	5	7	5	12	1	1
Width of span	7.5	10	7.5	10	7.5	7.5	10	7.5	10	7.5	7.5	10	7.5	10	7.5	7.5	10	7.5	10	7.5	10	10
Length	50	15	15	50	50	50	15	15	50	50	50	15	15	50	50	50	15	15	50	50	50	50
Floor area (m^2)	750	750	787.5	2500	4500	750	750	787.5	2500	4500	750	750	787.5	2500	4500	750	750	787.5	2500	4500	500	500
Ridge height (m)	• Gutter height +2.2 (for greenhouses with span = 7.5m), • Gutter height + 3 (for greenhouses with span = 10m)																					
Gutter Height (m)	1) 5.5, 2)7.5																					
Orientation	1) 0, 2) 30, 3) 60, 4) 90																					
Flooring Material	• Soil																					
Covers	1) ETFE (Ethylene tetrafluoroethylene), 2) HG (horticulture glass), 3) PC (polycarbonate), 4) PE (polyethylene), 5) PMMA (polymethylmethacrylate), 6) PO (polyolefin) film, 7) PVC (polyvinyl chloride), 8) Woven film																					

Table 2- 3: Number of scenarios

Shapes	22
Gutter Height	2
Orientation (0, 30, 60, 90)	4
Covers	8
Total Scenarios = 22 × 2 × 4 × 8 = 1408	

2.2.5.2. Model development in EnergyPlus™

Geometries of greenhouses were produced using SketchUp, a software that provides a user interface for the EnergyPlus™ dynamic simulation engine. The construction material was defined using Openstudio and allocated to each surface. Necessary input data influencing the simulation work of the study was then added to the exported files through EnergyPlus™'s different objects to the exported files from SketchUp[1]. The weather data used for the simulation is the typical meteorological year (TMY). Typical meteorological year files are representative of long-term weather data compiled from 20-30 years of data. The TMY file used in this study has been compiled from 2007 to 2021 for the location of the study. The calculation time specified for the simulation was between the 1st of January 2020 and the 31st of December 2020. Therefore, this annual duration includes typical wintertime in southern Alberta for off-season vegetable production, as well as summertime. Also, the optimum temperature range has been considered between 7°C and 28°C. The effect of student's attendance in the greenhouse environment has been considered. There are classroom visits during weekdays between 8 and 12:15 as well as 13:30 and 17:00, all year round except on holidays. There are 50 students in each classroom. Also, three employees work every day in the greenhouse. Schedule object in EnergyPlus™ has been used to define the influence of students' and employees' attendance. Air infiltration rates have a key role in determining greenhouse heating requirements. The infiltration rate has been considered as 0.9375 air changes per hour (ACH) in this study (Shelford and Both 2020).

A complete thermal model and an annual dynamic simulation were created and performed for all the defined scenarios for all mentioned parameters, to study the potential thermal

[1] Because of the modular structure of EnergyPlus™, each module is responsible for "getting" its own input [20]. Input can be defined under different objects in EnergyPlus™.

performance of the greenhouses during both cold and warm periods of the year for the considered location.

2.3. Results and discussion

EnergyPlus™ was run for all defined scenarios. As mentioned previously, the obtained results for the greenhouses are compared according to the hourly zone air temperature of greenhouses in one year, 2020. The related assessments were made according to the sum of the temperature deviations inside the greenhouse from the optimum temperature value. From the code definition in EnergyPlus™, the zone air temperature is the average temperature of the air temperatures at the system timestep. The zone heat balance represents a "well-stirred" model for a zone, therefore there is only one mean air temperature to represent the air temperature for the zone (NREL 2015).

2.3.1. Outdoor Climate

The daily variation of outdoor air temperature (Dry Bulb Temperature) and daily global radiation of TMY weather data used in this study are shown in Figures 2-6 and 2-7. These figures have been made with Data Viewer (DView) which is an application that can read TMY weather data files and is capable of visualizing time-series data at any timestep.

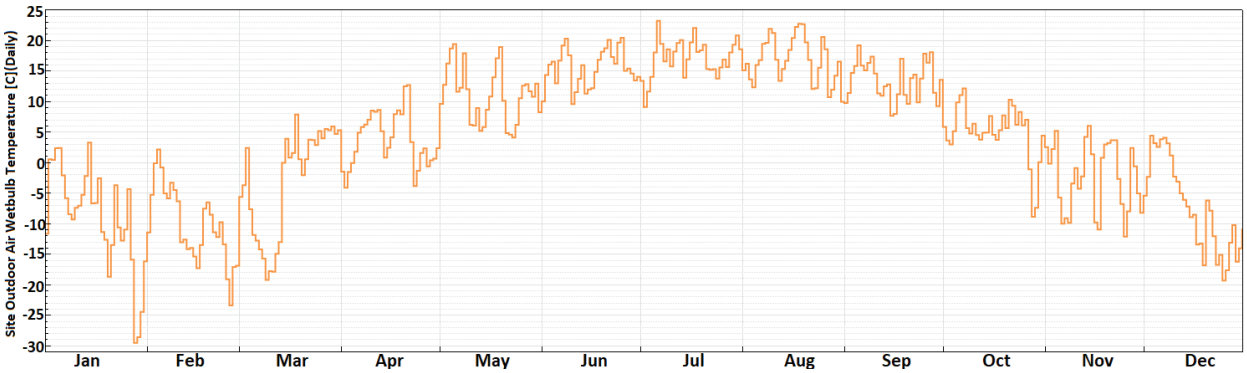

Figure 2- 6: Daily variation values of dry bulb Temperature

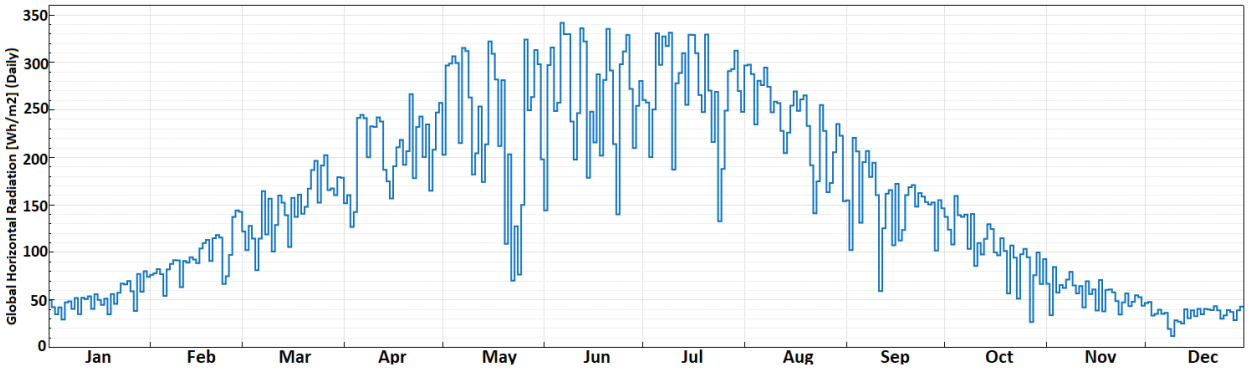

Figure 2- 7: Daily variation values of global radiation

During the whole year, the minimum and maximum monthly air dry bulb temperatures are around -30°C and 24°C observed in January and July, respectively.

2.3.2. Simulation results (most energy-efficient scenarios)

Figure 2-8 shows the top 10 of the most energy-efficient greenhouses among the defined scenarios of this study.

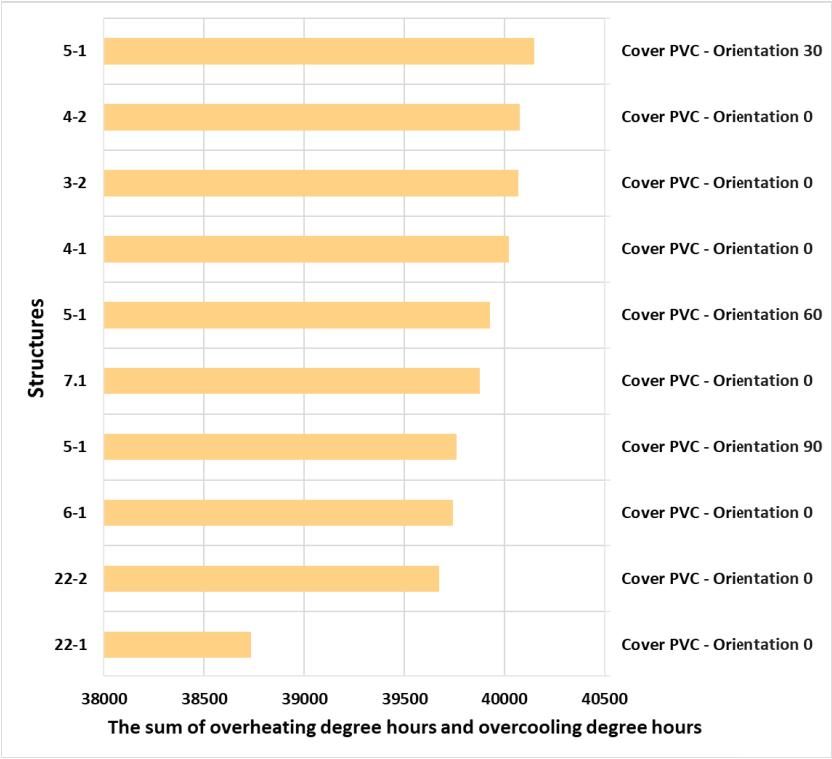

Figure 2- 8: Top 10 greenhouses among all scenarios[1]

[1] Structures include two numbers. According to Table 2-1, the first number is the number of shapes, and the second number is the number of gutter heights.

A total of 224 out of 1408 scenarios can be built on the OSCC land. The orientation of all these 224 greenhouses has been defined as 0 degrees. Figure 2-9 shows the top 10 energy-efficient greenhouses among these 224 scenarios. The best structure is Quonset with an area of 500 square meters, a total height of 8.5 meters, an orientation of west-east or 0 degrees, and the cover material of PVC. The total overheating degree hours and overcooling degree hours for this structure is 38732.7. This amount is 939.4, 1009.9, 1143.2, 1336.1, 1488.3, 1571.7, 1785.9, 2087.5, and 2518.7 less than the second to the tenth most efficient greenhouse design on OSCC land, respectively.

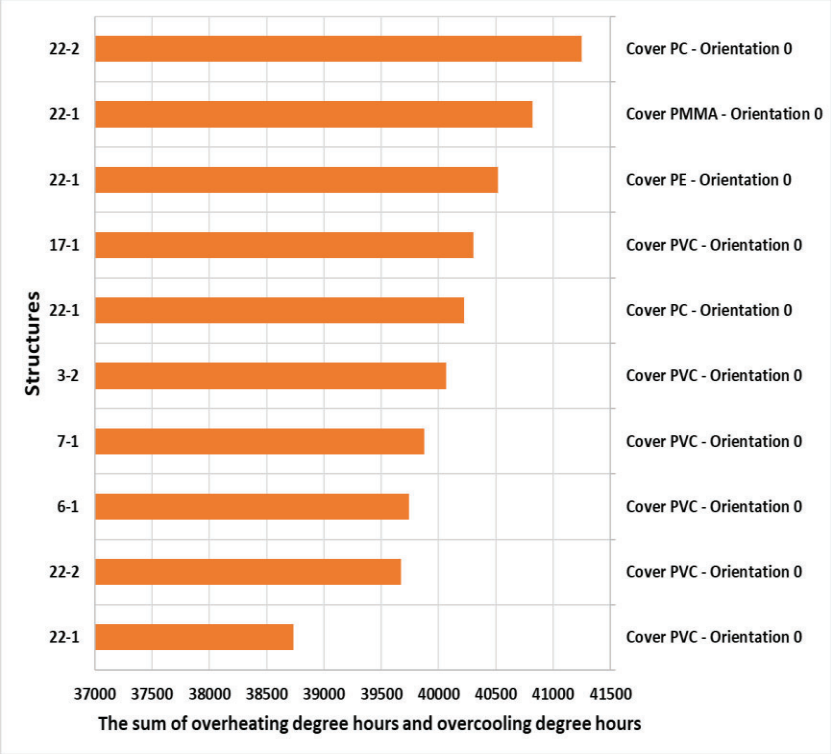

Figure 2- 9: Top 10 greenhouses among OSCC scenarios[1]

According to the results of the simulation for 224 scenarios, the Quonset shape with a total height of 8.5 meters is the first-most energy-efficient greenhouse on OSCC land among all 44 different structures and all cover materials, except woven film. However, Quonset is a single-

[1] Structures include two numbers. According to Table 2-1, the first number is the number of shapes, and the second number is the number of gutter heights.

span greenhouse with a minimum area between all the scenarios. As can be seen in Figure 2-8 and Figure 2-9, the best structures among multi-spans are Even-Span, Gothic, and Modified Arch, respectively. This finding aligns with the results of previous studies (Ahamed *et al*. 2018c; Mobtaker *et al*. 2019).

Figures 2-10(a) to 2-10(e) show the geometry of five most energy- efficient greenhouse structures on OSCC land. On the other hand, PVC cover material works the best in all different structures. The second-best cover material is PC in all structures.

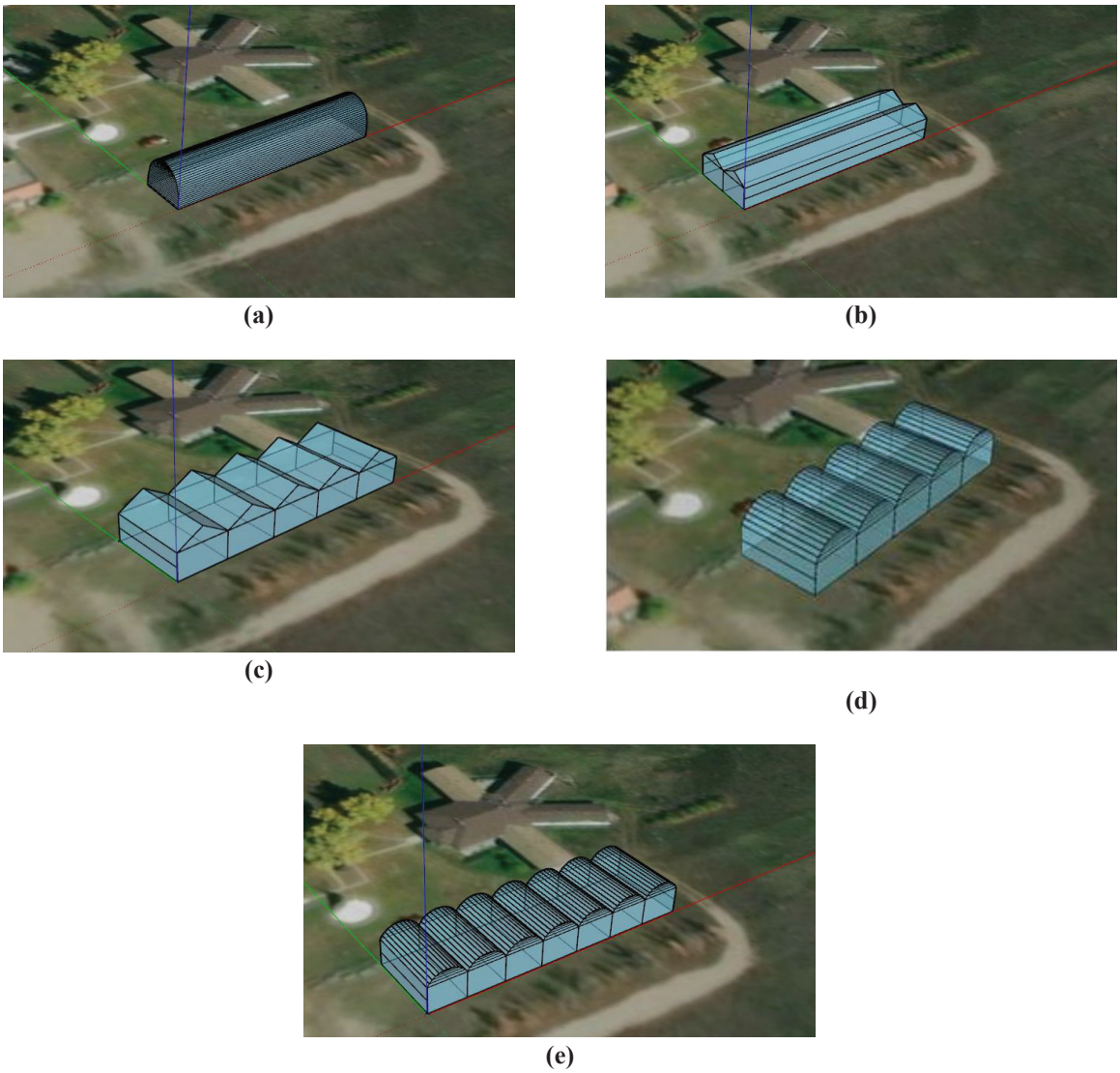

Figure 2- 10: Geometry of the (a): 1st, (b): 3rd, (c): 4th, (d): 5th, and (e): 7th most energy-efficient greenhouses on OSCC land

Figure 2-11 shows the variation of daily zone air temperature and how it changes during one year for the most energy-efficient status of the 5 structures mentioned above. An optimum temperature range of 7 to 28 can be seen in this graph as well. As can be seen, all five structures have a higher temperature compared to the outside temperature. The indoor temperature appears to fall below the minimum optimum growing temperature from late October to the middle of March. During the rest of the year, the indoor temperature is almost in the desired range except for some short periods, mostly during May and July. Overheating degree hours are low in comparison to overcooling degree hours during the cold seasons. This means that there is a higher demand for heating systems for the greenhouses in OSCC locations than for cooling systems.

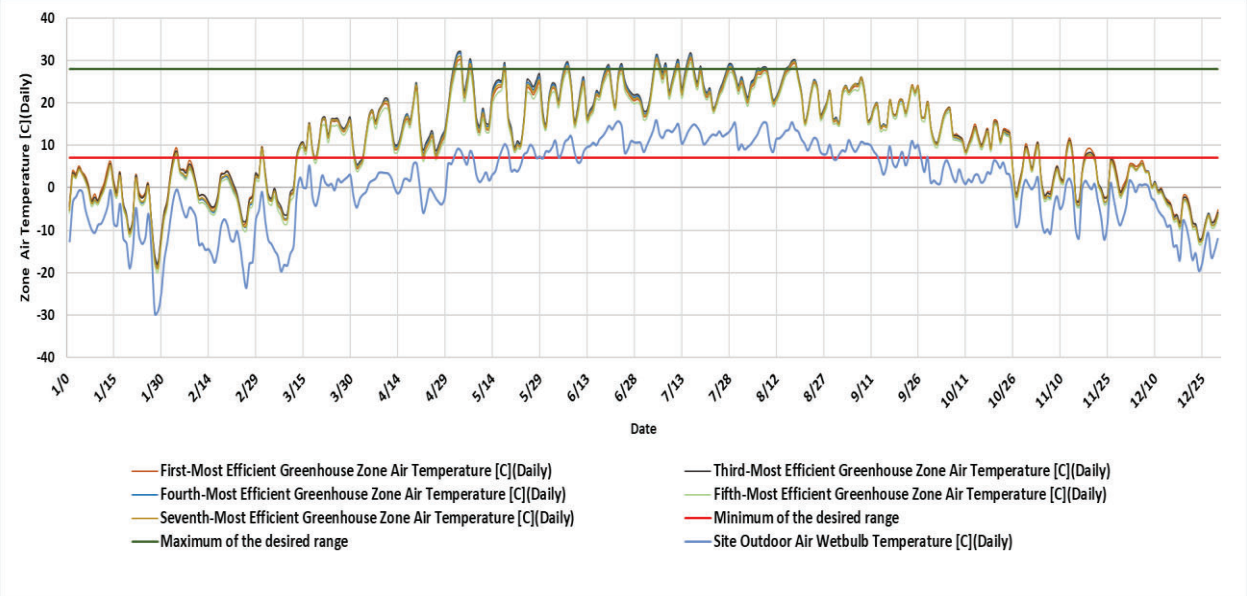

Figure 2- 11: Variation of daily zone air temperature for the 1st, 3rd, 4th, 5th, and 7th most energy-efficient greenhouses on OSCC land

Figure 2-12 shows how the monthly zone air temperature is changing during one year for these 5 structures. The annual temperature range increased in Quonset, Gothic, Modified Arch, Even-Span with two spans, and Even-Span with five spans, respectively. Considering monthly zone air temperature and variation in temperature range, Gothic has the minimum temperature

range between multi spans greenhouse. However, daily indoor temperature variation shows Even-Span with two spans and 5 spans, has less number of days with temperatures outside the optimum temperature range than Gothic, although these two have a wider range of temperature range during the year.

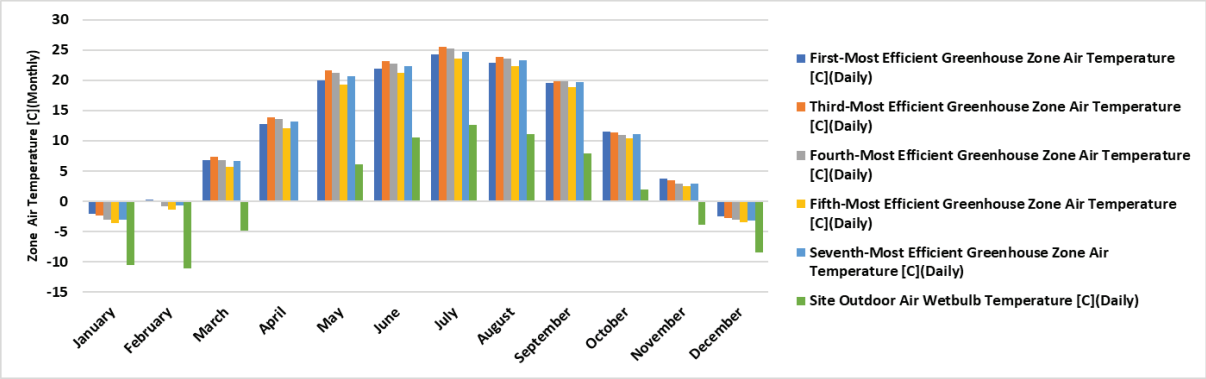

Figure 2- 12: Variation of monthly zone air temperature for the 1st, 3rd, 4th, 5th, and 7th most energy-efficient greenhouses on OSCC land

2.3.3. Overall comparison of all defined scenarios

As shown in Figure 2-13 around 630 greenhouses out of 1408 defined greenhouses have a total of overheating degree hours and overcooling degree hours between 44000 and 46000. This means that around 45% of the defined scenarios have a total temperature deviation somewhere between 44000 and 46000.

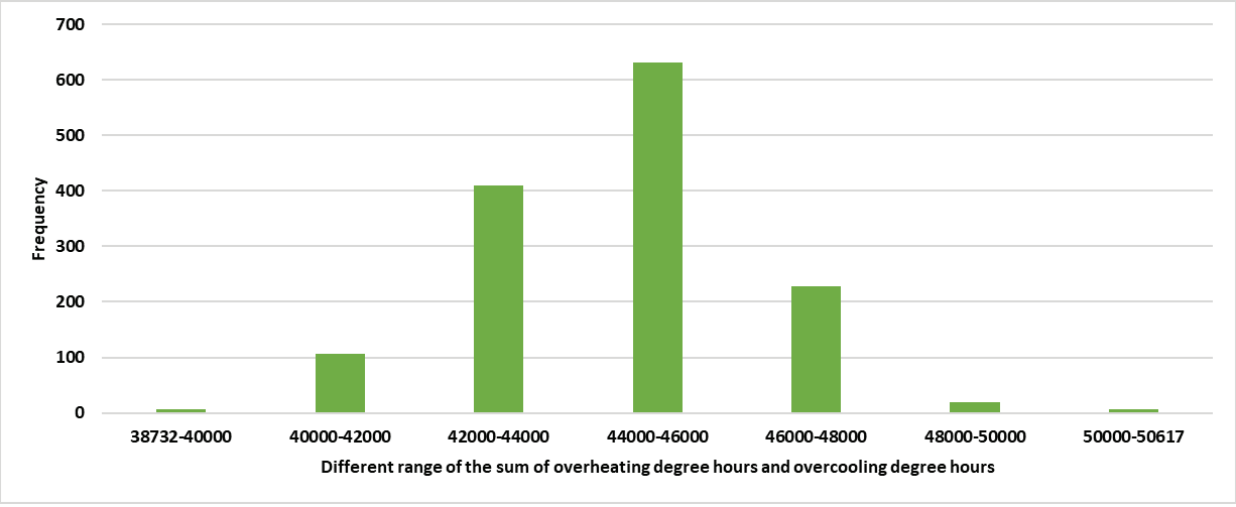

Figure 2- 13: Frequency of greenhouses deviating from desired temperatures (All scenarios)

In Table 2-4 the effect of varying covering materials, orientation, and gutter height on the thermal performance of each greenhouse shape can be seen. The most energy-efficient scenario of each greenhouse shape has been considered as the base-model. Obviously, PVC is the most energy-efficient covering material, followed by PC, PE, and PMMA. However, shape is a factor which should be considered in using PO film, HG, ETFE, and Woven film. According to the shape, one can work better than the other between the latter covering materials. The best orientation of the greenhouse is dependent on the shape of the greenhouse as well. For example, in the most energy-efficient structure of a Gothic shape greenhouse (regarding the size, span, covering material, and height), the best orientation is 90 degrees, followed by 60,30, and 0 degrees. However, this order is different from other greenhouse shapes. Also, the best gutter height is 5.5 meters in all shapes in Table 2-4, although the effect of changing the height on the thermal performance of a greenhouse is different. The maximum difference is in Modified Arch and the minimum is in Uneven-Span. This table illustrates how these parameters affect each other and the thermal performance of a greenhouse.

In Figure 2-14, the optimal orientation and cover material is identified if the shape of the greenhouse is kept fixed. In all cases, the best cover material is PVC. However, as mentioned above, it is not possible to decide which orientation works better. According to the results, it is obvious that for different shapes or cover materials, different orientations need to be considered to achieve an optimum result.

Table 2- 4: The effect of different covering materials, orientation, and gutter height on a greenhouse energy efficiency

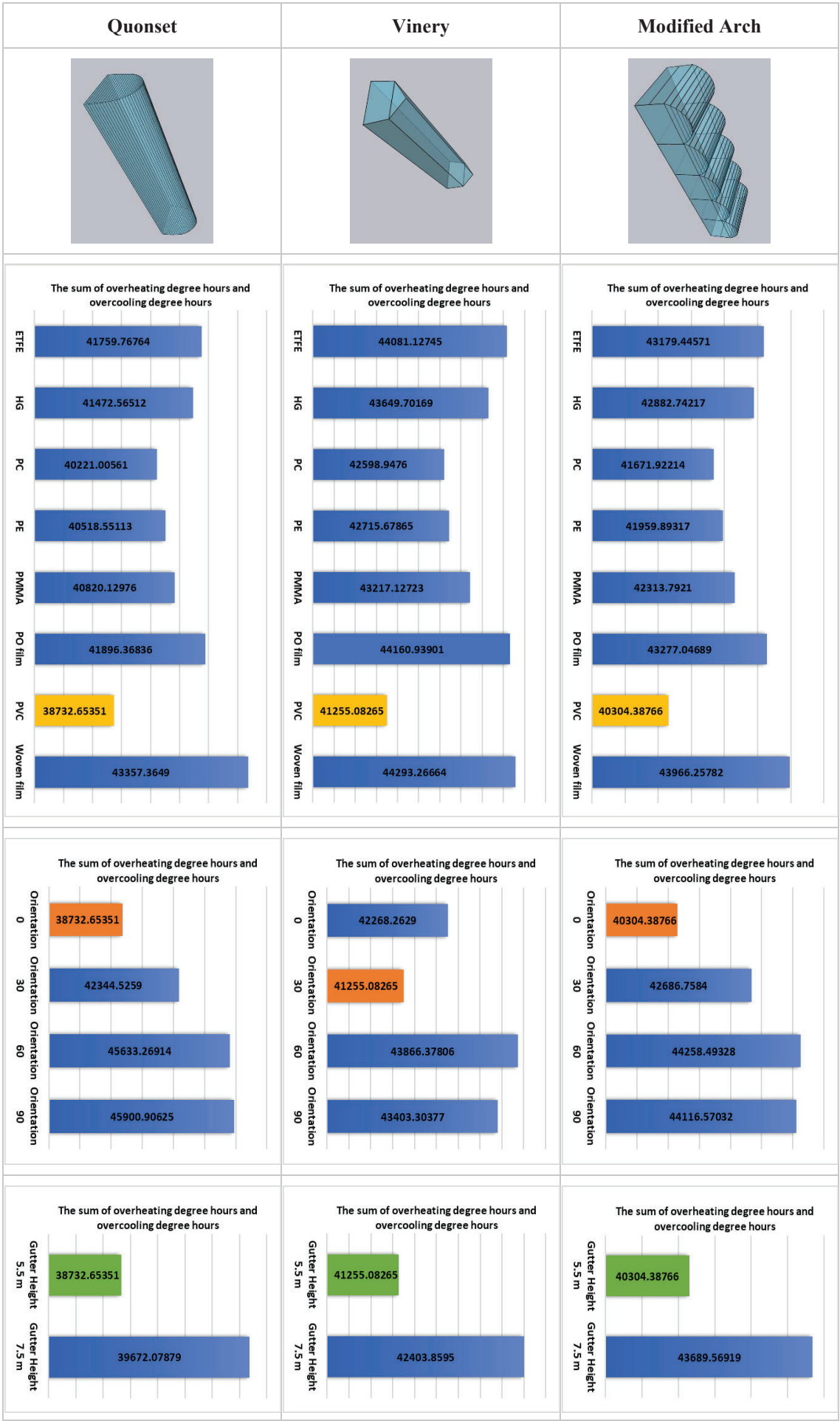
Quonset
Vinery
Modified Arch
The sum of overheating degree hours and overcooling degree hours
ETFE 41759.76764
HG 41472.56512
PC 40221.00561
PE 40518.55113
PMMA 40820.12976
PO film 41896.36836
PVC 38732.65351
Woven film 43357.3649
The sum of overheating degree hours and overcooling degree hours
ETFE 44081.12745
HG 43649.70169
PC 42598.9476
PE 42715.67865
PMMA 43217.12723
PO film 44160.93901
PVC 41255.08265
Woven film 44293.26664
The sum of overheating degree hours and overcooling degree hours
ETFE 43179.44571
HG 42882.74217
PC 41671.92214
PE 41959.89317
PMMA 42313.7921
PO film 43277.04689
PVC 40304.38766
Woven film 43966.25782
The sum of overheating degree hours and overcooling degree hours
Orientation 0 38732.65351
Orientation 30 42344.5259
Orientation 60 45633.26914
Orientation 90 45900.90625
The sum of overheating degree hours and overcooling degree hours
Orientation 0 42268.2629
Orientation 30 41255.08265
Orientation 60 43866.37806
Orientation 90 43403.30377
The sum of overheating degree hours and overcooling degree hours
Orientation 0 40304.38766
Orientation 30 42686.7584
Orientation 60 44258.49328
Orientation 90 44116.57032
The sum of overheating degree hours and overcooling degree hours
Gutter Height 5.5 m 38732.65351
Gutter Height 7.5 m 39672.07879
The sum of overheating degree hours and overcooling degree hours
Gutter Height 5.5 m 41255.08265
Gutter Height 7.5 m 42403.8595
The sum of overheating degree hours and overcooling degree hours
Gutter Height 5.5 m 40304.38766
Gutter Height 7.5 m 43689.56919

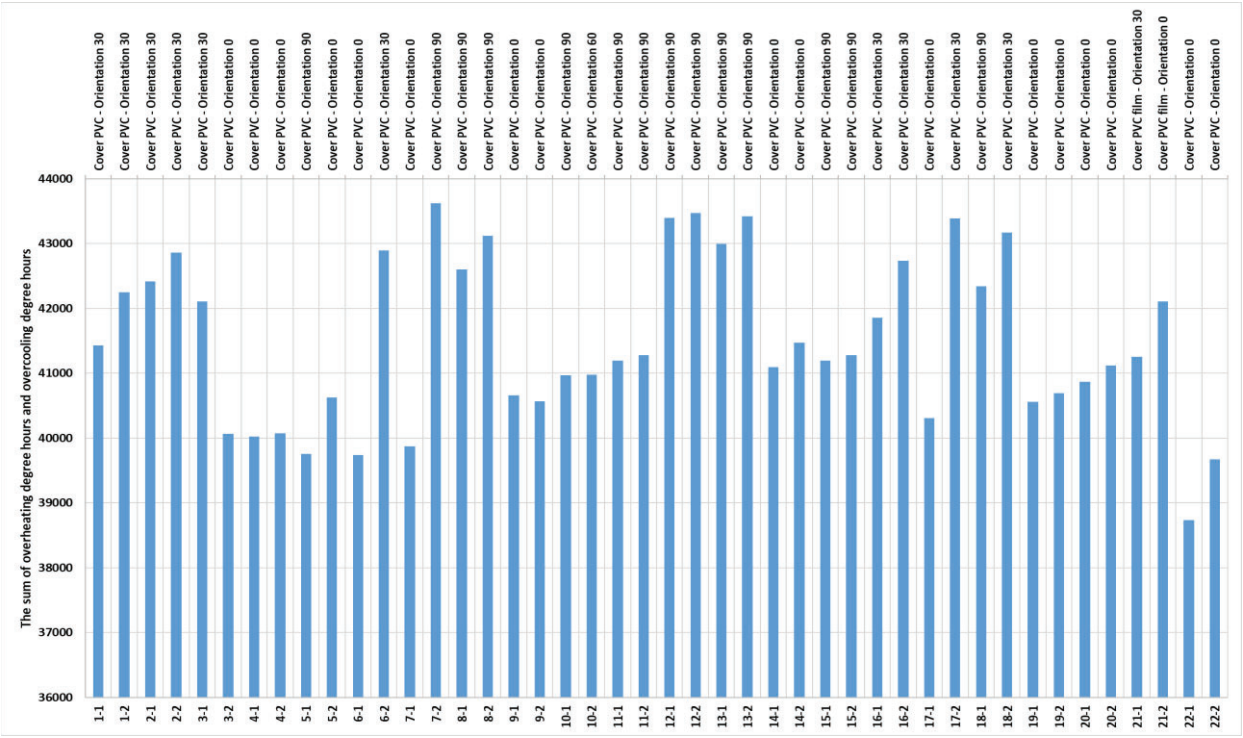

Figure 2- 14: The best orientation or cover material when the shape of the greenhouse is not changing (All scenarios)

Figure 2-15 indicates the opposite of Figure 2-14. Figure 2-15 demonstrates which shape works better, among all 1408 defined scenarios, if orientation and cover are kept fixed. For example, the structure of Gothic with 12 spans, an area of 4500 square meters, and a gutter height of 5.5 meters has the minimum total of overheating degree hours and overcooling degree hours for both orientations of 90 and 60 degrees, and each of the 8 cover materials. If the orientation and cover material do not change, except in three scenarios, the shape of the Gothic with 12 spans, an area of 4500 square meters, and a gutter height of 5.5 meters as well as the shape of Quonset with 1 span, the area of 500 square meters and the total height of 8.5 meters, works the best in comparison to the other structures. Also, it can be observed that in all the best cases, the gutter height is 5.5 meters, so it can be concluded that a gutter height of 5.5 meters results in a more efficient greenhouse.

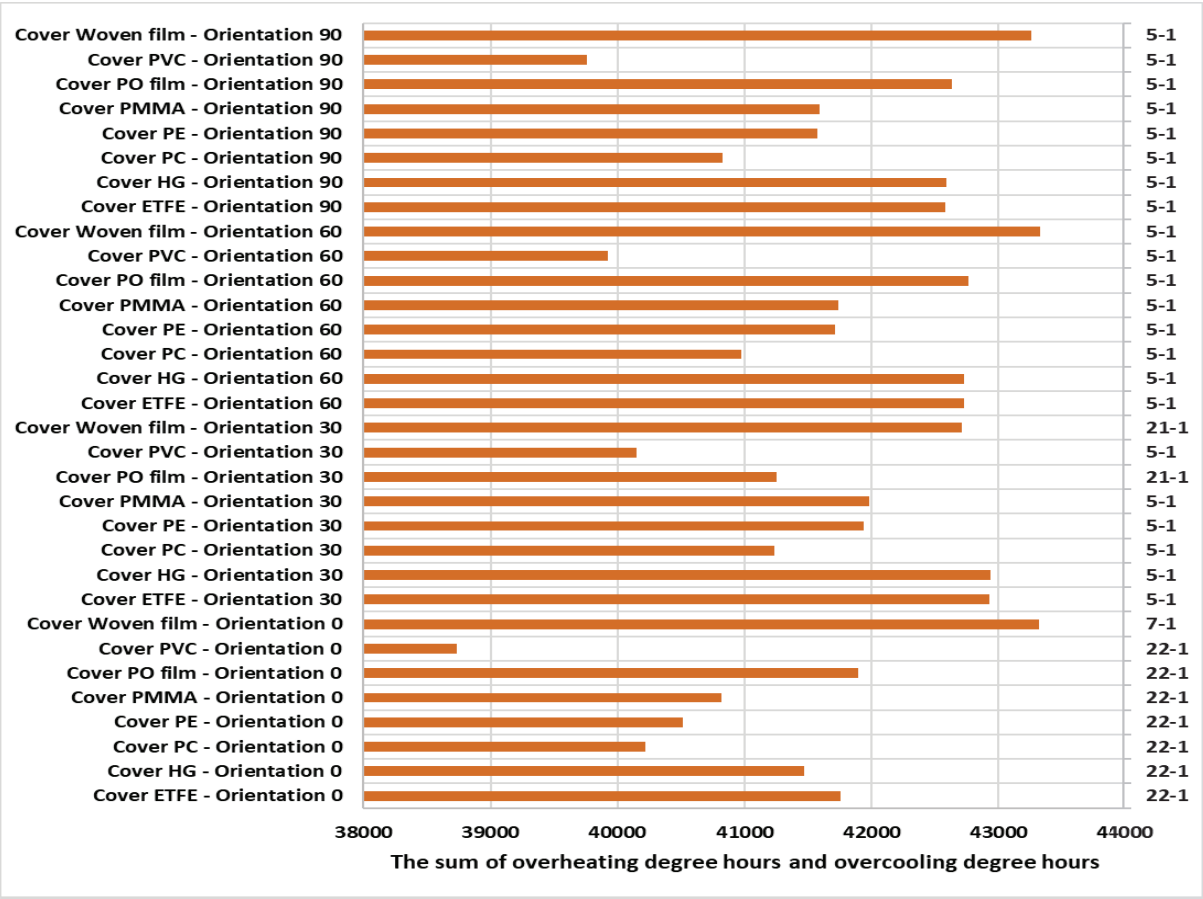

Figure 2- 15: The best shape of the greenhouse when orientation and cover are not changing (All scenarios)[1].

2.4. Conclusions

In this chapter, the amounts of total overheating and overcooling degree hours for 1408 defined scenarios were calculated. For this purpose, the six most common shapes of greenhouses (Gothic, Even-Span, Uneven-Span, Modified Arch, vinery, and Quonset type) in 2 different gutter heights, a variety of spans, 4 different orientations, and 8 different cover materials were compared. EnergyPlus™ was used to predict the internal temperatures of defined greenhouses for the year 2020. Based on the results of the simulation, the following conclusions were drawn:

[1]Structures include two numbers. According to Table 2-1, the first number is the number of shapes, and the second number is the number of gutter heights.

- The single-span Quonset shape greenhouse at east-west orientation, a total height of 8.5 meters, and PVC cover material has the minimum energy demand. However, this greenhouse has the minimum contact area with surrounding environment among all defined scenarios.
- Among the scenarios with an area of 750 m^2 and 787.5 m^2 designed for the OSCC land, Even-Span shape with two spans and a gutter height of 5.5 meters in an east-west direction, Even-Span shape with five spans and a gutter height of 5.5 meters in a north-south direction, Gothic shape with seven spans and a gutter height of 7.5 meters in a north-south direction, and Modified Arch shape with five spans and a gutter height of 5.5 meters in a north-south direction are the most energy-efficient greenhouses.
- Considering all 1408 scenarios and multi-span greenhouses, the most energy-efficient greenhouse after the Even-Span shape with two spans and a gutter height of 5.5 meters in an east-west direction, is the Gothic shape with twelve spans and a gutter height of 5.5 meters in a north-south direction. This scenario is a large commercial greenhouse with a 4500 m^2 area which is more energy-efficient than other options at high northern latitudes.
- PVC is the most energy-efficient cover material in all scenarios. PC is the second-best cover material.
- The result of the study corroborated the result of previous studies.
- The result of the study can be used as a reference to find the basic design of an energy-efficient greenhouse for any project's location in a cold climate like Southern Alberta.
- The restriction on the greenhouse area of the case study land can affect the economic efficiency of the greenhouse as it restricts greenhouse production. According to the results of the study, some of the large commercial greenhouses showed good thermal

performance. Considering the larger space to grow a larger yield in these greenhouses, they can be considered as energy-efficient structures with higher production profits.

Although one of the main goals of the project was to consider different options and values for the design parameters, because of EnergyPlus™ graphical limitations, it was not possible to consider a range of values for the angle of greenhouse roofs. The shapes considered in this chapter are all the common structures of conventional greenhouses. In future studies, it would be valuable if uncommon greenhouse structures such as Chinese Style Greenhouses, were compared with common greenhouse structures with respect to energy efficiency. However, economic criteria would need to be considered in such a study.

References

Ahamed, M. S., Guo, H., & Tanino, K. (2018a). A quasi-steady-state model for predicting the heating requirements of conventional greenhouses in cold regions. *Information Processing in Agriculture, 5* (1), 33–46.

Ahamed, M. S., Guo, H., & Tanino, K. (2018b). Development of a thermal model for simulation of supplemental heating requirements in Chinese-style solar greenhouses. *Computers and Electronics in Agriculture, 150*, 235–244.

Ahamed, M. S., Guo, H., & Tanino, K. (2018c). Energy-efficient design of greenhouse for Canadian Prairies using a heating simulation model. *International Journal of Energy Research, 42*(6), 2263-2272. doi:10.1002/er.4019.

Ahamed, M. S., Guo, H., & Tanino, K. (2020). Modeling heating demands in a Chinese-style solar greenhouse using the transient building energy simulation model TRNSYS. *Journal of Building Engineering, 29*. doi:10.1016/j.jobe.2019.101114.

Al Ka'bi, A. H. (2020). Comparison of energy simulation applications used in green building. *Annals of Telecommunications, 75*(7-8), 271-290. doi:10.1007/s12243-020-00771-6.

Alinejad, T., Yaghoubi, M., & Vadiee, A. (2020). Thermo-environomic assessment of an integrated greenhouse with an adjustable solar photovoltaic blind system. *Renewable Energy, 156*, 1-13. doi:https://doi.org/10.1016/j.renene.2020.04.070

Arenghi, A., Perra, C., & Caffi, M. (2021). Simulating and comparing different vertical greenery systems grouped into categories using EnergyPlus. *Applied Sciences, 11*(11). doi:10.3390/app11114802

Azhar, S., Brown, J., & Farooqui, R. (2009). BIM-based sustainability analysis: an evaluation of building performance analysis software. Proc 45th ASC Ann Conf 1(4):276–292.

Belkadi, A., Mezghani, D., & Mami, A. (2019). Energy design and optimization of a greenhouse: A heating, cooling and lighting study. *Engineering, Technology & Applied Science Research, 9*(3), 4235-4242. doi: 10.5281/zenodo.3249139.

Çakır, U., & Şahin, E. (2015). Using solar greenhouses in cold climates and evaluating optimum type according to sizing, position and location: A case study. *Computers and Electronics in Agriculture, 117*, 245-257. doi:10.1016/j.compag.2015.08.005.

Chen, C., Li, Y., Li, N., Wei, S., Yang, F., Ling, H., . . ., & Han, F. (2018). A computational model to determine the optimal orientation for solar greenhouses located at different latitudes in China. *Solar Energy, 165*, 19-26. doi:10.1016/j.solener.2018.02.022.

Chen, J., Ma, Y., & Pang, Z. (2020). A mathematical model of global solar radiation to select the optimal shape and orientation of the greenhouses in southern China. *Solar Energy, 205*, 380-389. doi:10.1016/j.solener.2020.05.055.

Choab, N., Allouhi, A., El Maakoul, A., Kousksou, T., Saadeddine, S., & Jamil, A. (2019). Review on greenhouse microclimate and application: Design parameters, thermal

modeling and simulation, climate controlling technologies. *Solar Energy, 191*, 109-137. doi:10.1016/j.solener.2019.08.042.

Deiana, A., Fabrizio, E., & Gerboni, R. (2014). *Energy performance optimization of typical Chinese solar greenhouses by means of dynamic simulation*. International Conference of Agricultural Engineering.

Esmaeli, H., & Roshandel, R. (2020). Optimal design for solar greenhouses based on climate conditions. *Renewable Energy, 145*, 1255-1265. doi:10.1016/j.renene.2019.06.090.

Fabrizio, E. (2012). Energy reduction measures in agricultural greenhouses heating: envelope, systems and solar energy collection. *Energy Build, 53*, 57–63.

Figueiroa, V., & Torres, J. P. N. (2022). Simulation of a small smart greenhouse. *Designs, 6*(6). doi:10.3390/designs6060106

Laate, E. A., & Dr. Mirza Consultants, I. (2020). Profile of the greenhouse industry in Alberta 2019: Alberta Agriculture and Forestry, Government of Alberta.

Lebre, B., Silva, P. D., Pires, L. C., & Gaspar, P. D. (2021). Computational modeling of the thermal behavior of a greenhouse. *Applied Sciences, 11*(24). doi:10.3390/app112411816

Liao, L., & Teo, E. A. L. (2018). Organizational change perspective on people management in BIM implementation in building projects. *Journal of Management in Engineering, 34*(3):4018008–4018009.

Ma, Y., Li, X., Fu, Z., & Zhang, L. (2019). Structural design and thermal performance simulation of shade roof of double-slope greenhouse for mushroom-vegetable cultivation. International *Journal of Agricultural and Biological Engineering, 12*(3), 126-133. doi:10.25165/j.ijabe.20191203.4852.

Ma, J., Du, X., Meng, S., Ding, J., Gu, X., Zhang, Y., . . . Wang, R. (2022). Simulation of thermal performance in a typical Chinese solar greenhouse. *Agronomy, 12*(10). doi:10.3390/agronomy12102255

Mobtaker, H. G., Ajabshirchi, Y., Ranjbar, S. F., & Matloobi, M. (2019). Simulation of thermal performance of solar greenhouse in north-west of Iran: An experimental validation. *Renewable Energy, 135*, 88-97. doi:10.1016/j.renene.2018.10.003.

Mazzeo, D., Romagnoni, P., Matera, N., Oliveti, G., Cornaro, C., & De Santoli, L. (2020). *Accuracy of the most popular building performance simulation tools: Experimental comparison for a conventional and a PCM-based test box*. Paper presented at the Proceedings of Building Simulation 2019: 16th Conference of IBPSA.

NREL, EnergyPlus, 2015. https://energyplus.net/.

Park, D. Y., Lee, H. J., Yun, S. I., & Choi, S. M. (2021). Simulation analysis of daylight characteristics and cooling load based on performance test of covering materials used in smart farms. *Energies, 14*(19). doi:10.3390/en14196331.

Rasheed, A., Lee, J., & Lee, H. (2018). Development and optimization of a building energy simulation model to study the effect of greenhouse design parameters. *Energies, 11*(8). doi:10.3390/en11082001.

Rasheed, A., Kwak, C. S., Kim, H. T., & Lee, H. W. (2020). Building an energy simulation model for analyzing energy saving options of multi-span greenhouses. *Applied Sciences, 10*(19). doi:10.3390/app10196884

Shelford, T. J., & Both, A. J. (2020). *Plant production in controlled environments*. In Holden, N. M., Wolfe, M. L., Ogejo, J. A., & Cummins, E. J. (Ed.), Introduction to Biosystems Engineering. https://doi.org/10.21061/IntroBiosystemsEngineering/Plant_Controlled_Environment

Shen, Y., Wei, R., & Xu, L. (2018). Energy consumption prediction of a greenhouse and optimization of daily average temperature. *Energies, 11*(1). doi:10.3390/en11010065

Van Beveren, P. J. M., Bontsema, J., Van Straten, G., & Van Henten, E. J. (2015). Minimal heating and cooling in a modern rose greenhouse. *Applied Energy, 137*, 97-109. doi:10.1016/j.apenergy.2014.09.083

Chapter 3: Comparison of Thermal Performance, Energy Demand, and Costs of Conventional Greenhouses, Chinese Style Greenhouses, and Plant Factories: A Case Study in Southern Alberta

3.1. Introduction and background

The world's population reached 8 billion on 15 November 2022. The United Nations predicts that by mid-century, the global population could grow to around 9.7 billion, followed by an increase to 10.4 billion during the 2080s and remaining at that level until 2100 (UN 2022). In addition to population growth, the world faces numerous constraints such as climate change, the depletion of fossil fuels, beside the steady increase in energy demand (Ouazzanİ ChahİDİ and Mechaqrane 2021). Hence, ensuring a supply of food, using energy-efficient systems which can produce fresh food locally, is of paramount importance. Greenhouse agriculture seems to be one of the most practical techniques for providing sustainable, locally produced, high-quality products. By protecting plants against harsh ambient conditions, these structures can secure local harvests even in regions with the most challenging climates. It should be considered that reliably producing high-quality high-yields in greenhouses consumes significantly more energy in comparison to free land (outdoor) cultivation (Vadiee and Martin 2014). A report from the Institute for International Energy Studies (IIES) showed that the high-energy consumption in greenhouse agriculture is primarily due to heating demands (Chaysaz *et al.* 2019). The heating energy requirements for northern regions greenhouses have been reported to be 90% to 95% of the total energy demand for greenhouse production (Ahmed *et al.* 2018c; Lristinsson 2006). These high energy needs increase production costs with consequent increases in the market price. Excess energy use (if from fossil sources) also has detrimental effects on the environment by contributing to climate change through greenhouse gas emissions. It seems that high energy demands in greenhouse construction and operation are thus contradictory to the main goal behind utilizing them in the first place; therefore, a reliable framework for planning, designing,

implementing, and managing greenhouses is required to control the energy requirements in this sector.

The greenhouse is complex, multiparametric, non-linear and depends on a set of external and internal factors (Escamilla-García *et al*. 2020). Designing a greenhouse requires scrupulous planning for each of its many components, including shape, orientation, covering materials, construction material, thermal control equipment, heating and cooling systems (particularly in cold and hot climates), water usage, irrigation equipment, light supplementations, growing media, fertilizers, chemical or biological pesticides, CO_2 demand, and emissions. Each of these factors can have a significant impact on the energy efficiency of the greenhouse. Most of these factors are interdependent, thus their influence on energy efficiency must be considered *in situ* (Belkadi *et al.* 2019). Accordingly, it will be necessary to optimize these factors to decrease total energy demand. Of note, is that the design parameters of a greenhouse that results in energy efficiency under a study situation might not be applicable to every other greenhouse and the optimal value can vary with the location of the greenhouse (Lebre *et al*. 2021).

Greenhouse facilities can be categorized based on their main light energy source for plants, which fall into three types: (1) greenhouses using only sunlight, (2) greenhouses that supplement sunlight with artificial lighting, and (3) closed-growth rooms with fully artificial lighting (Brandon *et al*. 2016; Kim *et al.* 2022).

The first type of greenhouse facility, a greenhouse using only sunlight, might be covered in a transparent medium. In this case, the incident short wavelength radiation through the medium and solar irradiance provides sufficient light for plant growth (Chaob *et al*. 2019). The rate of thermal energy consumption by this type of greenhouse depends on the amount of solar radiation entering the greenhouse (Mobtaker *et al*. 2019). The optimal design of solar greenhouses leads to the best use of solar energy and reduces the energy consumption in the greenhouse (Karambasti

et al. 2022). Belkadi *et al.* (2019) developed a new approach to optimize the energy consumption of a greenhouse based on an energy balance equation. The influence of four different shapes (elliptic, even-span, uneven-span, and rectangular) and five different cover materials (Acrylic, Polycarbonate, Polyethylene film, Glass, and Low-E Glass) was discussed. When adopting an uneven-span form and using polyethylene film as cover material they demonstrated significant improvement in energy efficiency. Çakır and Sahin (2015) developed a model to optimize design parameters including orientation, roof shape, floor area, and the ratio of the greenhouse's length to width (K number) to maximize energy input from the sun. With this model, they were able to find the optimal K numbers and orientations for any greenhouse type. They concluded that the roof shape had the predominant influence on efficiency. The Elliptic shape was the optimal form in their site of study.

An efficient greenhouse design with the lowest heat load in winter and lowest cooling load in summer was sought by Karambasti *et al.* (2022), using solar radiation distribution model integrated into a multi-parameter optimization. The optimal physical parameters (floor area size, inclined surfaces of roof, and orientation) were investigated for three types of greenhouses (Even-Span, Modified Arch, and Quonset). They showed the best direction of placement is east-west orientation while length-to-width ratio is maximized. With regards to optimal solar radiation capture and total solar friction, the Quonset greenhouse exhibited the best performance, improving on the Even-Span and Modified Arch types. Ahmed *et al.* (2019) presented a comprehensive review of the potential techniques causing reduction in the heating requirement and cost of conventional-style winter greenhouses. Finding the best shape, orientation, and cover material, using opaque north walls and thermal screens, and insulating the greenhouse, especially the perimeter and the side wall near the ground, are some of the techniques that can result in decreased energy requirement. They showed that at high northern latitudes, the east-west

orientation of the greenhouse is more energy efficient during the winter, demonstrating that by using any thermal screen in winter greenhouses can save 20% of energy, as they reduce the loss of thermal radiation to the sky during the winter nights.

The second type of greenhouse employs supplemental lighting when sunlight is suboptimal (Brandon *et al*. 2016). For instance, opaque walls on the north side, used to reduce thermal energy demand, often require supplemental lighting in nearby shaded areas. Mobtaker *et al*. (2019) investigated the amount of total solar radiation that can be captured by the six different shapes of greenhouses including uneven-span, even-span, single-span, vinery, quonset, and arch type. They also developed a dynamic thermal model for estimating temperatures of the inside air, soil surface, and the inner surface of the north wall of a single-span greenhouse. They showed that a single-span-shaped greenhouse with an east-west orientation receives the maximum solar radiation during the cold season and that the temperature on the inner surface of the north wall plays a significant role in raising greenhouse air temperature; thus by erecting a brick wall on the northern side energy loss is reduced by an average of 68%.

The most common structure of the second type of greenhouse is known as Chinese Style Greenhouse (CSG). Generally, CSGs have three opaque walls on the north, east, and west sides of the structure. These walls are typically made of brick containing heat-absorbing material on the inside and insulating material on the outside (Ma *et al*. 2022). The south side of the building has a transparent cover material that allows for the maximum sun exposure. The energy captured during the day is thus stored in the thermal mass of the walls and subsequently released at night. As the walls are opaque, supplemental lighting will be required at certain times during the day (Ahmed *et al*. 2019). CSGs also make use of an insulation sheet, or heating blanket, that is rolled out over the south side to slow the rate of heat loss. By considering the combination of factors such as solar exposure, thermal energy storage, and the minimization of thermal losses, it is

possible to maintain the indoor temperature of a CSG above the outdoor temperature during cold periods in northern latitudes.

Ma *et al.* (2019) used EnergyPlus™ to evaluate the thermal performance and energy consumption of a double-slope greenhouse with a wall in the middle of the greenhouse (double-side CSG). EnergyPlus™ is a whole building energy simulation software that uses heat and mass transfer models, heating and air conditioning variables, and simulation of interactions of thermal zones within the building and environment to model energy consumption (NREL 2015). Their objective was to design a new roof for the side of the greenhouse oriented away from the sun, known as shade room of the greenhouse, by selecting the best inner surface, insulation, and outer surface materials and calculating the minimum required insulation thickness for the designed roof. They concluded that the new roof increased the indoor temperature, resulting in reduced energy consumption. Ahamed *et al*. (2020) modelled the transient heating load of a fully environmental controlled CSG for the year-round production at high northern latitudes using TRNSYS (Transient System Simulation Tool), which is an energy systems simulation software package (TRNSYS 2017). They showed that minimized heating costs during production can be achieved for CSGs at high northern latitudes with appropriate adaptations.

Thermal performance for typical CSGs was evaluated by Ma *et al*. (2022) using EnergyPlus™. They showed that acceptable heat conservation of all components inside the CSG on cold weather days was achievable, while maintaining acceptable air temperatures during the night. Deiana *et al.* (2014) assessed the energy performance of three different CSGs, varying in the use of glazed surfaces, opaque walls, and thermal blankets, as well as ventilation rate of the structure, using EnergyPlus™. Improvements in solar greenhouse construction by changing the simple characteristics of the structure and defining a more complex design can cause an increase in energy efficiency. This means a higher minimum internal temperature during the cold periods

can be achieved which may obviate the need for auxiliary heating systems, or allow the switch to the cultivation of different types of crops with higher market values. This design has the potential to be economical, if higher costs of construction can be recovered with the improved market value and production volume of the crops.

The third type of facility is completely isolated from the outside environment (*i.e.* a closed system) thus necessitating artificial lighting (Brandon *et al.* 2016). Maximizing fertility, production volume, and efficient resource usage are some of the features of this closed system (Graamans *et al*. 2018). Vertical farming and hydroponics are the most common methods employed in such facilities. Although vegetable production is possible in most climates and locations using such plant factories, providing the desired indoor condition and artificial lighting will lead to higher electrical energy requirements (Weidner *et al.* 2021). Graamans *et al.* (2018) compared the energy requirements for lettuce production in plant factories with greenhouses in three different climate regions. They confirmed higher energy demand for plant factories due to artificial lighting; however, showed that they confer other advantages such as improved efficiency in resource utilization, uniformity of interior climate, and higher quantity and quality of production. Using a new model, Weidner *et al.* (2021) optimized and compared the energy consumption of three types of controlled-environment agriculture (CEA) systems including a plant factory, a non-ventilated greenhouse, and a ventilated greenhouse for a variety of climate zones. He also conducted a sensitivity analysis to determine the most influential operational and design parameters. They predicted that the specific energy consumption of ventilated greenhouses was significantly lower than the other systems for the location of their study.

The greenhouse industry is adaptable to the application of sustainable agricultural practices (Karambasti *et al*. 2022). As a result, food security can be ensured virtually anywhere, especially in the north and under conditions of seasonal temperature fluctuations and limited

light. However, reducing energy demand within agricultural greenhouses should be a key goal in order to advance sustainable development in this sector (Iddio *et al*. 2020). Therefore, this chapter seeks to find the most energy-efficient greenhouse facility located in the continental climate of Southern Alberta, and in particular at the Old Sun Community College in Siksika First Nation of the Blackfoot Confederacy (east of Calgary, AB, Canada).

3.1.1. Objective

The objectives of this study are as follows:

- To make a comparison between three different proposed greenhouse facilities (Conventional Greenhouses, Chinese Style Greenhouses, and Plant Factories), located in Southern Alberta during the year 2020, regarding their thermal performance and energy requirement using the EnergyPlus™ simulation model.
- To validate the simulation model based on measured data from an existing greenhouse located in Olds, Alberta, Canada during two time periods (from the 5th to the 10th of February 2020 and from the 25th to the 30th of July 2020).
- To adapt EnergyPlus™ to consider the effect of plants evapotranspiration latent heat
- To investigate the effect of increasing volume (increasing height) and two different opaque wall construction materials on the energy efficiency of each greenhouse facility, by type.
- To perform an energy and capital investment cost analysis to assess the potential profitability of these facilities.

3.2. Methodology

The focus of this study is on modelling a Conventional Greenhouse (CG), a Chinese Style Greenhouse (CSG), and a Plant Factory (PF) located in Southern Alberta. The decision-making

on the efficiency of each greenhouse facility requires both consideration of the energy consumption and an economic analysis. The energy consumption of each facility is derived from the combination of HVAC (Heating, Ventilation, and Air Conditioning) and artificial lighting loads, which are calculated using EnergyPlus™. Furthermore, an economic analysis was performed to identify the most cost-effective and energy-efficient design for a greenhouse facility in the region of study. In this study, it has been assumed that the greenhouse is operational all year round, and that HVAC systems are used when the greenhouse indoor temperature is outside the desired range of 16°C and 27°C. These assumptions are just for the sake of comparison between the defined cases.

3.2.1. Description of the existing greenhouse for EnergyPlus™ validation

A Chinese Style Greenhouse located in Olds, Alberta, Canada is considered as the case study to validate the model used in this study (Figure 3-1). Figure 3-2 details the supporting structure of the existing greenhouse model and its dimensions. Table 3-1 summarizes the greenhouse's geometrical and structural parameters.

Figure 3- 1: The experimental greenhouse used to validate the simulation model of this study

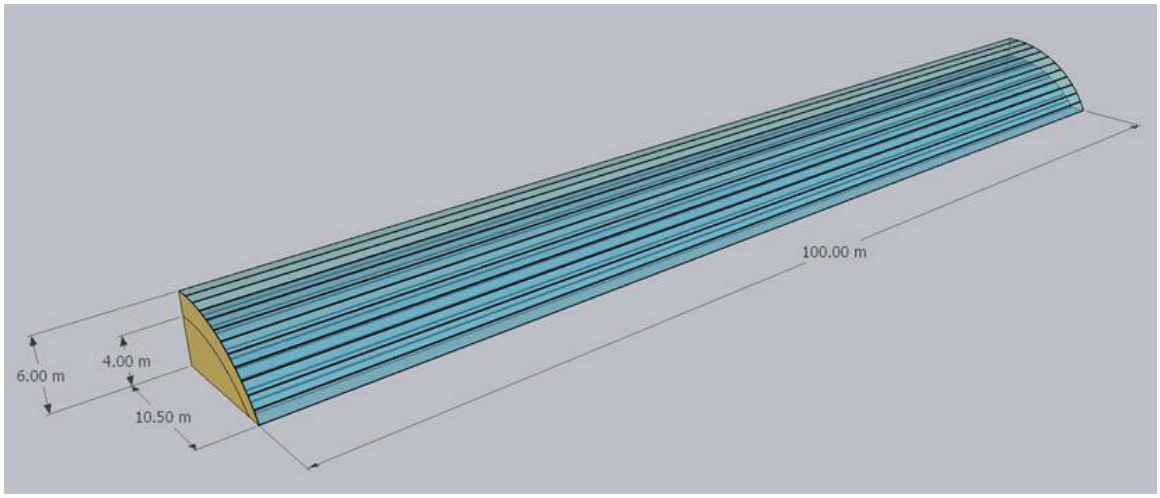

Figure 3- 2: The geometry of the experimental greenhouse model developed in SketchUp

The north wall, a composite structure, is 6 meters tall. The outside is a 1-m-thick layer of clay, covered with a tarp. The inside layer is made of a black colour metal sheet for the first 4 m from the ground and followed by an insulation blanket for the last 2 m. There is a 2-metre space between the first and second layer of covering material on the south roof. The first layer is at 4 metres above the ground and the second layer is two metres above it. The covering material is made of Poly film on the south roof. There is an insulation blanket on top of the first layer of covering material.

Table 3- 1: Detailed existing greenhouse structural specifications used to make the model

Latitude	51.76697
Longitude	-113.97065
Greenhouse Type	Passive solar
Width of span	Outer perimeter: 10.5 m Inner perimeter: 9 m
Length	100 m
Ridge height	6 m
Gutter Height	4 m
Orientation	South
Flooring Material	Soil
Covering material	2 layers of Poly film plastic
North Side wall materials	Outside layer: tarp Middle layer: 1-meter-thick clay Inner layer: Black color Metal Sheet for 4 m – Insulation blanket on top
Insulation material (Heating Blanket)	fabric on top of the first layer of cover material

To validate the model in predicting the average temperature inside the greenhouse, the simulated temperature was compared with the actual temperature between the 5th and 10th of February 2020 as the winter duration and between the 25th and 30th of July 2020 as the summer duration. For the duration of the study, the insulation blanket has been closed all day during winter and open during summer. Natural ventilation has been utilized during summer. An infiltration rate of 1.5 ACH has been defined for the model.

3.2.2. Dynamic energy simulation model

Energy simulation models aid in developing energy-efficient designs with lowered energy costs, increased natural energy resources (e.g., solar energy) usage, and reduced negative impacts of fossil fuel on the surrounding environment (Al Ka'bi 2020; Azhar *et al*. 2009; Liao and Teo 2018). In this study, the simulation of the greenhouse energy consumption and thermal performance was carried out using EnergyPlus™.

3.2.2.1. EnergyPlus™

EnergyPlus is a whole-building energy simulation model, developed by the U.S. Department of Energy and the Lawrence Berkeley National Laboratory. EnergyPlus™ can simulate both the heat transfer process with a non-uniform temperature field, the heating and cooling load of buildings, the annual dynamic energy consumption, and output detailed real-time data, such as the average indoor hourly temperature, humidity, and the system's hourly heating and cooling power (Ma *et al.* 2019; Crawley *et al.* 2001). In recent years, EnergyPlus™ has been used in several studies to analyse the thermal performance and energy consumption of greenhouses (Ma *et al.* 2022; Ma *et al.* 2019; Chen *et al.* 2018; Deiana *et al.* 2014).

3.2.2.1.1. Energy balance in EnergyPlus™

EnergyPlus™ is a heat balance-based simulation program based on the principle of energy conservation. The rate of change of air temperature inside the greenhouse can be proposed as the result of heat exchange between the inside and outside of the greenhouse. By assuming that air is well mixed inside the greenhouse so that there is not any spatial temperature variation (thermal equilibrium), the energy balance for a greenhouse can generally be elucidated as the following differential equation for temperature (Esmaeili and Roshandel 2020; Shen *et al.* 2018; Alinejad *et al.* 2020; Van Beveren *et al*. 2015):

$$m_{air}C_{p,air}\frac{dT_{in}}{dt} = Q_{sun} + Q_{light} + Q_{people} + Q_{heatSys} - Q_{coolSys} - Q_{long} - Q_{loss} - Q_{vent} - Q_{crop} \pm Q_{store} \pm Q_{soil} \pm Q_{inf} \quad (3\text{-}1)$$

This study considers energy balance that is influenced by the aforementioned thermal fluxes as shown in Figure 3-3. A description of each of the variables in the equation above can be found in Table 3-2.

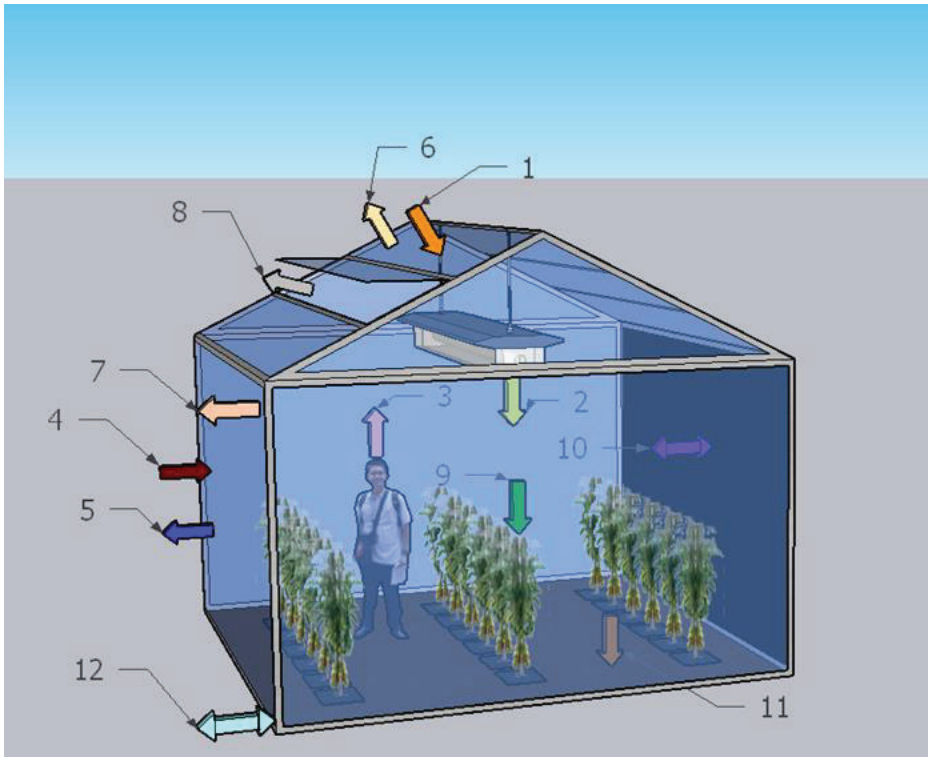

Figure 3- 3: The schematic illustration of the thermal fluxes inside a greenhouse

Table 3- 2: Explanation of different greenhouse energy fluxes

Different greenhouse energy fluxes and related arrows' colors					
1	Heat gains due to absorbed solar radiation through greenhouse cover (Shortwave)	Q_{sun}	**7**	Heat loss due to conduction and convection	Q_{loss}
2	Heat gains due to artificial lighting	Q_{light}	**8**	Heat loss due to natural ventilation	Q_{vent}
3	Heat gains due to students/workers	Q_{people}	**9**	Heat loss due to crop evapotranspiration	Q_{crop}
4	Heat gains due to the auxiliary heating system	$Q_{heatSys}$	**10**	Heat exchange via convection between the heat storage wall and inside air	Q_{store}
5	Heat loss due to the auxiliary cooling system	$Q_{coolSys}$	**11**	Heat exchange via conduction between indoor air and soil	Q_{soil}
6	Heat loss due to transferring thermal radiation (Longwave)	Q_{long}	**12**	Heat exchange between outdoor and indoor air due to infiltration	Q_{inf}

EnergyPlus™ uses different models to calculate greenhouse energy fluxes mentioned above such as the Perez sky model, TARP (Thermal Analysis Research Program) model, and Kiva (ground heat transfer) model to calculate Q_{sun}, Q_{loss}, Q_{soil}, respectively. One of the main limitations of EnergyPlus™ is that it does not account for indoor plant environments (Fabrizio 2012; Harbick and Albright 2016).

Crop evapotranspiration results in a cooling effect on the surroundings (Arenghi *et al.* 2021). In order to modify the EnergyPlus™ deficiency, the energy loss from greenhouse air due to this process, Q_{crop}, can be expressed by:

$$Q_{crop} = ET \times l \times A_{CultivatedGround} \tag{3-2}$$

ET ($gr_{H_2O}.day^{-1}.m^{-2}$) is the amount of water entering the greenhouse by evapotranspiration and l ($Cal.gr_{H_2O}{}^{-1}$) is the latent heat of the vaporization of water. ET can be calculated as follows:

$$ET = ET_{rate} \times \rho \tag{3-3}$$

$$ET_{rate} = ET_o \times K_c \tag{3-4}$$

ET_{rate} ($cm.day^{-1}$) is the evapotranspiration rate, ρ ($gr.cm^{-3}$) density of water, and K_c is the dimensionless crop coefficient representing the crop type and the development of the crop over the growth period (Alinejad *et al.* 2020; Arenghi *et al.* 2021; Kumar *et al.* 2016). The value for K_c is between 0.15 and 0.30 for vegetables (Ponce 1989), which has been considered 0.25. In this study, Priestley and Taylor's formula which is the radiation part of the Penman equation (Allen *et al*. 1998) has been used for the calculation of ET_o ($cm.day^{-1}$) (Priestley and Taylor 1972):

$$ET_o = \frac{1.26\Delta(\frac{R_n}{\rho l})}{\Delta + \gamma} \tag{3-5}$$

R_n (Cal.$cm^{-2}.day^{-1}$) is the net radiation at the crop surface, γ ($mb.℃^{-1}$) is a psychrometric constant that is equal to 0.66 $mb.℃^{-1}$, and Δ ($mb.℃^{-1}$) is the slope vapour

pressure curve which is a function of the air temperature and can be calculated as follows (Linsley *et al.* 1982):

$$\Delta = (0.00815T_a + 0.8912)^7 \quad (3\text{-}6)$$

T_a (℃) is the overlaying air temperature. The hourly latent heat flux due to evapotranspiration was calculated using Equations 3-1 to 3-6 and integrated into the general energy balance of EnergyPlus™ using its advanced settings ("OtherEquipment" object and "EnergyManagementSystem" objects).

3.2.3. Model description

3.2.3.1. Location of the models

The land south of Old Sun Community College (OSCC) in Siksika Indian Reserve, Calgary Region, Alberta, Canada, will be the location for a greenhouse to be used for educational purposes. This land is 55 metres long and 15 metres wide. Latitude and longitude of the land are 50.93 and -112.94, respectively.

The hourly weather data used for the simulation are representative of long-term weather data compiled from 2007 to 2021 for the location of the study and were retrieved from (Lawrie and Crawley 2022). The calculation time specified for the simulation was between 1 January 2020 and 31 December 2020.

3.2.3.2. Description of model key design parameters

A total of 16 cases have been defined for the three facilities (CG, CSG, and PF) by determining different shapes, heights, and construction materials. Six cases have been considered as "base model case". The geometry of these base model cases can be seen in Figures 3-4(a) to 3-4(f). Table 3-3 shows defined cases and model inputs.

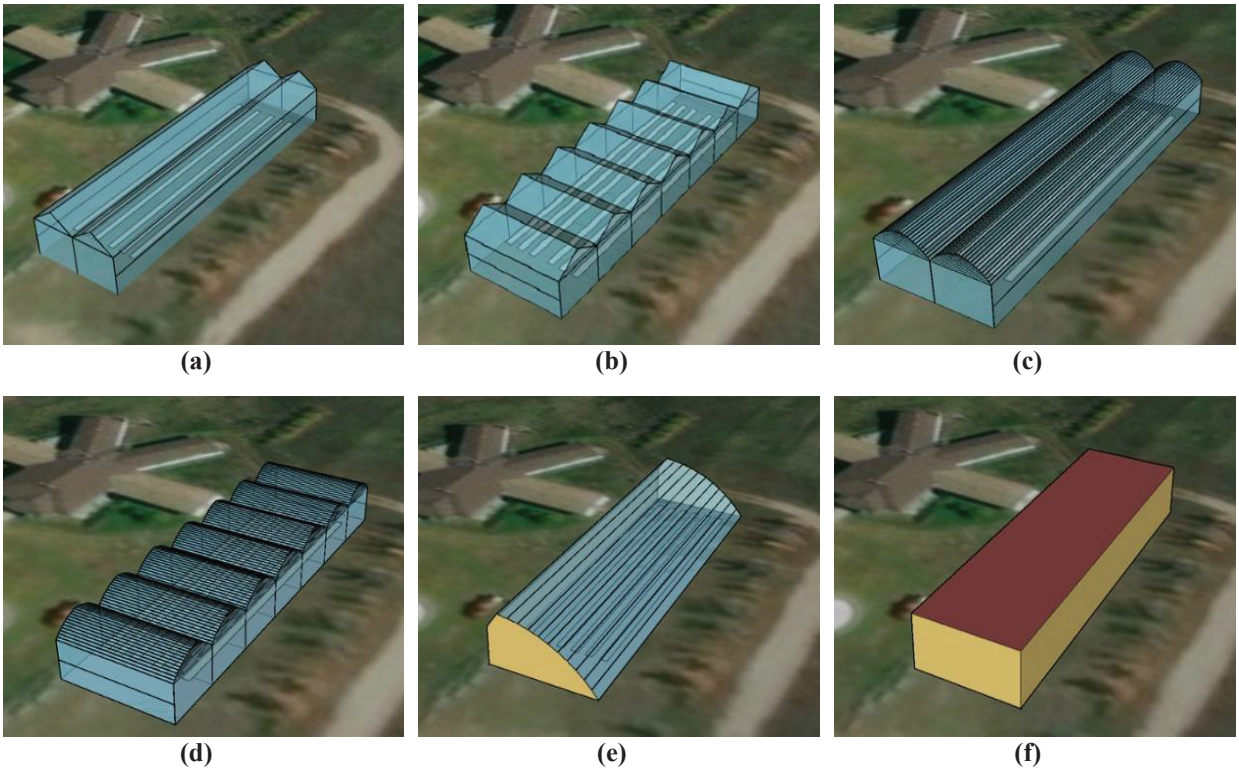

Figure 3- 4: The geometry of 6 base models of the study developed by SketchUp. (a) Even-Span with 2 spans; (b) Even-Span with 7 spans; (c) Gothic with 2 spans; (d) Gothic with 7 spans; (e) CSG; (f) PF

3.2.3.2.1. Cover/Wall/Heating blanket construction

Two layers of Polycarbonate (PC) have been considered for covering CGs and the south roof and wall of CSGs. PC is the most common covering material used by the greenhouse industry in Canada. PFs contain opaque walls on all sides and CSGs have opaque walls on the North, East, and West sides. Construction materials with the lowest possible U-value (coefficient of heat transmission) and high insulation characteristics have been considered for these opaque façades. A heating blanket has been considered for CGs and CSGs during the nights and when the indoor temperature is less than 20°C. The construction materials, and materials used to make them can be seen in Tables 3-4 and 3-5.

Table 3- 3: Cases defined for 3 greenhouse facilities of CGs, CSGs, and PFs as EnergyPlus™ models; their geometry and operational inputs

		Conventional Greenhouses (CGs)								Chinese Style Greenhouses (CSGs)				Plant Factories (PFs)			
		Base Model Case 1	Case 1	Base Model Case 2	Case 2	Base Model Case 3	Case 3	Base Model Case 4	Case 4	Base Model Case 5	Case 5	Case 6	Case 7	Base Model Case 6	Case 8	Case 9	Case 10
		Even-Span (2 Span)		Even-Span (7 Span)		Gothic (2 Span)		Gothic (7 Span)		CSG Sandwich Panel		CSG Spray Foam-Concrete		PF Sandwich Panel		PF Spray Foam-Concrete	
Orientation		E-W	E-W	N-S	N-S	E-W	E-W	N-S	N-S	E-W	E-W	E-W	E-W	E-W	E-W	E-W	E-W
Length (m)		52.5	52.5	15	15	52.5	52.5	15	15	52.5	52.5	52.5	52.5	52.5	52.5	52.5	52.5
Number of Spans		2	2	7	7	2	2	7	7	1	1	1	1	1	1	1	1
Width of Each Span (m)		7.5	7.5	7.5	7.5	7.5	7.5	7.5	7.5	-							
Width (m)		15	15	52.5	52.5	15	15	52.5	52.5	15	15	15	15	15	15	15	15
Height (m)	Ridge Height	2.2	2.2	2.2	2.2	2.2	2.2	2.2	2.2	2.2	2.2	2.2	2.2	-	-	-	-
	Gutter Height	5.5	5.5	7.5	7.5	5.5	5.5	7.5	7.5	5.5	7.5	5.5	7.5	-	-	-	-
	Total Height	7.7	7.7	9.7	9.7	7.7	7.7	9.7	9.7	7.7	9.7	7.7	9.7	7.7	9.7	7.7	9.7
Floor Area (m2)		787.5															
Transparent Wall Area		745.12	1014.48	821.82	1088.62	752.7	1021.5	848.35	1115.15	-							
Opaque Wall Area (m2)		30.38	31.02	36.18	39.38	175.74	229.44	80.89	99.09	446.64	680.44	446.64	680.44	1039.5	1309.5	1039.5	1309.5
Transparent Roof Area (m2)		890.32	890.32	886.07	886.07	677.13	677.13	673.9	673.9	782.68	848.09	782.68	848.09	0			
Opaque Roof Area (m2)		22.7	22.7	26.95	26.95	253.3	253.3	256.53	256.53	195.03	192.92	195.03	192.92	787.5	787.5	787.5	787.5

Cultivation Area (m2)	252			756	1260
Heating Setpoints	16				
Cooling Setpoints	27				
infiltration Rate	0.9375	0.5		0	
Duration of lighting Period	N.A.	before sunrise and after sunset (from 4:00 to 20:00)		16 hours (from 17:00 to 9:00)	
Floor Construction Material	Floor				
Facade Construction Material (Opaque Facade)	CG Wall	PF-CSG Facade (Sandwich Panel)	PF-CSG Facade (Concrete spray foam)	PF-CSG Facade (Sandwich Panel)	PF-CSG Facade (Concrete spray foam)
Facade Construction material (Transparent Facade)	CG-CSG Covering material	CG-CSG Covering material	CG-CSG Covering material	N.A.	N.A.
Roof Construction Material (Opaque Facade)	CG Wall	PF Roof & CG Wall	PF Roof & CG Wall	PF Roof	PF Roof
Roof Construction material (Transparent Facade)	CG-CSG Covering material	CG-CSG Covering material	CG-CSG Covering material	N.A.	N.A.
Lighting System	Sunlight	Sunlight + LED		LED	
Number of Lighting Equipment	N.A.	126		378	630
Heating Blanket	During the Night and When the Inside Temperature is Less Than 20°C			N.A.	
Natural Ventilation	Affected when the indoor temperature is more than 25°C not affected when the indoor temperature is less than 20°C (75 ACH)			N.A.	

Table 3- 4: Different construction materials, their thermal resistance, and the materials considered in each construction material's layers

Name	Floor	CG Wall	PF-CSG Facade (Spray Foam-Concrete)	PF-CSG Facade (Sandwich Panel)	PF-CSG Roof	CG-CSG Covering material	Heating Blanket
Outside Layer	Soil	Galvanized Steel	Polyurethane foam medium density closed cell	Concrete Block: Medium Mass Aggregate: 2 or 3 cores	Metal Siding	PC 10 mm	Polythene
Layer 2			Polyurethane foam medium density closed cell	Metal Siding	Rock wool board	Air	Polyester
Layer 3			Concrete Block: Medium Mass Aggregate: 2 or 3 cores	Rock wool board	Metal Siding	PC 6 mm	Glass Fibre
Layer 4			Polyurethane foam low-density open cell	Metal Siding			Polyester
Layer 5							Polythene
Thermal Resistance (m^2.K/W)	0.67	0.001	5.715	3.126	2.86	0.151	1.116

Table 3- 5: Thickness and thermal conductivity of different materials used in different layers of construction materials

Name	Concrete Block: Medium Mass Aggregate: 2 or 3 cores	Metal Siding	Galvanized Steel	Polyurethane foam low-density open cell	Polyurethane foam medium density closed cell	Rock wool board	Glass Fibre	PC 10 mm	Polythene	PC 6 mm	Polyester	Air	Soil
Thickness (m)	0.3	0.0015	0.05	0.09	0.04	0.1	0.051	0.01	0.0001	0.006	0.012	0.002	0.2
Thermal Conductivity (W/m. K)	1.13	44.96	50	0.04	0.025	0.035	0.048	0.19	0.33	0.19	0.45	0.03	0.3

3.2.3.2.2. Production layer

PFs with a height of 7.7 meters and 9.7 meters have 3 and 5 production layers, respectively and that for the CGs and CSGs is just one. The area of each production layer is 252 m^2.

3.2.3.2.3. Lighting

In this study, CGs have been illuminated completely with natural light. A lighting period of 16 hours has been considered for both CSGs and PFs cases. In CSGs, artificial lights have been used between 4:00 and 20:00, before sunrise and after sunset. In PFs, only artificial lights have been scheduled to turn off from 09:00 to 17:00 and are on during the rest of the day.

3.2.3.2.4. HVAC equipment

The only contribution of the total energy demand in GCs is heating during the cold periods of the year and cooling during the warm periods of the year. Both are considered when the heat management through layers and insulation covers are insufficient. In CSGs and PFs energy demand is related to both lighting systems as well as heating and cooling systems.

To cope with heating and cooling loads, an ideal HVAC system has been defined for the model using “HVACTemplate:Thermostat” and “HVACTemplate:Zone:IdealLoadsAirSystem” objects of EnergyPlus™. This HVAC system can provide the plant comfort limit temperature setpoints. Typical setpoints for HVAC in different greenhouses facilities vary (Jans-Singh *et al*. 2021). In this study, cooling is activated if internal temperatures surpass 27℃ for one scenario. Also, a heating setpoint of 16℃ was considered. The setpoints work for most of the vegetables including tomato, cucumber, eggplant, green bean, melon, and pepper (Mostafavi & Rezaei 2019). HVAC-required energy depends on how much the temperature of the greenhouse deviates from the plant comfort limit (Baglivo *et al*. 2020).

3.2.4. Economic analysis

A brief cost analysis has been done in this study. The initial cost of greenhouse construction and energy cost for one year have been calculated for each case. The profit from selling greenhouse production for one year has been considered and subtracted from the sum of the initial cost and energy cost to find the net total cost of the first year of operation:

$$Net\ total\ cost = Initial\ Cost + Energy\ Cost - Profit\ of\ Selling\ productions \quad (3\text{-}7)$$

Prices related to construction materials are based on market prices on January 2022 and includes all materials, labour to install, transportation, and equipment costs (Rsmeans 2022). In this study, natural gas has been considered to provide heating and cooling demands. Lighting equipment uses electricity.

It has been assumed that half of the cultivated area is planted with tomatoes and the other half with sweet bell peppers with 6 plants in one square metre while they are being replanted annually. The target yield for tomato is 55 kg/m^2 and for sweet bell pepper is 23 kg/m^2 (Statistics Canada). The production cycle for both vegetables has been considered for one year. Table 3-6 demonstrates the prices for different components considered in economic analysis.

Table 3- 6: Price list for different items used in economic analysis

Component Name	Price in $	Component Name	Price in $
PF-CSG Façade (Concrete spray foam)	415 per m^2	Natural Gas	4.26 per GJ
CG Wall	16 per m	Electricity	0.30 per kWh
PF-CSG Façade (Sandwich Panel)	370 per m^2	Tomato plant	2.5 per each
PF-CSG Roof	40 per m^2	Sweet Bell plant	4.75 per each
CG-CSG Covering material	42 per m^2	Tomato	4.87 per Kg
Heating Blanket	80 per m^2	Sweet Bell Pepper	9.39 per Kg

3.3. Results and discussion

3.3.1. Model validation – Comparison of measured data with predicated data

Figures 3-5(a) and 3-5(b) show the simulation result and measured data on the variation of the inside and outside air temperature of the experimental greenhouse located in Olds, Alberta, obtained on the 5th to 10th of February (winter duration) and 25th to 30th of July (summer duration).

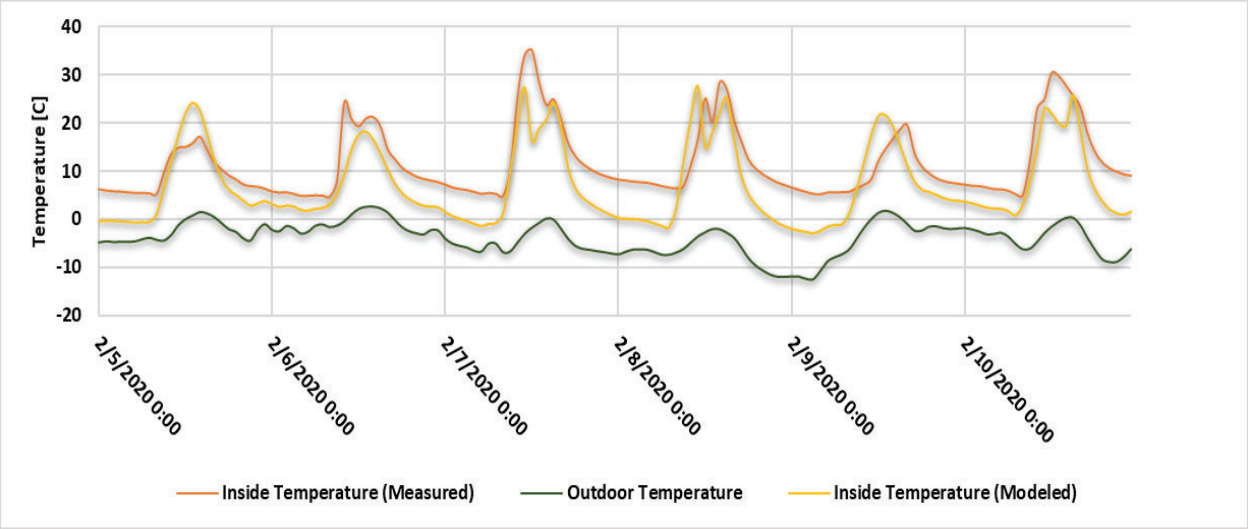

(a)

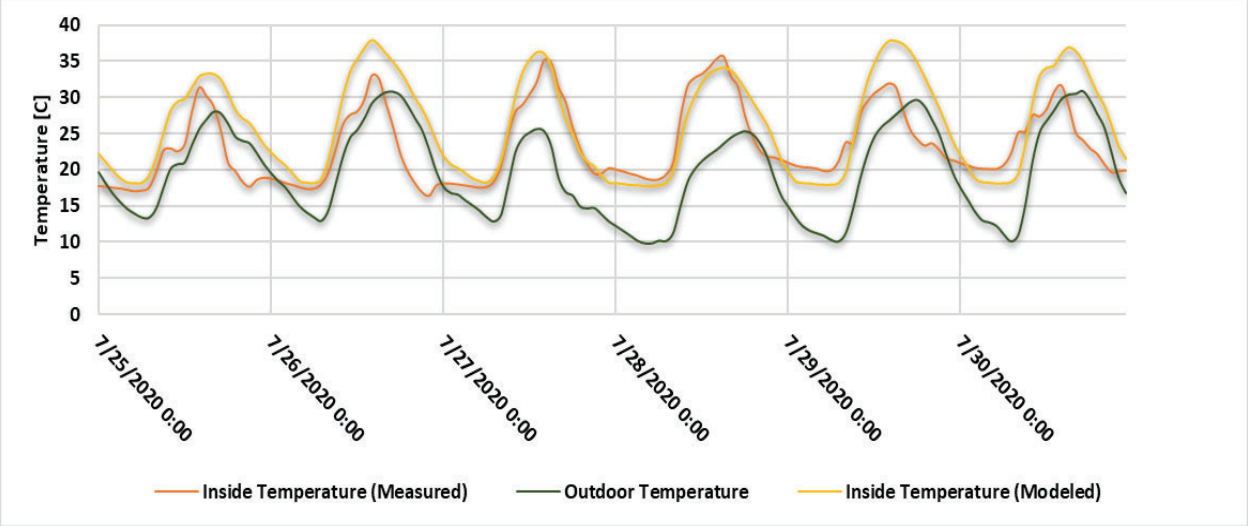

(b)

Figure 3- 5: Comparison of simulation results and measured data of the inside and outside air temperature of the experimental greenhouse located in Olds. (a) Winter duration between the 5th and the 10th of February; (b) Summer duration between the 25th and the 30th of July

The trend of the indoor air temperature is similar in both simulated and real data. In the winter period, the simulated data is mostly below the measured data while it is the opposite in the summer period.

Both heating blanket and natural ventilation are controlled manually in the experimental greenhouse. This can be the main reason for the difference between measured and predicted data. Also, finding the accurate thermal conductivity of construction materials is impossible and that can be the other reason for this difference. Overall, the comparison results demonstrate a reasonable prediction of the indoor environment's average temperature of the greenhouse using EnergyPlus™.

3.3.2. General comparison of base models

The annual solar radiation and outside air dry bulb temperature variation curves in the proposed greenhouse location is shown in Figures 3-6.

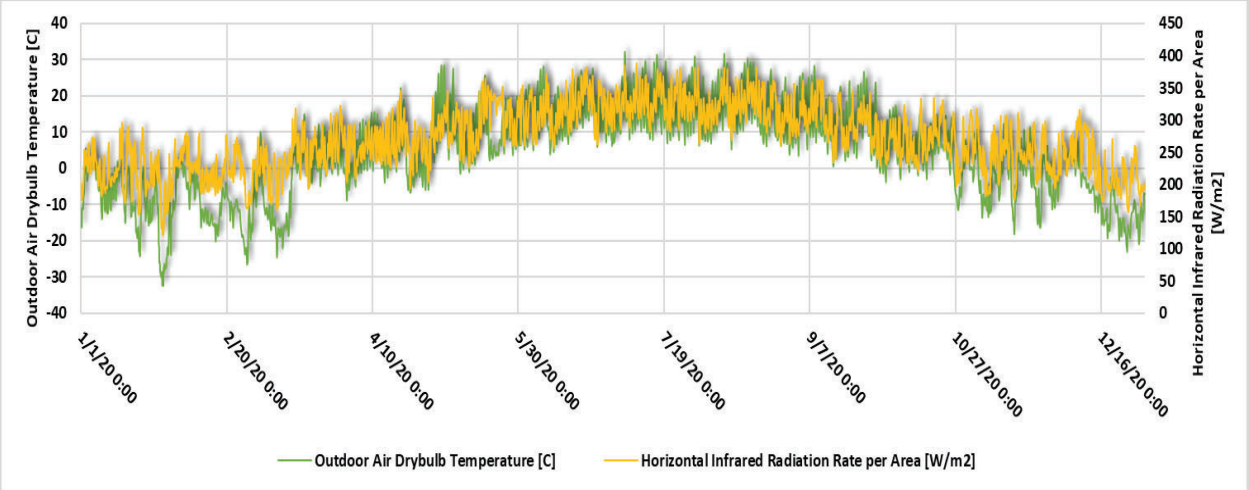

Figure 3- 6: The case study location annual solar radiation [W/m2] and outside air drybulb temperature [°C]

The annual average temperature of the base models indoor environment can be seen in Figures 3-7(a) to 3-7(e). The cooling and heating setpoints defined for the models can be seen in this figure as well.

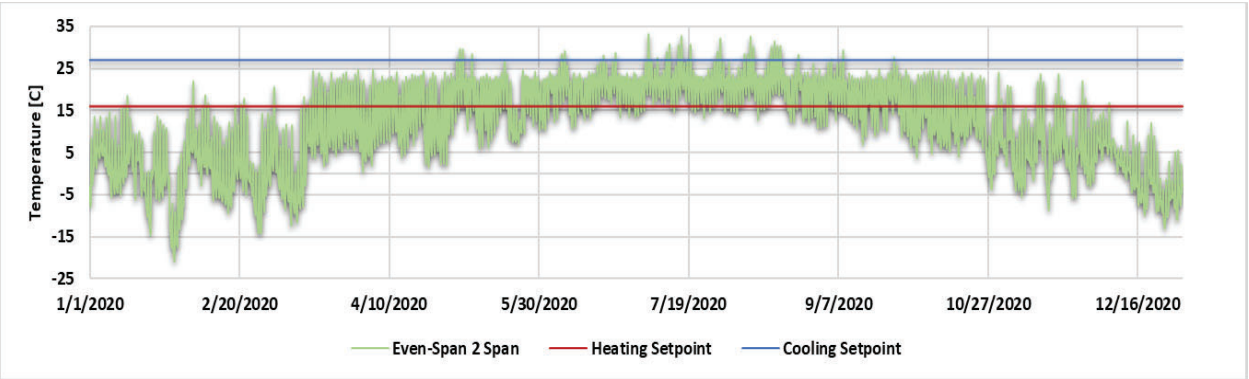
35
25
15
5
-5
-15
-25
Temperature [C]
1/1/2020
2/20/2020
4/10/2020
5/30/2020
7/19/2020
9/7/2020
10/27/2020
12/16/2020
Even-Span 2 Span
Heating Setpoint
Cooling Setpoint

(a)

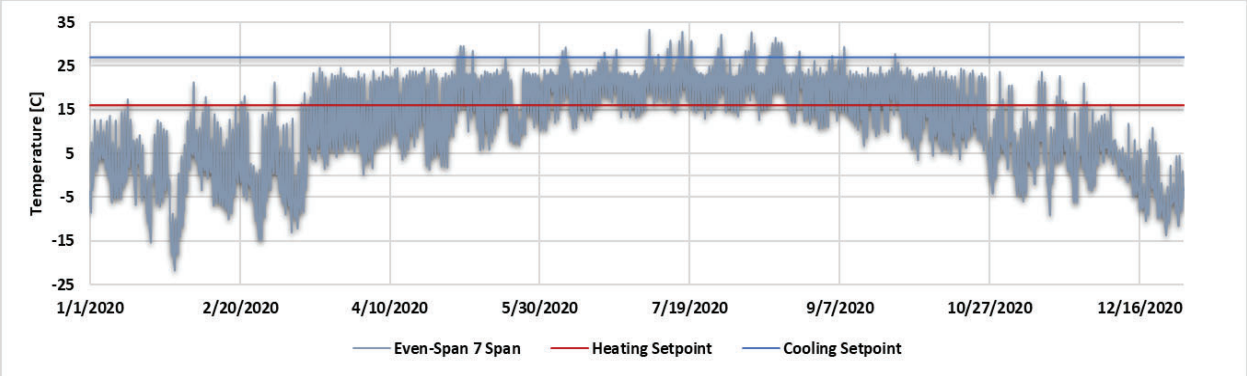
35
25
15
5
-5
-15
-25
Temperature [C]
1/1/2020
2/20/2020
4/10/2020
5/30/2020
7/19/2020
9/7/2020
10/27/2020
12/16/2020
Even-Span 7 Span
Heating Setpoint
Cooling Setpoint

(b)

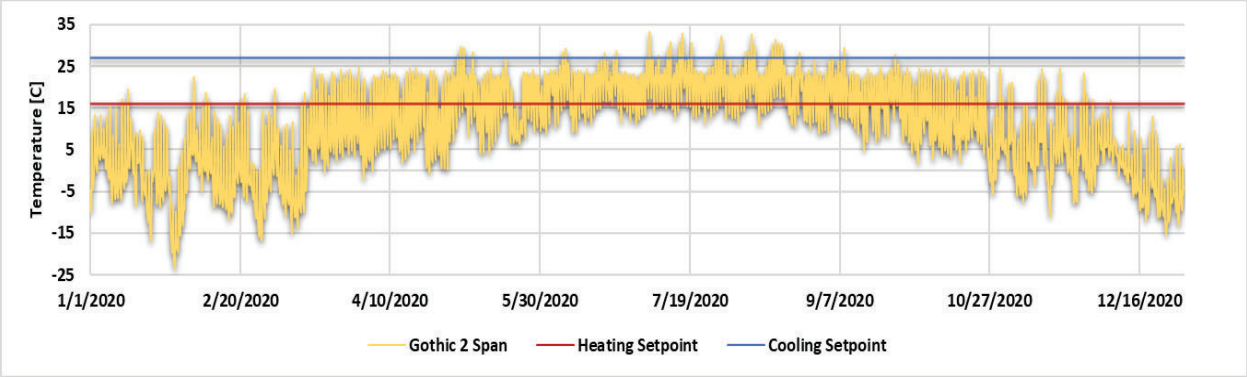
35
25
15
5
-5
-15
-25
Temperature [C]
1/1/2020
2/20/2020
4/10/2020
5/30/2020
7/19/2020
9/7/2020
10/27/2020
12/16/2020
Gothic 2 Span
Heating Setpoint
Cooling Setpoint

(c)

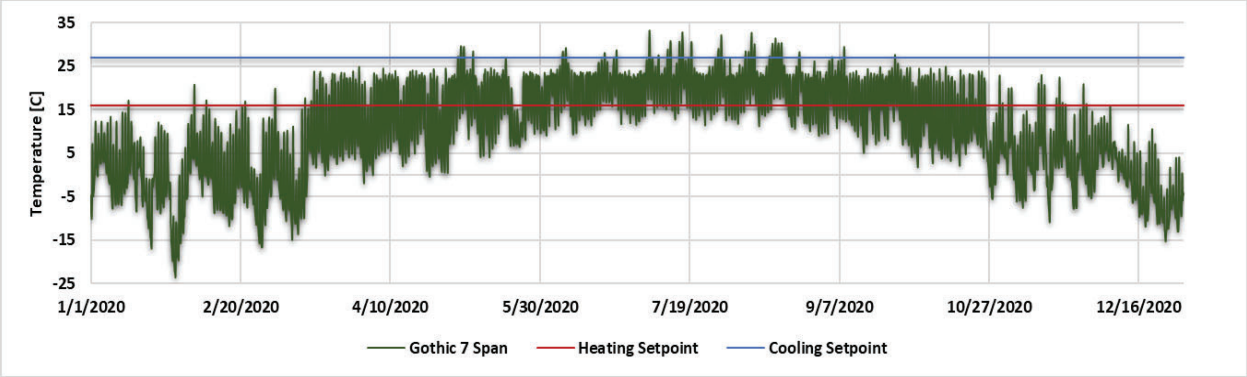
35
25
15
5
-5
-15
-25
Temperature [C]
1/1/2020
2/20/2020
4/10/2020
5/30/2020
7/19/2020
9/7/2020
10/27/2020
12/16/2020
Gothic 7 Span
Heating Setpoint
Cooling Setpoint

(d)

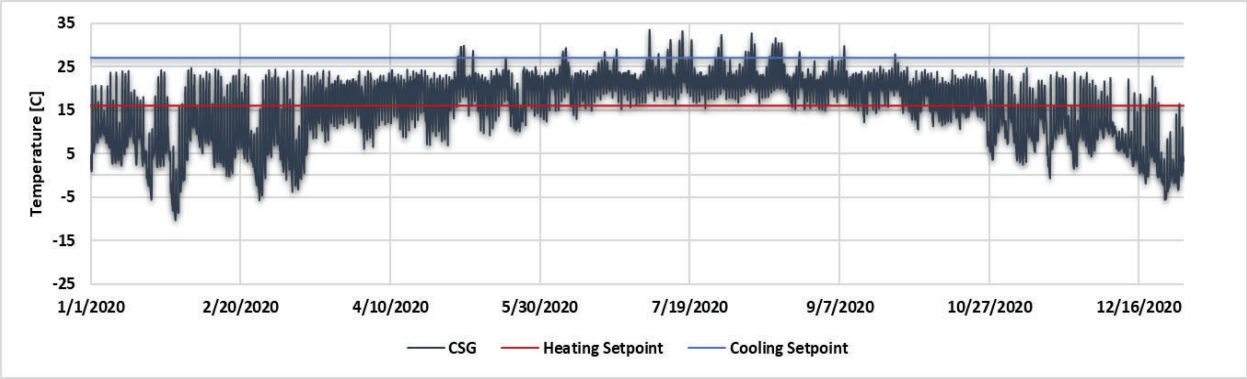

(e)

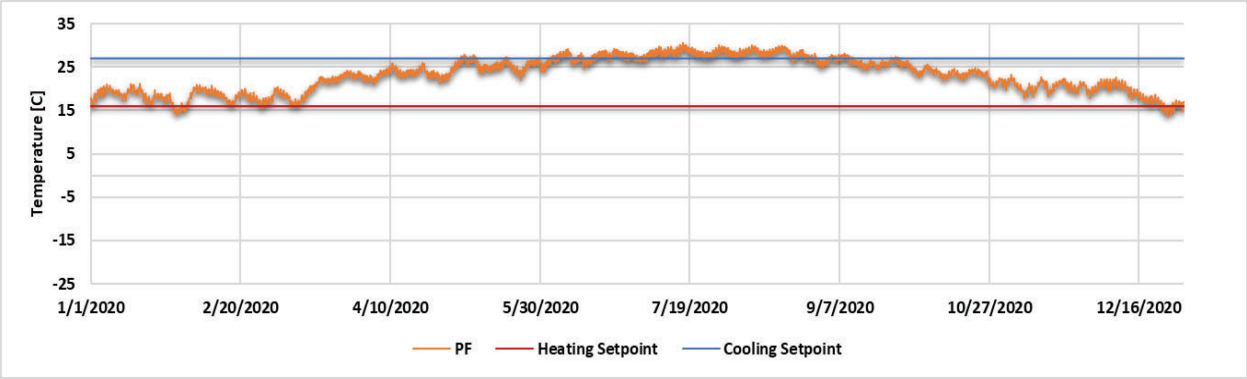

(f)

Figure 3- 7: The annual average temperature [°C] of the base models indoor environment and heating and cooling setpoints, which are 16°C and 27°C, respectively

Temperature is below the desired temperature during winter in CGs and CSG base models. During summer, the temperature for these models is mostly within the desired temperature range but there are some hours in which the temperature is out of range. The temperature exceeded the desired temperature during summer in PF's base model. Although PF's temperature is mostly within the range during the winter, there are a few days the temperature goes below 16°C.

As expected, for crops to survive in this location, both heating and cooling loads are required inside the greenhouse facilities. This energy demand has been defined to better evaluate the thermal performance of different proposed scenario cases. Figure 3-8 demonstrates the base models' cooling, heating, and artificial lighting electricity annual load simulated using

EnergyPlus™. The total annual energy demand is obtained by the sum of every heating/cooling rate for every time step defined for the model in the simulation period.

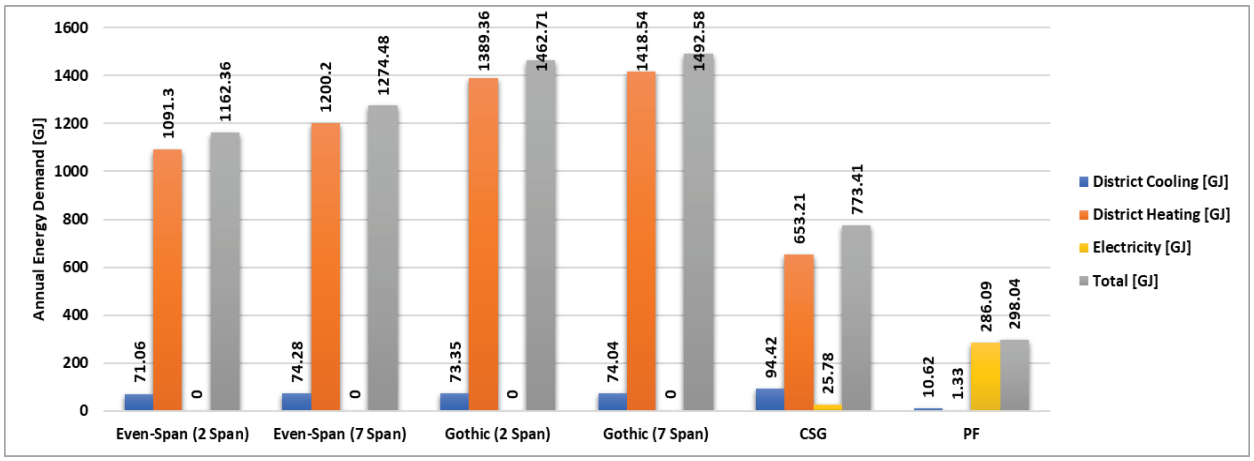

Figure 3- 8: Cooling, heating, and artificial lighting electricity annual load of the Conventional Greenhouse (CG) in different scenarios, Chinese Style Greenhouse (CSG), and Plant Factory (PF)

The maximum cooling load is for CSG, and it is 94.42 GJ. The maximum heating load is for the Gothic greenhouse with 5 spans, and it is 1418.54 GJ. Natural ventilation through the south side of the facility is not enough and it can cause a higher cooling energy demand in comparison to other base models.

CGs' energy consumption (in all four different shapes) in comparison to CSG clearly shows the positive impact of existing an insulated wall on the north, east, and west sides of this type of greenhouse facility regarding the heating demand (Figure 3-8).

The minimum heating load is related to PF which is 1.33 GJ. The minimum cooling load is for PF as well and it is 10.62 GJ (Figure 3-8). Obviously, being totally insulated has caused a lower cooling and heating load in PF. Although, plant evapotranspiration can be the main reason for the cooling load being less than the other base models. As mentioned before, the cultivated area in the PF base model is three times more than the other base models.

The other energy demand is related to artificial lighting energy consumption (Figure 3-8). Electricity load related to PF's lighting is around 11 times more than CSG as it uses the sunlight

and lights are turning on just before sunrise and after sunset between 4 am to 8 pm. No lighting system has been defined for CGs and the lighting energy usage is zero. Figure 3-8 clearly demonstrates that PF is more energy efficient than the other greenhouse facilities followed by CSG as the second most energy-efficient facility.

3.3.3. Comparison of models with different height

The energy consumption of each base model (7.7 meters in height) has been compared with a similar case with a greater height (9.7 meters in height) in Figures 3-9(a) and 3-9(b). As could be expected, more energy is needed to heat the greenhouse with greater height in all cases except in PF's models. This can be the result of gaining extra heat by using more artificial lighting in five layers of the cultivated area instead of three layers. Subsequently, this causes a higher difference between the cooling loads of two PF cases with different heights and lighting system electricity usage.

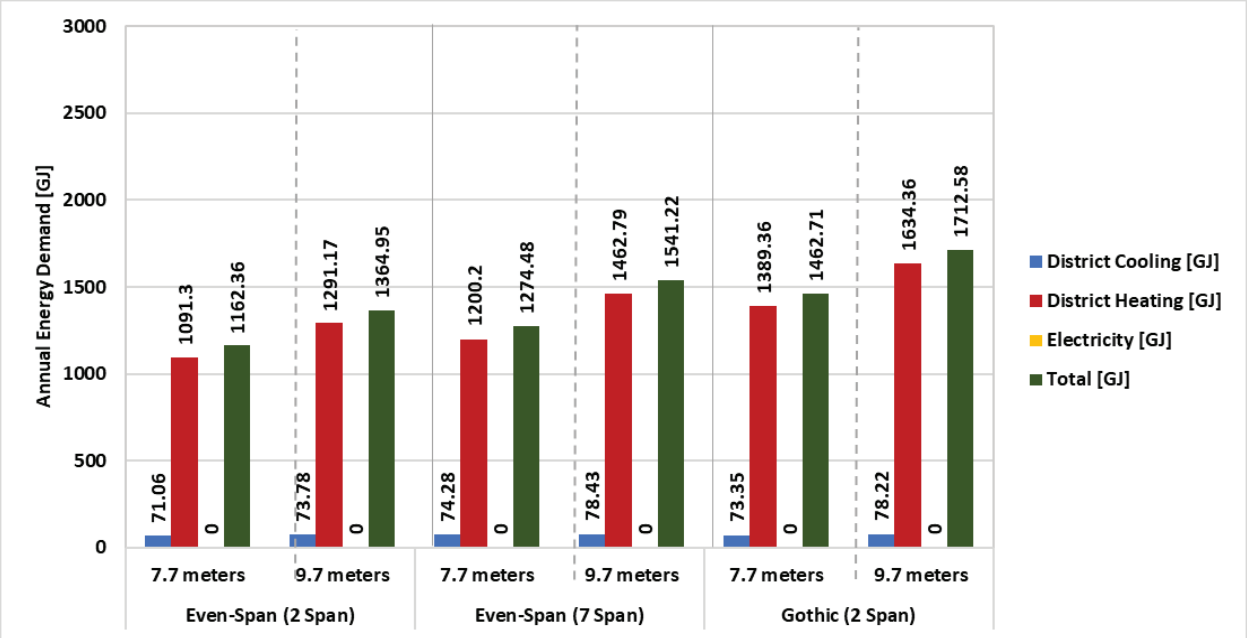

(a)

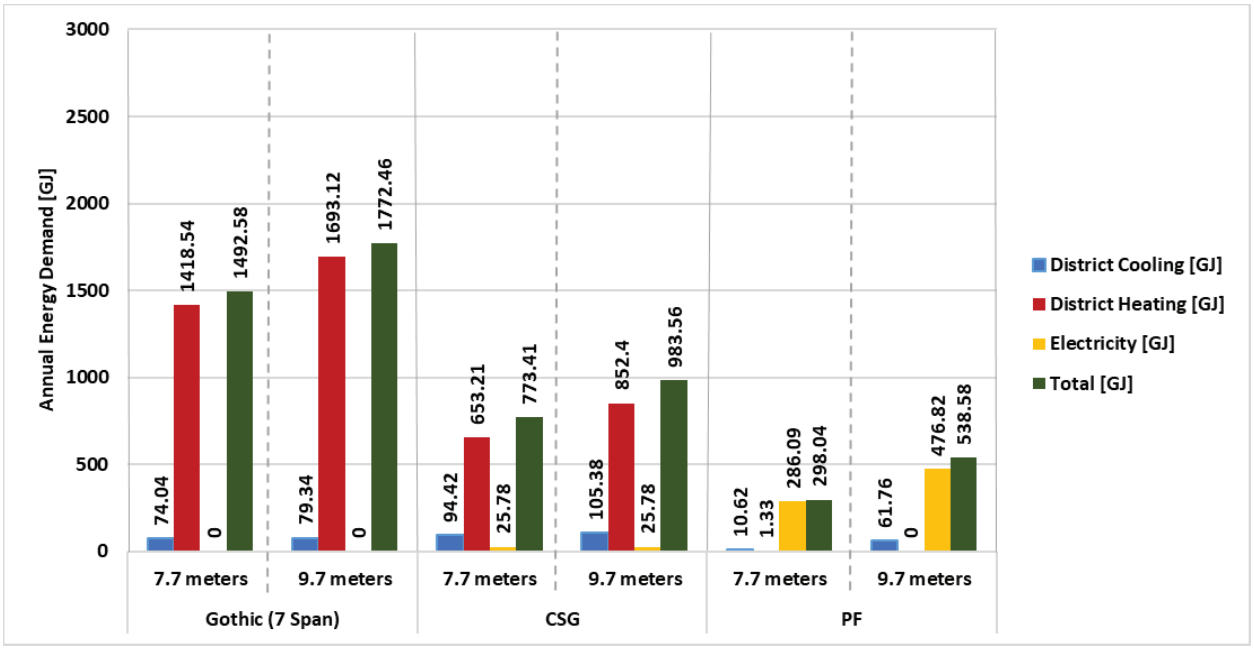

(b)

Figure 3- 9: Comparison of the energy consumption of each base model (7.7 meters in height) with a similar case with a greater height (9.7 meters in height)

3.3.4. Comparison of models with different construction materials

In Figure 3-10, the energy demand of CSG and PF base models using sandwich panels as opaque wall construction material has been compared with similar cases using spray foam-concrete as opaque wall construction material.

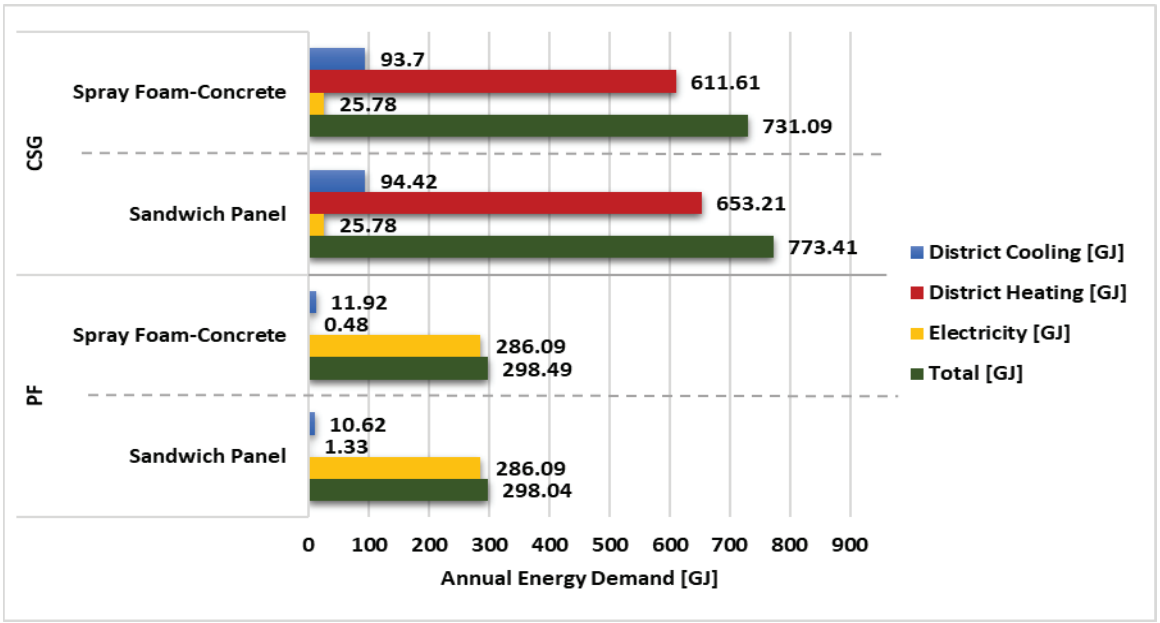

Figure 3- 10: The effect of using Sandwich Panels and Spray Foam-Concrete on the energy consumption of CSGs and PFs

As can be observed, there is not a big difference between heating and cooling loads between each of the construction materials for each of the facility cases. This is because the thermal roughness of these two construction materials is almost the same. The lighting energy demand is not being affected by changing opaque wall construction material.

3.3.5. Comparison of models considering economic aspects

The price of construction materials, artificial lighting equipment, annual electricity/ natural gas usage, the annual total cost of each defined case, and profit from selling greenhouse yield in this study can be seen in Table 3-7.

The minimum total cost is $28,932 per year for Even-Span with 2 spans and 7.7 metres in height. The maximum net total cost is $121,939 per year for Plant Factory constructed with Spray Foam-Concrete and 9.7 metres in height. This difference is related to both the electricity usage of lighting equipment and the upfront cost of the plant factories.

Although the upfront cost of a plant factory is around 2.5 times more than Even-Span, this greenhouse saves money by not requiring energy to provide heat. The annual costs for plant factory cases are more than for the other cases. Without considering the amount of production, plant factories are the least economic options. However, the profit of plant factories can make up for the higher annual cost and energy when there is vertical production in them. The highest projected profit is $192,472 which is for a plant factory with 9.7 metres in height, sandwich panel as construction material, and 5 cultivated layers.

Table 3- 7: Comparison of the annual net total cost of all 16 defined cases

		Transparent Wall ($)	Opaque Wall ($)	Transparent Roof ($)	Opaque Roof ($)	Heating Blankets ($)	Lighting Equipment ($)	Upfront Cost ($)	Annual Mortgage Cost ($/yr.)[a]	Heating Load ($/yr.)	Cooling Load ($/yr.)	Lighting Electricity ($/yr.)	Tomato & Sweet Bell Pepper cost ($/yr.)	Annual Cost (&/yr.)	Projected Production ($/yr.)	Projected Profit ($/yr.)
Conventional Greenhouses (CGs)	Base Model Case 1	31,295	9,722	37,393	7,264	130,835		216,509	18,499	4,649	303	0		28,932		32,029
	Case 1	42,608	9,926	37,393	7,264	152,384		249,576	21,324	5,500	314	0		32,620		28,341
	Base Model Case 2	34,516	11,578	37,215	8,624	136,631		228,564	19,529	5,113	316	0		30,439		30,522
	Case 2	45,722	12,602	37,215	8,624	157,975	0	262,138	22,397	6,231	334	0		34,444		26,517
	Base Model Case 3	31,613	56,237	28,439	81,056	114,386		311,732	26,634	5,919	312	0		38,346		22,615
	Case 3	42,903	73,421	28,439	81,056	135,890		361,710	30,904	6,962	333	0	5,481	43,681	60,961	17,280
	Base Model Case 4	35,631	25,885	28,304	82,090	121,780		293,689	25,093	6,043	315	0		36,932		24,029
	Case 4	46,836	31,709	28,304	82,090	143,124		332,063	28,371	7,213	338	0		41,403		19,558
Chinese Style Greenhouses (CSGs)	Base Model Case 5	0	165,257	32,873	42,810	62,614	12,600	316,153	27,012	2,783	402	2,149		37,827		23,134
	Case 5		251,763	35,620	42,134	67,847		409,964	35,027	2,605	399	2,149		45,661		15,300
	Case 6		185,356	32,873	42,810	62,614		336,252	28,729	3,631	449	2,149		40,439		20,522
	Case 7		282,383	35,620	42,134	67,847		440,584	37,643	3,535	436	2,149		49,244		11,717
Plant Factories (PFs)	Base Model Case 6	0	384,615	0	31,500	0	37,800	453,915	38,782	6	45	23,841	16,443	79,117	182,884	103,767
	Case 8		484,515		31,500			553,815	47,318	2	51	23,841		87,655		95,229
	Case 9		431,393		31,500		63,000	525,893	44,932	0	263	39,735	27,405	112,335	304,807	192,472
	Case 10		543,443		31,500			637,943	54,506	0	293	39,735		121,939		182,868

[a] This mortgage payment has been calculated with a 5% interest rate and amortization period of 20 years.

3.4. Conclusion

This study compares the thermal performance and energy consumption of three greenhouse facilities including Conventional Greenhouses (CGs), Chinese Style Greenhouses (CSGs), and Plant Factories (PFs). Different cases have been defined for each facility to better evaluate the effect of shape, height, and construction materials. An economic analysis has also been done to determine the approximate cost of each case total cost and compare the cases considering economic aspects. It was assumed that the greenhouses are under production status throughout the year.

The results of the study can be summarised as follows:

- As it has been assumed that the greenhouse has production all year round and the temperature is kept between 16℃ and 27℃, there are annual heating and cooling loads in all cases.
- Considering an ideal HVAC system, the highest amount of heating and cooling loads is for CGs. This can be the result of using a transparent construction material with low thermal resistance.
- The lowest heating and cooling energy consumption is for PFs. This is mainly the result of insulated walls and ceilings as well as being fully enclosed (no infiltration). In reality, it is impossible to build a building with 0 infiltration rate but 0 infiltration rate was an assumption used in this study to better understand the effect of infiltration on thermal load.
- The highest usage of electricity for lighting purposes can be seen in PFs. This is obviously the result of using artificial lighting as the only source of light for production.
- The impact of greater height is the same in all cases except in PFs. Higher greenhouse facilities have higher cooling and heating demand. As there are more cultivated layers in

taller PFs, the heating energy coming from lighting equipment decreases the heating loads and increases cooling loads approximately four times more in comparison to the increase in the other cases.

- Using sandwich panels and spray foam-concrete as opaque walls' construction materials results in approximately the same amount of energy loads in PFs and CSGs.
- The upfront cost to build the most expensive PF is around 2.5 times more than the cheapest case of CG facilities. There is a better quantity and quality of yield, though, from PF facilities, especially when plants are growing in several vertical layers. If not grown this way, the huge electricity usage for lighting purposes and the upfront costs of construction makes PFs the least economical greenhouse facility to operate one.
- According to the assumptions and related results of this study, PFs, CSGs, and CGs are the most energy-efficient facilities for the location of this study, respectively. However, some cases of CGs are more economical than CSGs. The upfront cost is higher in CSGs in comparison to CGs but by considering a cheaper construction material that has a similar thermal resistance to what is considered in this study, CSGs can be made both economical and energy-efficient.
- The quality and quantity of yield is dependent on the amount of sunlight during the year. It is suggested that some artificial lighting be provided in CGs to prevent any production problems when sunlight is not sufficient during the year, although this will increase the annual cost of CGs.
- Consideration of the effects of other environment-controlling equipment and greenhouse facility frames on energy demand and the final total cost was out of the scope of this study. For a more accurate comparison, these should be taken into account in future studies.

References

Ahamed, M. S., Guo, H., & Tanino, K. (2018). Energy-efficient design of greenhouse for Canadian Prairies using a heating simulation model. *International Journal of Energy Research, 42*(6), 2263-2272. doi:10.1002/er.4019

Ahamed, M. S., Guo, H., & Tanino, K. (2019). Energy saving techniques for reducing the heating cost of conventional greenhouses. *Biosystems Engineering, 178*, 9-33. doi:10.1016/j.biosystemseng.2018.10.017

Ahamed, M. S., Guo, H., & Tanino, K. (2020). Modeling heating demands in a Chinese-style solar greenhouse using the transient building energy simulation model TRNSYS. *Journal of Building Engineering, 29*. doi:10.1016/j.jobe.2019.101114.

Al Ka'bi, & A. H. (2020). Comparison of energy simulation applications used in green building. *Annals of Telecommunications, 75*(7-8): 271-90. doi:https://doi.org/10.1007/s12243-020-00771-6

Alinejad, T., Yaghoubi, M., & Vadiee, A. (2020). Thermo-environomic assessment of an integrated greenhouse with an adjustable solar photovoltaic blind system. *Renewable Energy, 156*, 1-13. doi:https://doi.org/10.1016/j.renene.2020.04.070

Allen, R.G., Pereira, L.S., Raes, D., & Smith, M. (1998). Crop evapotranspiration-Guidelines for computing crop water requirements. *FAO Irrigation and Drainage paper 56*. Fao, Rome, 300(9).

Arenghi, A., Perra, C., & Caffi, M. (2021). Simulating and comparing different vertical greenery systems grouped into categories using EnergyPlus. *Applied Sciences, 11*(11). doi:10.3390/app11114802

Azhar, Salman, Brown, Justin, and Farooqui, Rizwan. (2009). BIM-Based sustainability analysis: An evaluation of building performance analysis software.

Baglivo, C., Mazzeo, D., Panico, S., Bonuso, S., Matera, N., Congedo, P. M., & Oliveti, G. (2020). Complete greenhouse dynamic simulation tool to assess the crop thermal well-being and energy needs. *Applied Thermal Engineering, 179*. doi:10.1016/j.applthermaleng.2020.115698.

Belkadi, A., Mezghani, D., & Mami, A. (2019). Energy design and optimization of a greenhouse: A heating, cooling and lighting study. *Engineering, Technology & Applied Science Research, 9*(3), 4235-4242. doi: 10.5281/zenodo.3249139.

Brandon, M. F., Kozai, T., Yamaguchi, T., Takagaki, M., Maruo, T., & Yamori, W. (2016). *Next revolution of Agriculture: A review of innovations in plant factories*. (3rd) edited by CRC press. pp. 18.

Çakır, U., & Şahin, E. (2015). Using solar greenhouses in cold climates and evaluating optimum type according to sizing, position and location: A case study. *Computers and Electronics in Agriculture, 117*, 245-257. doi:10.1016/j.compag.2015.08.005

Chaysaz, A., Seyedi, S. R. M., & Motevali, A. (2019). Effects of different greenhouse coverings on energy parameters of a photovoltaic–thermal solar system. *Solar Energy, 194*, 519-529. doi:10.1016/j.solener.2019.11.003

Chen, C., Li, Y., Li, N., Wei, S., Yang, F., Ling, H., . . . Han, F. (2018). A computational model to determine the optimal orientation for solar greenhouses located at different latitudes in China. *Solar Energy, 165*, 19-26. doi:10.1016/j.solener.2018.02.022

Choab, N., Allouhi, A., El Maakoul, A., Kousksou, T., Saadeddine, S., & Jamil, A. (2019). Review on greenhouse microclimate and application: Design parameters, thermal modeling and simulation, climate controlling technologies. *Solar Energy, 191*, 109-137. doi:10.1016/j.solener.2019.08.042.

Crawley, D.B., Lawrie, L.K., Winkelmann, F.C., Buhl, W.F., Huang, Y.J., Pedersen, C.O., Strand, R.K., et al. (2001). EnergyPlus: Creating a new-generation building energy simulation program. *Energy and Buildings* 33(4): 319-31. doi:https://doi.org/https://doi.org/10.1016/S0378-7788(00)00114-6. doi: https://www.sciencedirect.com/science/article/pii/S0378778800001146.

Deiana, A., Fabrizio, E., & Gerboni, R. (2014). *Energy performance optimization of typical Chinese solar greenhouses by means of dynamic simulation*. International Conference of Agricultural Engineering.

Escamilla-García, A., Soto-Zarazúa, G. M., Toledano-Ayala, M., Rivas-Araiza, E., & Gastélum-Barrios, A. (2020). Applications of artificial neural networks in greenhouse technology and overview for smart agriculture development. *Applied Sciences, 10*(11). doi:10.3390/app10113835

Esmaeli, H., & Roshandel, R. (2020). Optimal design for solar greenhouses based on climate conditions. *Renewable Energy, 145*, 1255-1265. doi:10.1016/j.renene.2019.06.090

Fabrizio, E. (2012). Energy reduction measures in agricultural greenhouses heating: envelope, systems and solar energy collection. *Energy Build. 53*, 57–63

Graamans, L., Baeza, E., van den Dobbelsteen, A., Tsafaras, I., & Stanghellini, C. (2018). Plant factories versus greenhouses: Comparison of resource use efficiency. *Agricultural Systems, 160*, 31-43. doi: https://doi.org/10.1016/j.agsy.2017.11.003

Harbick, K., & Albright, L.D. (2016). Comparison of energy consumption: greenhouses and plant factories. *Acta Horticulture, 1134*, 285–292. DOI: 10.17660/ActaHortic.2016.1134.38

Iddio, E., Wang, L., Thomas, Y., McMorrow, G., & Denzer, A. (2020). Energy efficient operation and modeling for greenhouses: A literature review. *Renewable and Sustainable Energy Reviews, 117*. doi:10.1016/j.rser.2019.109480

Jans-Singh, M., Ward, R., & Choudhary, R. (2021). Co-simulating a greenhouse in a building to quantify co-benefits of different coupled configurations. *Journal of Building Performance Simulation, 14*(3), 247-276. doi:10.1080/19401493.2021.1908426

Karambasti, B. M., Naghashzadegan, M., Ghodrat, M., Ghorbani, G., Simorangkir, R. B. V. B., & Lalbakhsh, A. (2022). Optimal solar greenhouses design using multi-objective genetic algorithm. *IEEE Access, 10*, 73728-73742. doi:10.1109/access.2022.3189348

Kim, Y., Shin, H.-R., Oh, S.-h., & Yu, K.-H. (2022). Analysis on the economic feasibility of a plant factory combined with architectural technology for energy performance improvement. *Agriculture, 12*(5). doi:10.3390/agriculture12050684.

Kumar Singh, V., Tiwari, K. N., & Dt, S. (2016). Estimation of crop coefficient and water requirement of Dutch roses (*Rosa hybrida*) under greenhouse and open field conditions. *Irrigation & Drainage Systems Engineering, 05*(03). doi:10.4172/2168-9768.1000169

Lawrie, L. K., & Crawley, D. B. (2022). Development of global typical meteorological years (TMYx). Doi:http://climate.onebuilding.org

Lebre, B., Silva, P. D., Pires, L. C., & Gaspar, P. D. (2021). Computational modeling of the thermal behavior of a greenhouse. *Applied Sciences, 11*(24). doi:10.3390/app112411816

Liao, L, & Teo, E. A. L. (2018). Organizational change perspective on people management in BIM implementation in building projects. *Journal of Management in Engineering, 34*(3):4018008–4018009.

Linsley, R. K., Kohler, M. K. & Paulhus, J. L. H. (1982). *Hydrology for engineers*, 3d. Ed. Newyork: McGraw-Hill.

Lristinsson, J. (2006). *The energy-producing greenhouse*. The 23rd Conference on Passive and Low Energy Architecture, Geneva, Switzerland.

Ma, J., Du, X., Meng, S., Ding, J., Gu, X., Zhang, Y., . . . Wang, R. (2022). Simulation of thermal performance in a typical Chinese solar greenhouse. *Agronomy, 12*(10). doi:10.3390/agronomy12102255.

Ma, Y., Li, X., Fu, Z., & Zhang, L. (2019). Structural design and thermal performance simulation of shade roof of double-slope greenhouse for mushroom-vegetable cultivation. *International Journal of Agricultural and Biological Engineering, 12*(3), 126-133. doi:10.25165/j.ijabe.20191203.4852.

Mobtaker, H. G., Ajabshirchi, Y., Ranjbar, S. F., & Matloobi, M. (2019). Simulation of thermal performance of solar greenhouse in north-west of Iran: An experimental validation. *Renewable Energy, 135*, 88-97. doi:10.1016/j.renene.2018.10.003v

Mostafavi, S. A., & Rezaei, A. (2019). Energy consumption in greenhouses and selection of an optimized heating system with minimum energy consumption. *Heat Transfer-Asian Research, 48*(7), 3257-3277. doi:10.1002/htj.21540

NREL, EnergyPlus, 2015. https://energyplus.net/.

Ouazzanİ ChahİDİ, L., & Mechaqrane, A. (2021). Energetic and economic analysis for improving greenhouse energy efficiency. *Journal of Energy Systems*. doi:10.30521/jes.950754

Ponce, V. M. (1989*). Engineering Hydrology: Principles and Practices:* Prentice Hall.

Priestley, C. H. B., & Taylor, R. J. (1972). On the assessment of surface heat flux and evaporation using large scale parameters. *Monthly Weather Review, 100*, 81-92.

Shen, Y., Wei, R., & Xu, L. (2018). Energy consumption prediction of a greenhouse and optimization of daily average temperature. *Energies, 11*(1). doi:10.3390/en11010065

Statistics Canada. Table 18-10-0245-01 Monthly average retail prices for selected products. DOI: https://doi.datacite.org/dois/10.25318%2F1810024501-eng

TRNSYS 17 Manual (2017). Volume 5, Multizone building modeling with Type56 and TRNBuild. Solar Energy Laboratory, University of Wisconsin, Madison, WI

Rsmeans. (2022). *Yardsticks for Costing: 62012*: RSMeans.

United Nations Department of Economic and Social Affairs, Population Division. (2022). World Population Prospects 2022: Summary of Results. UN DESA/POP/2022/TR/NO. 3.

Vadiee, A., & Martin, V. (2014). Energy management strategies for commercial greenhouses. *Applied Energy, 114*, 880-888. doi:10.1016/j.apenergy.2013.08.089

Van Beveren, P. J. M., Bontsema, J., Van Straten, G., & Van Henten, E. J. (2015). Minimal heating and cooling in a modern rose greenhouse. *Applied Energy, 137*, 97-109. doi:10.1016/j.apenergy.2014.09.083

Weidner, T., Yang, A., & Hamm, M. W. (2021). Energy optimisation of plant factories and greenhouses for different climatic conditions. *Energy Conversion and Management, 243*. doi:10.1016/j.enconman.2021.114336

Chapter 4: A Feasibility Study on Designing a Hybrid Renewable Energy System to Provide Greenhouse Facility Energy Demand Using EnergyPlus™ and HOMER: A Case Study in South of Alberta, Canada

4.1. Introduction and background

Conventional local food production may not only meet the future's food market needs, but it also cannot provide for today's demand. The greenhouse industry is the fastest-growing agriculture sector worldwide (Manonmani *et al*. 2016) and it represents an effective strategy to meet the growing demand for food (Esmaeili and Roshandel 2020). Greenhouses are widely used across the world to supply fresh vegetables and fruits during the off-season period (Chen *et al.* 2019) by providing favourable climate conditions for crops to protect them from outdoor weather conditions. However, using different systems to provide a well-controlled micro-environment within the greenhouse to obtain good quality and quantity of crop yields can increase the energy demand of this sector and, subsequently, the operational costs (Rasheed *et al*. 2018). In the severe climate conditions of the northern latitudes, using heating systems to achieve the desired temperature conditions inside the greenhouse for optimal crop growth for one year can be the main part of energy consumption. In Canada greenhouses approximately one-fifth to one-third of the total production costs are related to heating (Ahmed *et al*. 2019; Yang *et al.* 2012). Apart from a higher production cost, this can lead to a negative impact on the global environment, especially when energy is sourced from fossil fuels. Finding ways to manage, to save, to produce, and to store energy in the greenhouse sector has gained a lot recent attention (Rasheed *et al*. 2018). Using hybrid renewable energy systems helps to significantly reduce the energy footprint of greenhouses. Accordingly, by predicting the energy consumption in design process of greenhouses, it is possible to design the optimal energy system, which is economically, environmentally, and technically feasible.

Several of the studies listed below have tried to find the best method of providing greenhouses energy demand. Cuce *et al.* (2016) in their outstanding study introduced the possibility of using semi-transparent PV modules as a façade and roof material, seasonal thermal energy storage via vertical ground heat exchangers, and solar-assisted heat pump systems to minimize the cost of cultivation and thus, maximize profits. The result showed up to 80% energy saving can be achieved through appropriate retrofitting of conventional greenhouses. Zhuang *et al*. (2019) have developed a comprehensive mathematical model to propose an energy management scheme for a greenhouse with the integration of renewable energy sources to minimize the cost of greenhouse operations. Vourdoubas (2015) reviewed applications of solar energy, geothermal energy, and biomass (olive kernel wood which is a CO_2-neutral fuel) as renewable energy sources in a commercial flower greenhouse. The result showed lower CO_2 emissions in flower cultivation greenhouse because of using solid biomass for heating and solar-PV cells for electricity generation. By developing a mathematical model, Mirzamohammadi *et al*. (2020) determined an energy supply planning for greenhouses in both micro-grid and grid-connected modes using mathematical programming and optimized the exploitation of renewable energy units along with energy storage units. Ronay and Dumitru (2015) demonstrated the advantages of a renewable energy-based hydroponic tomato greenhouse instead of a conventional greenhouse, which uses grid power and conventional gas heating systems. The result showed how using this kind of technologies can contribute to have self-sustained and economical greenhouses. Ntinas *et al*. (2020) demonstrated that the establishment of renewable energy systems in a solar collector greenhouse and transferring the excess energy to other buildings can result in sustainable production and optimum growth conditions for greenhouse crops with negative carbon footprint, a potential of financial profit and saving energy, water, and fertilizer as well as CO_2 emissions. They considered cumulative energy demand, carbon footprint, and water

use efficiency as climate change indicators. By developing a mathematical model in Matlab/Simulink platform, Kıyan *et al*. (2013) analyzed the effect of integrating a solar collector heating system (consisting of evacuated tube solar collectors with thermal storage, control, and piping units) as a hybrid solar heating system to a greenhouse which already has a fossil fuel heating system. Results showed that although combining the existing fossil fuel system with the proposed hybrid system requires a slightly longer payback period than expected, it is economically feasible. Furthermore, such integration can lower CO_2 and other harmful greenhouse gas emissions, significantly, which will contribute to the protection of the environment and the preservation of natural resources.

The aim of this study is to optimize a hybrid renewable energy system to provide the energy load of an educational greenhouse located in Southern Alberta which has cold winters and hot summers. Meanwhile, the feasibility of combining this greenhouse crop production with solar and wind electricity generation within the same building will be assessed.

4.1.1. Objectives

The objective of this study is as follows:

- Predicting the annual heating, cooling, and electricity loads of an educational greenhouse located in Old Sun Community College in Siksika First Nation of the Blackfoot Confederacy (east of Calgary, Alberta, Canada) using EnergyPlus™.
- Defining different scenarios of off-grid and on-grid energy systems considering the different combinations of the energy system components including the grid, generator, PV panels, wind turbine, and battery.
- Determining the optimum hybrid renewable energy system by considering economic, technical, and environmental criteria among defined scenarios using HOMER results

- Performing a sensitivity analysis on grid power price and sellback rate for the most optimum hybrid renewable energy system

4.2. Materials and methods

4.2.1. Study area

The educational greenhouse is located in the South of Old Sun Community College (OSCC) in Siksika Indian Reserve, Calgary Region, Alberta, Canada. The location of the Siksika Indian Reserve in Alberta can be seen in Figure 4-1. The potential of using wind turbines and photovoltaic panels according to the amount of solar radiation and wind speed can be seen in this figure as well.

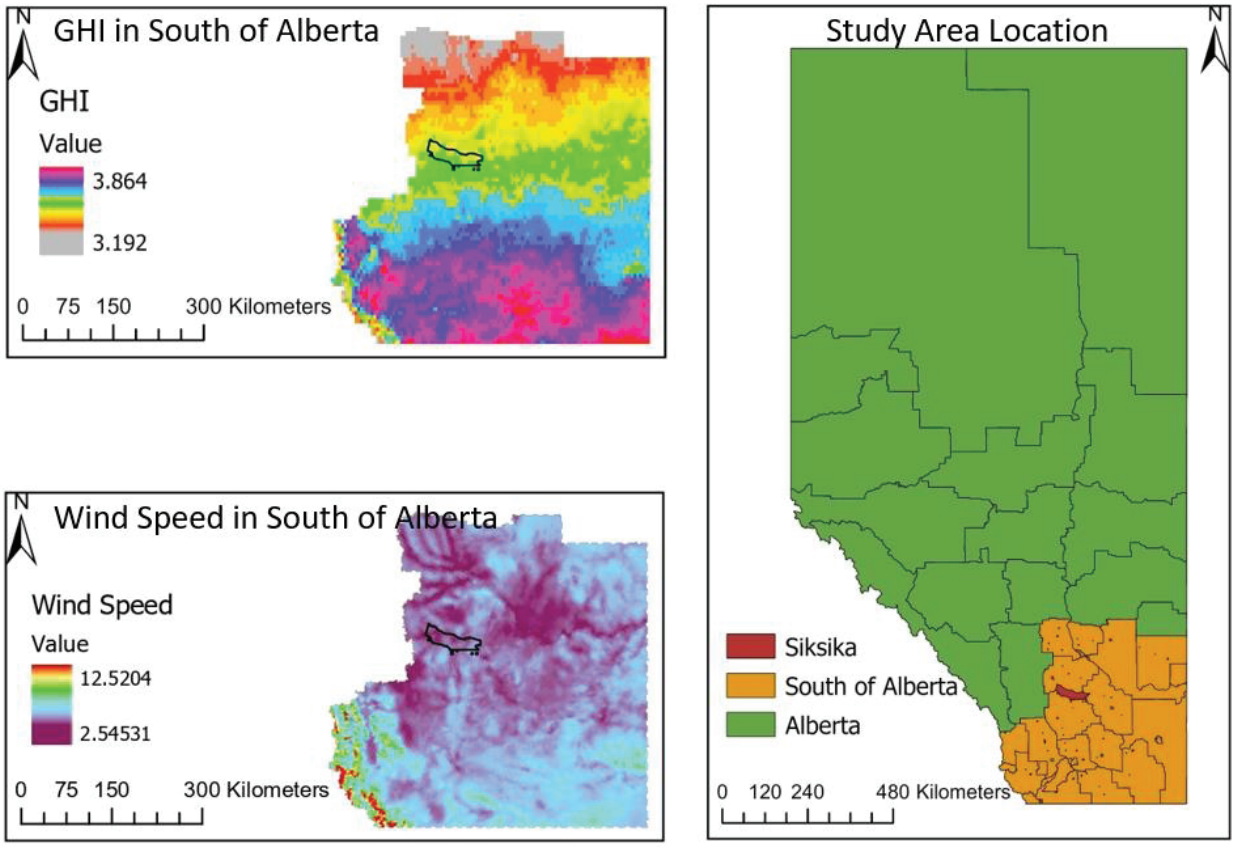

Figure 4- 1: The location of the study area in the South of Alberta and the status of Global Horizontal Irradiance (GHI) (kWh/m^2/day) (Sengupta *et al.* 2018) and wind Speed (m/s) (Draxl *et al.* 2015a and b; King *et al.* 2014; Lieberman-Cribbin *et al.* 2014)

Average monthly wind speed (m/s) at 50 meters above the surface was obtained from NASA's prediction of worldwide energy resource database for 30 years (January 1984 to December 2013) and entered as input data to HOMER. Other input data was monthly average Solar Global Horizontal Irradiance (GHI) (kWh/m^2/day) obtained also from NASA's prediction of worldwide energy resource database for 22 years (July 1983 to June 2005). Figures 4-2 and 4-3 show the profile of wind speed and solar radiation data, respectively.

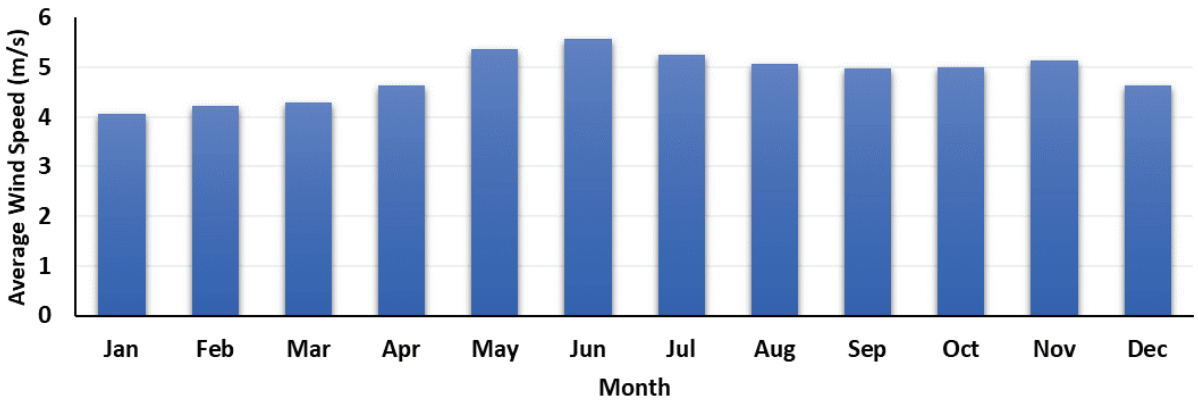

Figure 4- 2: Wind speed data at 50 meters above the surface for the location of the study

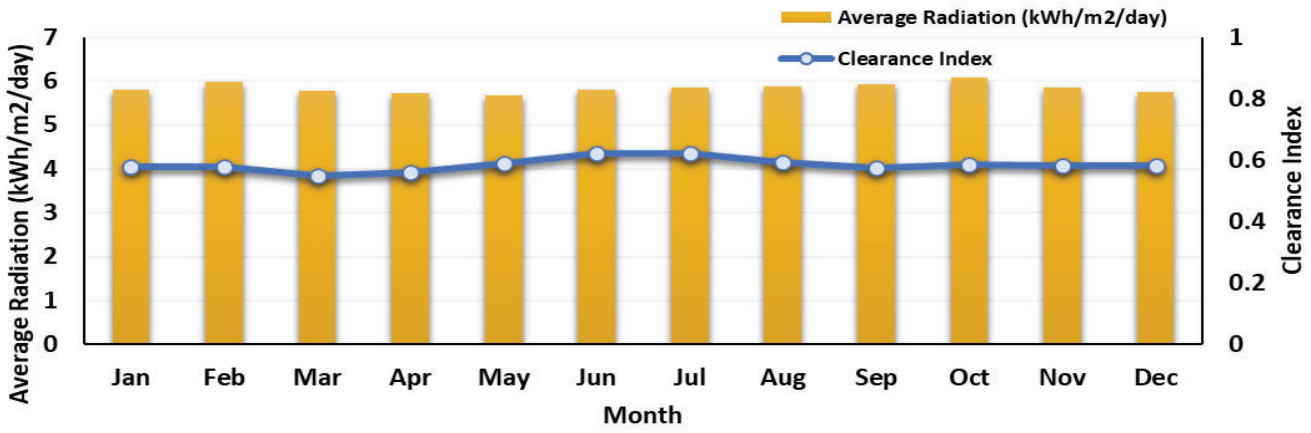

Figure 4- 3: Solar Global Horizontal Irradiance (GHI) and clearance index[1] data for the location of the study

[1] Clearance index is the ratio of the measured global solar radiation at the Earth's surface to the extra-terrestrial solar radiation at the top of the atmosphere and was entered to HOMER Pro as one of the input data.

4.2.2. Greenhouse model's characteristics

Figure 4-4 shows the geometry of the greenhouse considered in this study. Table 4-1 summarizes the greenhouse's geometrical and structural parameters. The greenhouse is a Chinese Style Greenhouse (CSG). The production layer consists of 6 separate rows of growing surfaces located 1.5 metres far from the floor surface and 1 metre far from each other. In total, 252 m^2 of growing area has been considered for this greenhouse. A lighting period of 16 hours has been considered for the greenhouse during the day. Artificial lights are used between 4:00 and 20:00 (before sunrise and after sunset). The heating blanket opens when the indoor temperature goes below 20°C.

It should be noted that the assumptions regarding the Chinese Style Greenhouses characteristics, operation and schedules in this study had to be made to fit into the EnergyPlus™ simulation capabilities.

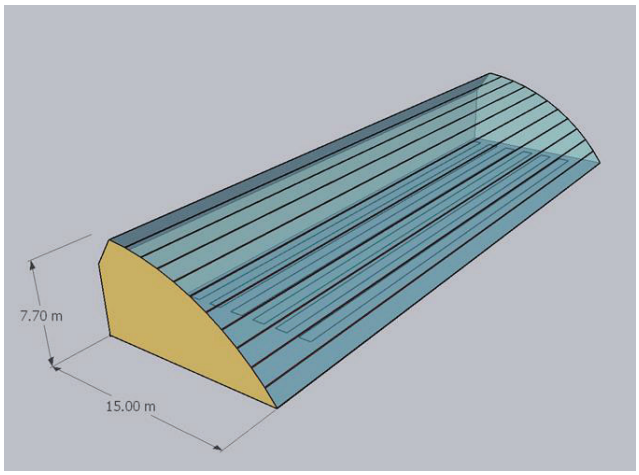

Figure 4- 4: The geometry of the Chinese Style Greenhouse

Table 4- 1: Geometrical and structural properties of the greenhouse

Latitude	50.85
Longitude	-113.06
Width of span (m)	15
Length (m)	52.5
Back Wall Height (m)	7.7
Orientation	East-West
Flooring Material	Soil
Covering material	2 layers of Polycarbonate
North Side wall materials	- **Outside layer:** 8cm of polyurethane foam medium density closed cell - **Middle layer:** 30cm of concrete wall - **Inner layer:** 9cm of Polyurethane foam low-density open cell

4.2.3. Greenhouse load estimation using EnergyPlus™

Energy consumption of the education greenhouse was calculated using EnergyPlus™, a whole building energy simulation software/platform (EnergyPlus 2021). EnergyPlus™ can simulate the heating and cooling load of buildings, the annual dynamic energy consumption, and the system's hourly heating and cooling power (Ma *et al.* 2019; Crawley *et al.* 2001). Energy demand is related to both lighting systems whenever the lights are on as well as heating and cooling systems. An ideal HVAC system has been defined for the greenhouse model to provide the plants' comfort temperature limits.[1] These temperatures for heating and cooling have been considered at 13°C and 27°C, respectively, which is an optimum temperature range for most vegetables (Mostafavi and Rezaei 2019).

Figures 4-5 and 4-6 show the monthly and annual load profiles for the greenhouse, respectively. Greenhouse's average daily energy consumption is 225.33 kWh/day and the peak of the load is 207.87 kW. The annual energy load is 82194 kWh.

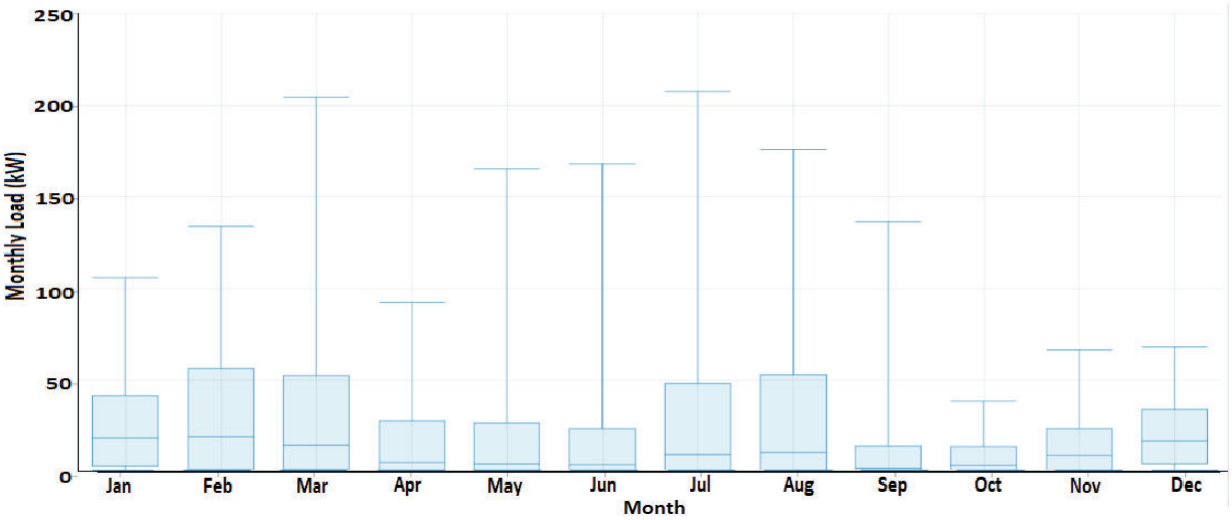

Figure 4- 5: Monthly load graph of the greenhouse

[1] "HVACTemplate:Thermostat" and "HVACTemplate:Zone:IdealLoadsAirSystem" objects of EnergyPlus™ have been used to define an ideal HVAC system.

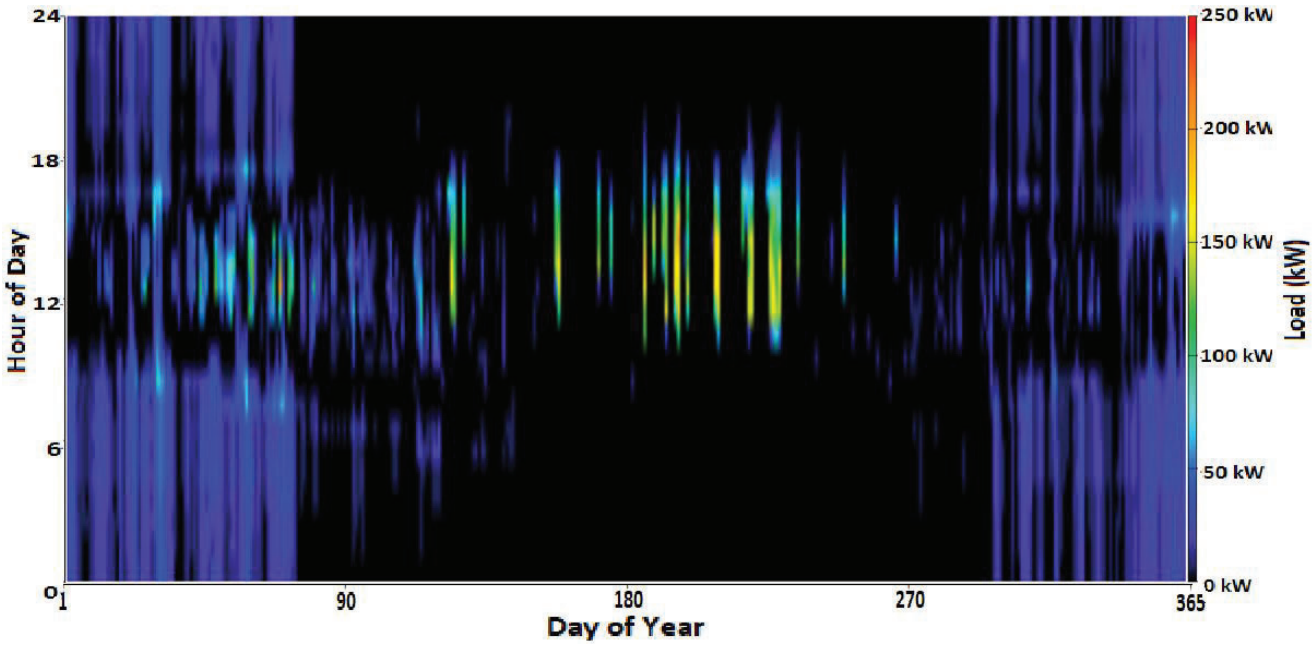

Figure 4- 6: Annual load graph of the greenhouse

4.2.4. Power system design

Hybrid Optimization of Multiple Electric Renewables (HOMER) software developed by the National Renewable Energy Laboratory (NREL) was used in this study to simulate and size the scenario's power systems. Using several possible combinations of input variables, HOMER can optimize the power system (Hoarcă *et al*. 2023). Figure 4-7 demonstrates a general view of the methodology used in this study to find the most optimum power system. The simulation-optimization approach was done for the year 2020. The economic, technical, and environmental criteria considered in this study were 1) providing the greenhouse energy demand; 2) minimizing NPC; 3) minimizing LCOE; 4) minimizing environmental impact.

In this study, different combinations of the power systems' components including grid, generator, PV array, wind turbine, and battery were considered to define scenarios. The schematic of these scenarios and the description of each scenario has been shown in Table 4-2.

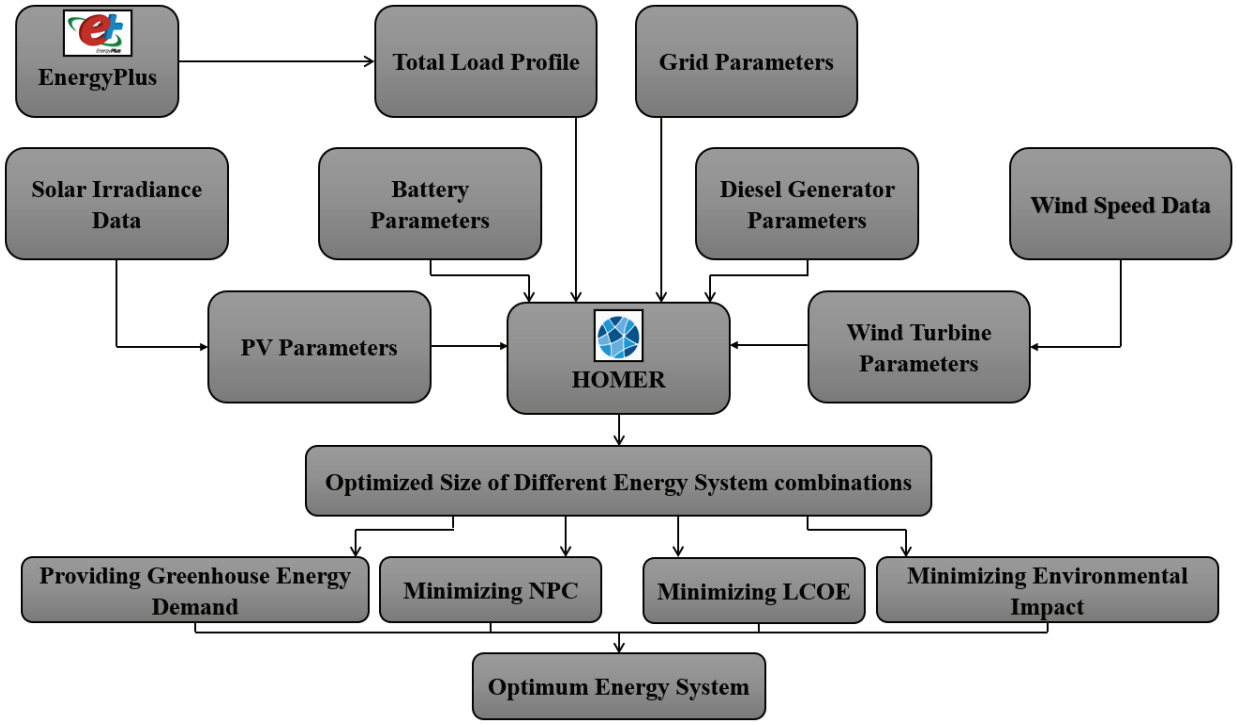

Figure 4- 7: General view of the methodology used in this study

Table 4- 2: Defined scenarios for different combinations of the grid, generator, PV array, wind turbine, and battery

Scenario Number	Schematic	Scenario's Name	Description on scenarios' components
1	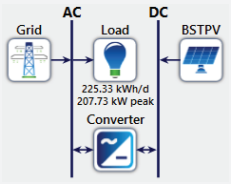	PV-Gr	The components of this scenario include: 1- PV 2- Grid
2	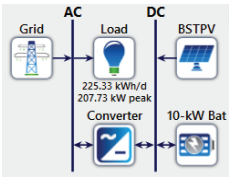	PV-Gr-B	The components of this scenario include: 1- PV 2- Grid 3- Battery
3	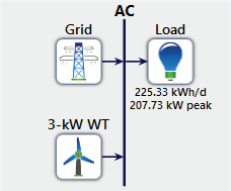	WT-Gr	The components of this scenario include: 1- Wind Turbine 2- Grid
4	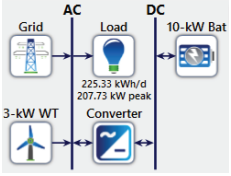	WT-Gr-B	The components of this scenario include: 1- Wind Turbine 2- Grid 3- Battery

5	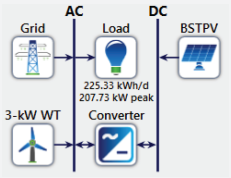	**PV-WT-Gr**	The components of this scenario include: 1- PV 2- Wind Turbine 3- Grid
6	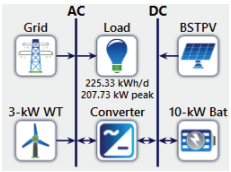	**PV-WT-Gr-B**	The components of this scenario include: 1- PV 2- Wind Turbine 3- Grid 4- Battery
7	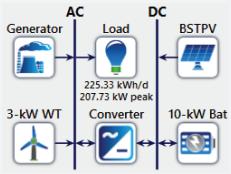	**PV-WT-Ge-B**	The components of this scenario include: 1- PV 2- Wind Turbine 3- Generator 4- Battery

In this study, the size of the converter and the number of batteries were optimized by HOMER in all on-grid scenarios. According to the explanation in sections 4.2.5.3 and 4.2.5.4, the search space for the optimum PV panel produced energy and the number of wind turbines has been limited. In all 7 scenarios, the search space for PV is between 0 kW and 77 kW energy production, and for the number of wind turbines is between 0 and 12. The PV-WT-Ge-B scenario has been defined as a hybrid renewable energy system that uses a generator as a backup. The search space for the number of batteries was set between 0 and 20 in this scenario (peak load is around 200 kW).

4.2.5. Describing the components of the scenarios

4.2.5.1. Grid

It has been assumed that the greenhouse relies on grid electricity, except in the PV-WT-Ge-B scenario. In this study, grid power price and grid sell-back price have been considered at $ 0.3 CAD/kW and $ 0.05 CAD/kW[1], respectively.

[1] Sell-back rate is a fraction of the power price.

4.2.5.2. Diesel generator

PV-WT-Ge-B scenario is an off-grid power system and it has been assumed that it uses a diesel generator as a backup. HOMER calculates the rate of diesel generator fuel consumption concerning power output using Equation 4-1 (Chisale *et al*. 2023).

$$F(t) = F_0 P_{rated} + F_1 P_{gen}(t) \tag{4-1}$$

Where, F_0 is intercept coefficient, F_1 is the slope of the fuel curve, P_{rated} is rated output power of diesel generator, and $P_{gen}(t)$ is the real power output power of a diesel generator. The cost of a 10-kW generator is around $ 5000 CAD in Canada. Considering the shipping costs, $ 600 CAD/kW and $ 540 CAD/kW have been used as the initial and replacement cost of the generator, respectively.

4.2.5.3. PV panels

HOMER calculates the electrical power produced by PV panels using the following equation [Homerenergy]:

$$P_{pv} = Y_{pv} f_{pv} \left(\frac{\bar{G}_T}{\bar{G}_{T,STC}} \right) \left[1 + \alpha_P (T_c - T_{c,STC}) \right] \tag{4-2}$$

Where, P_{pv} (kW) is the PV array power produced, Y_{pv} (kW) is the rated capacity of the PV array, f_{pv} (%) is the PV derating factor, $\bar{G}_T$ (kW/m^2) is the solar radiation incident on the PV array in the current time step, $\bar{G}_{T,STC}$ (kW/m^2) is the incident radiation at standard test conditions, α_P (%/℃) is the temperature coefficient of power, T_c (℃) is the PV cell temperature in the current time step, and $T_{c,STC}$ (25℃) is the PV cell temperature under standard test conditions. PV power depends on incident radiation and the temperature of the cell (Cristian *et al*. 2017).

The Bifacial Semi-Transparent Photovoltaic (BSTPV) module has been considered in this study as a component that can improve the daylight performance and energy efficiency of a greenhouse covering material and produce renewable energy (Mun *et al*. 2020). This module can serve as both a PV and covering material on the roof of the greenhouse. BSTPV panels with 0.44 kW capacity and an area of 2.234 m^2 have been used in this study. The price of each panel is $ 435 CAD, on average. A replacement cost of $ 391.5 CAD and a lifetime of 25 years have also been considered. Considering the area of the greenhouse roof, which is 782.68 m^2, a maximum number of 175 BSTPV panels can be mounted on the greenhouse roof if a checkerboard pattern is used[1]. This results in a maximum of 77 kW of electricity production using BSTPV panels.

4.2.5.4. Wind Turbine

HOMER calculates the power production of wind turbines using Equation 4-3 (Cristian *et al*. 2017).

$$P_{max} = \frac{16}{27} \times P_0 \tag{4-3}$$

$P_0\ (W)$ is the power on the upstream section and can be calculated as follows:

$$P_0 = \frac{1}{2} \times \rho_{Local} \times A_R \times V_{Local}^3 \tag{4-4}$$

Where, $P_W\ (W)$ is the wind turbine power produced, $\rho_{Local}\ (kg/m^3)$ is the local density of air at rotor height, $A_R\ (m^2)$ is the swept area of the rotor, and $V_{Local}\ (m/s)$ is the local wind speed at the location of the system. The performance of these systems is obviously dependent on local wind conditions as there is a cubic relationship between the wind speed and the power

[1] It has been assumed that during the daytime, enough light for growing plants goes through the bifacial panels when they are installed in a checkerboard pattern.

produced by a wind turbine. Theoretically, according to Equation 4-3, wind turbines can produce 60% power generated by the wind but this amount decreases to 40% in reality (Hoarcă *et al*. 2023).

3 kW wind turbines (3-kW WT) with 3.3 metres blades were considered to be installed on the edge of the greenhouse roof through the length. Assuming 4.3 metres of space between wind turbines, a maximum of 12 wind turbines can be installed. A roof height of 7.7 metres, and hub height of 12 metres were considered for the wind turbine. The average price of a 3-kW wind turbine is $ 6000 CAD plus installation. The replacement cost and useful lifetime have been set as $ 5400CAD and 20 years, respectively.

4.2.5.5. Battery

HOMER calculated the capacity of the battery using Equation 4-5 (Hoarcă *et al*. 2023).

$$C = \left(E \times N_{day}\right)/\left(\eta_{converter} \times \eta_{battery} \times DOD\right) \tag{4-5}$$

Where, $E\ (volt)$ is the charging voltage, N_{day} is the number of days without charging, $\eta_{converter}$ is the convertor efficiency, $\eta_{battery}$ is the battery efficiency, and DOD is the depth of discharge. A 9.32 kWh 48-volt battery with a lifetime of 18 years was used in this study. The price of a battery with these properties is around $ 6500 CAD. The replacement cost was considered $ 5850 CAD.

4.2.5.6. Power converter

As any system that contains both AC and DC elements needs a converter (HOMEREnergy), a converter was considered in scenarios that have PV, Battery, or both. HOMER uses Equation 4-6 to calculate the converter capacity (Chisale *et al*. 2023).

$$P_{converter} = \frac{E_{L,max}}{\eta_{DC/AC}} \tag{4-6}$$

Where, $P_{converter}$ is the capacity of a power converter, $E_{L,max}$ (Wh) is the maximum energy demand required by the load, and $\eta_{DC/AC}$ is conversion efficiency. The price of a 10-kW converter is around $10,000 CAD in Canada which has been used in this study with 15 years lifetime and $ 9,000 CAD/kW of replacement cost.

4.2.6. Economic, technical, and environmental criteria

Net Present Cost (NPC) is considered as one of the economic criteria. It is defined as follows (HOMEREnergy):

$NPC = Present\ value\ of\ installing\ and\ operating\ component\ costs$ − Present value of the revenues (4-7)

HOMER calculates NPC for each of the components over the project lifetime to find the NPC of the whole system. HOMER's optimization objective is to minimize the NPC. This is considered as a disadvantage as it is not able to do a multi-objective optimization (Hoarcă *et al*. 2023; Bukar *et al*. 2019; Carroquino *et al*. 2018).

The other economic criterion is the Levelized Cost of Electricity (LCOE) which is the average cost per kWh of useful electrical energy produced by the system (HOMEREnergy). LCOE can be calculated as follows (Jacobson 2020):

$$LCOE = \frac{\sum_{t=1}^{n} \frac{A_{Capital} + A_{O\&M,t} + A_{Fuel,t} + A_{Decomm}}{(1+i)^t}}{\sum_{t=1}^{n} \frac{E_t}{(1+i)^t}} \tag{4-8}$$

Where, $A_{Capital}$ is the annualized upfront capital cost over the project's lifetime, $A_{O\&M,t}$ is the annual operation and maintenance cost in year t, $A_{Fuel,t}$ is the annual fuel cost in year t,

A_{Decomm} is the annualized decommissioning cost at the end of the project, n is the time between financing and the end of decommissioning of the power system, i is the discount rate which is assumed to be constant over n years[1], and E_t is the energy production by the power system.

Renewable energy fraction is generally the share of the energy supplying the demand which has been produced by renewable energy sources. HOMER calculates the renewable energy fraction using Equation 4-8 (HOMEREnergy).

$$f_{ren} = 1 - \frac{E_{nonren}}{E_{served}} \tag{4-8}$$

Where, $E_{nonren}(kWh/yr.)$ is the non-renewable energy production, and $E_{served}(kWh/yr.)$ is the total electrical load. Renewable energy fraction is considered a technical criterion for comparison.

The emission of Carbon Dioxide (CO_2) has been considered as the environmental criterion. It has been assumed that there is 632 g of Carbon Dioxide emissions to produce 1.0 kWh of grid power. Also, by using 1.0 L of diesel fuel to run the generator in the PV-WT-Ge-B scenario, there is 2.618 kg Carbon Dioxide emissions (HOMEREnergy).

4.2.7. Sensitivity analysis

A sensitivity analysis has been done on the cost of grid power and the rate of sellback for a kWh electricity production by BSTPV and 3-kW wind Turbine to see how the optimal system changes with these variations in cost. A range of $ 0.3 to $ 4.5 has been considered for the price of the energy purchased from the grid. $ 0.05 to $ 1.5 is the range defined for the sellback price of the

[1] A discount rate of 5% has been considered in this study.

generated electricity by renewable energy systems to the grid. These ranges have been defined for the sake of doing a complete and inclusive sensitivity analysis.

4.3. Results and discussion

4.3.1. HOMER optimization results

The results of the power system simulation in each scenario including optimized size/quantity of each component, Net present value (NPC), levelized cost of electricity (LCOE), Initial Capital or Capital Expenditure (CapEx), Operation cost (OC), Energy Production (EP), Excess Electricity (EE), payback time and Carbon Dioxide (CO_2) emissions for each scenario can be seen in Table 4-3. As mentioned before, HOMER's optimization objective in finding the best combination is minimizing NPC.

Table 4- 3: The optimized size and quantity of each scenario's components using the HOMER simulation

	PV-Gr	PV-Gr-B	WT-Gr	WT-Gr-B	PV-WT-Gr	PV-WT-Gr-B	PV-WT-Ge-B
BSTPV (kW) (Quantity)	77 (175 panels)	77 (175 panels)			77 (175 panels)	77 (175 panels)	77 (175 panels)
BSTPV Energy Production (kWh/yr.)	131,380	131,380			131,380	131,380	131,380
3-kW WT			12	12	1	1	12
3-kW WT Energy Production (kWh/yr.)			41,609	41,609	3,467	3,467	41,609
10-kW Bat		1		1		1	20
Converter (kW)	51	50.4		0.0251	51.8	52	61.9
Generator (kW)							230
Generator Energy Production (kWh/yr.)							37,496
Grid Energy Purchased (kWh/yr.)	55,916	55,954	71,409	71,409	55,062	55,054	
Grid Energy Sold (kWh/yr.)	94,516	94,116	30,772	30,772	97,619	97,713	
Renewable Energy Fraction (%)	68.4	68.3	36.9	36.9	69.4	69.4	54.4
NPC ($)	203,764	212,221	372,068	380,554	204,947	213,425	1.28M
LCOE ($/kW)	0.0580	0.0605	0.166	0.169	0.0573	0.0596	0.784
CapEx ($)	127,144	132,988	72,000	78,525	133,947	140,625	477,993
OC ($/yr.)	3,553	3,984	15,088	15,186	3,570	3,660	40,462
Simple Payback (yr.)	5.76	6.03	6.99	7.62	5.97	6.26	2.65
Discounted Payback (yr.)	6.14	6.46	7.55	8.29	6.38	6.71	2.75
CO_2 (kg/yr.)	35,339	35,363	45,130	45,130	34,799	34,794	31,748

4.3.2. Comparing on-grid scenario

The amount of NPC for each scenario is shown in Figure 4-8. The results show that the hybrid system, which is a combination of BSPV, and Grid (PV-Gr) has the lowest NPC of $ 203,764 CAD.

The LCOE for each scenario can be seen in Figure 4-9. PV-WT-Gr scenario's LCOE is $ 0.0573 per 1 kW energy production, which is the lowest amount of the scenarios.

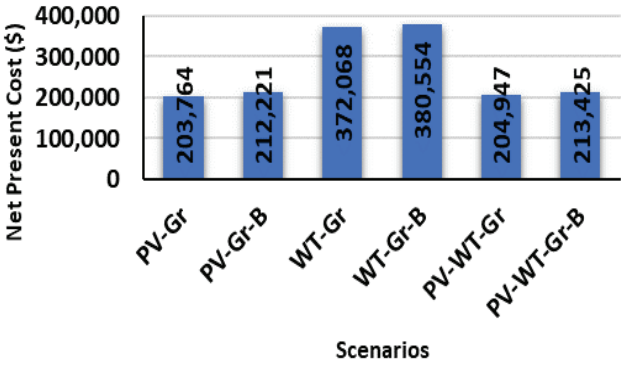

Figure 4- 8: Net Present Cost (NPC) of scenarios

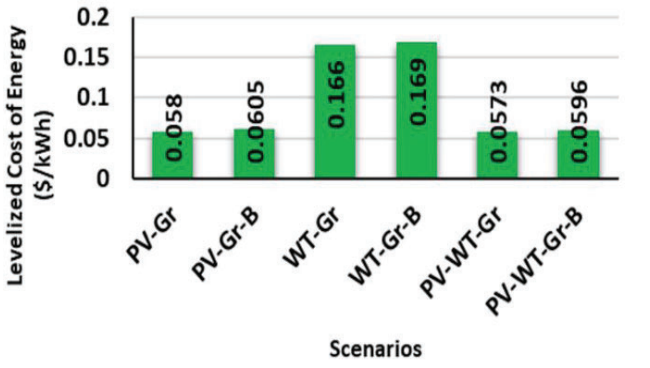

Figure 4- 9: Levelized Cost of Energy (LCOE) of scenarios

Figure 4-10 shows the share of renewable energy sources in each scenario. PV-WT-Gr and PV-WT-Gr-B have the maximum renewable energy fraction in the system (69.4%).

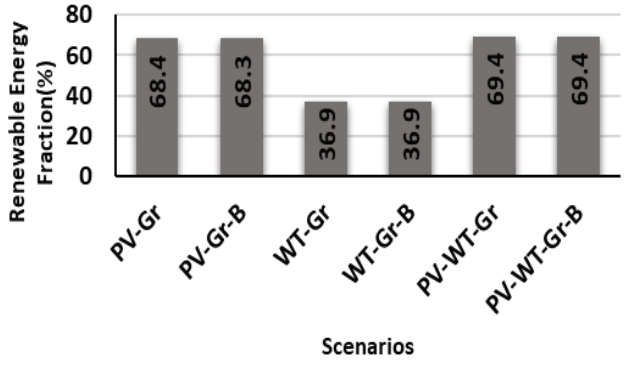

Figure 4- 10: Renewable energy fraction of scenarios

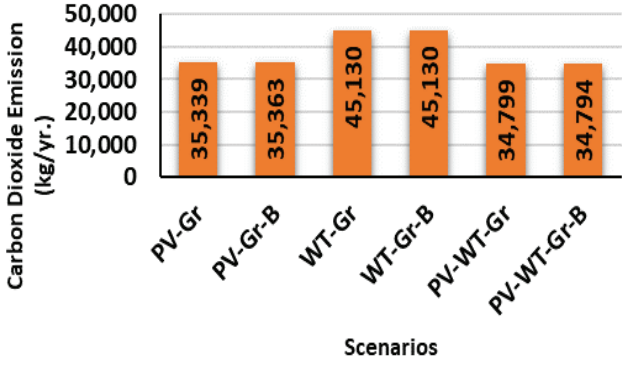

Figure 4- 11: Carbon Dioxide (CO_2) emissions of scenarios

The amount of CO_2 emission in each scenario can be seen in Figure 4-11. PV-WT-Gr-B has the minimum CO_2 emission, which is 34,794 kg for each kW of energy production by the grid. PV-WT-Gr CO_2 emission is close to PV-WT-Gr-B, and it is just 5 kg more per year.

The hybrid system, which is a combination of BSPV, Wind Turbine and Grid (PV-WT-Gr) has the minimum Levelized Cost of Energy (LCOE). The Net Present Costs (NPC) for PV-WT-Gr is $ 1,183 CAD more than the system using BSPV and Grid (PV-Gr), which is not a significant difference over the lifetime of a project. There is less energy purchased from the grid in the hybrid system, which is a combination of BSPV, Wind Turbine, Battery, and Grid (PV-WT-Gr-B) and more energy sold to the grid. Using a battery would result in a higher NPC, and LCOE. As the amount of CO_2 emissions is almost the same between PV-WT-Gr and PV-WT-Gr-B scenarios, and they both have the highest fraction of renewable energy sources, PV-WT-Gr is considered the optimum on-grid combination.

BSTPV has the greatest annual energy production contribution in the PV-WT-Gr scenario, 131,380 kWh. Considering the annual energy demand of 82194 kWh, BSTPV produces more than enough to supply the energy load. The extra energy produced by BSTPV and 3-kW WT is sold back to the grid. There are some hours in which there is no energy production by BSTPV and 3-kW WT so the energy is provided through the grid during those hours. The payback time for this scenario is 5.93 years.

The profile of load, BSTPV, and 3-kW WT output power, energy purchased from the grid and sold to the grid, for a summer and winter duration with the highest energy demand during 2020 can be seen in Figures 4-12 and 4-13.

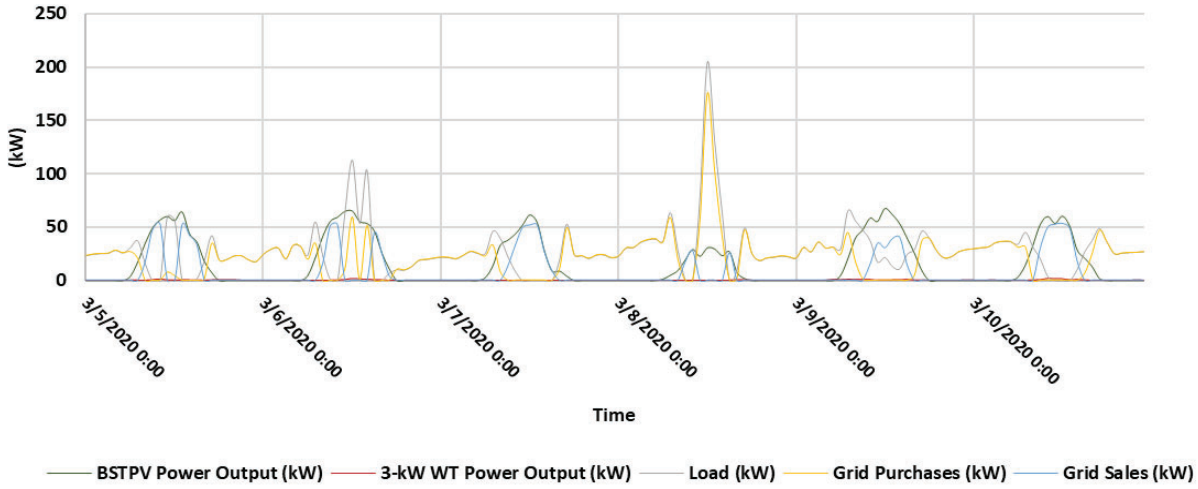

Figure 4- 12: The profile of load, BSTPV, and 3-kW WT output power, energy purchased from the grid and sold to the grid for the winter duration, of 2020

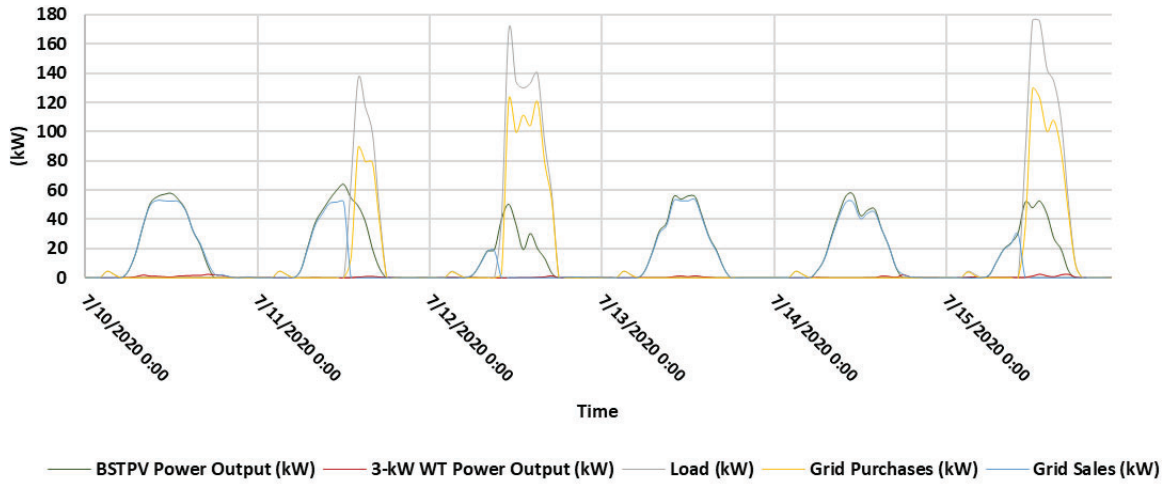

Figure 4- 13: The profile of load, BSTPV, and 3-kW WT output power, energy purchased from the grid and sold to the grid for the summer duration of 2020

Figure 4-14 depicts the monthly value of the load, BSTPV, and 3-kW WT output power, energy purchased from the grid and sold to the grid, and the amount of energy provided to the greenhouse using the PV-WT-Gr combination. Figures 4-15 and 4-16 demonstrate the annual output power of BSTPV and 3-kW WT. Obviously, BSTPV produces more energy annually than 3-kW WT.

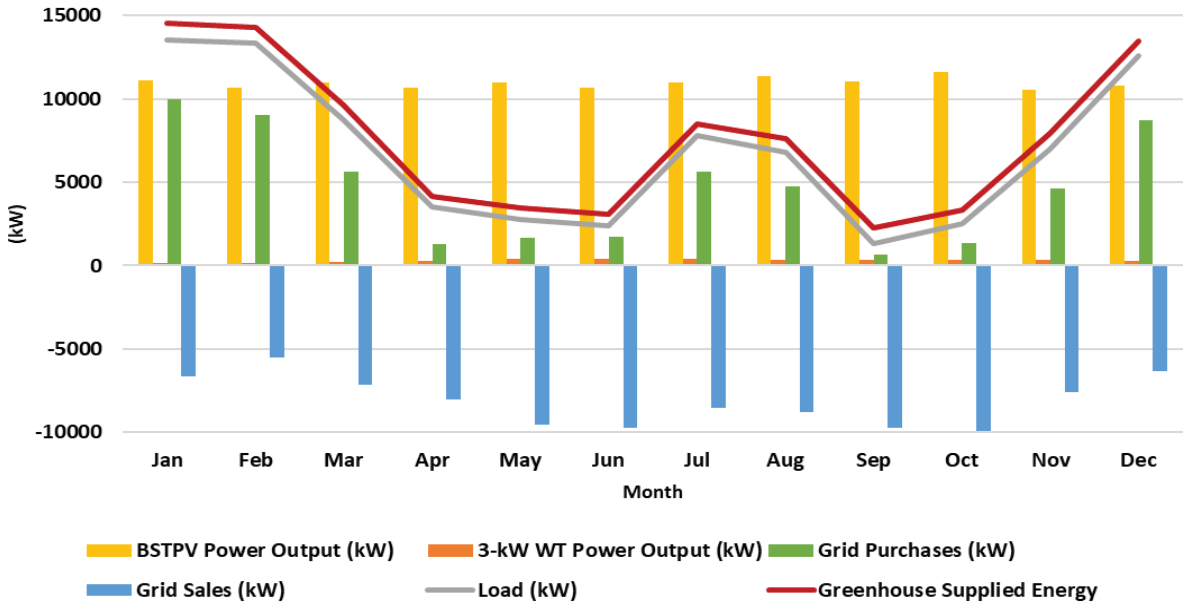

Figure 4- 14: Monthly value of the load, BSTPV and 3-kW WT output power, energy purchased from the grid and sold to the grid, and total supplied energy to the greenhouse

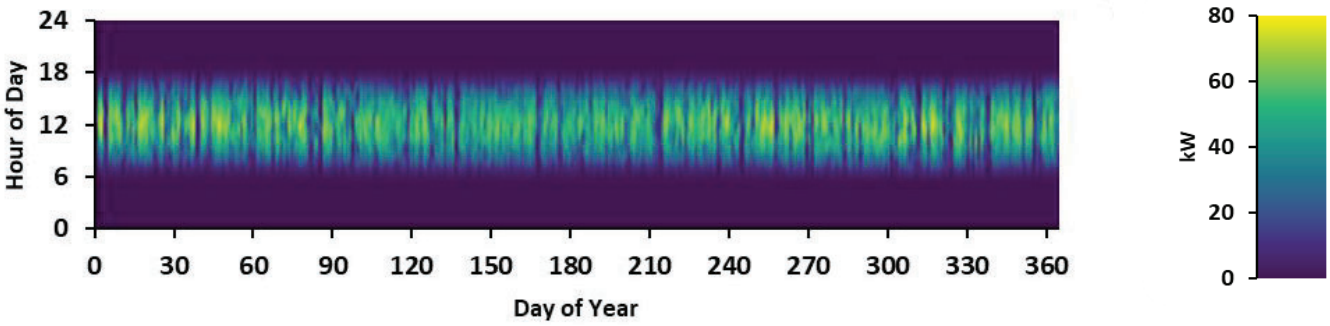

Figure 4- 15: The annual output power of BSTPV

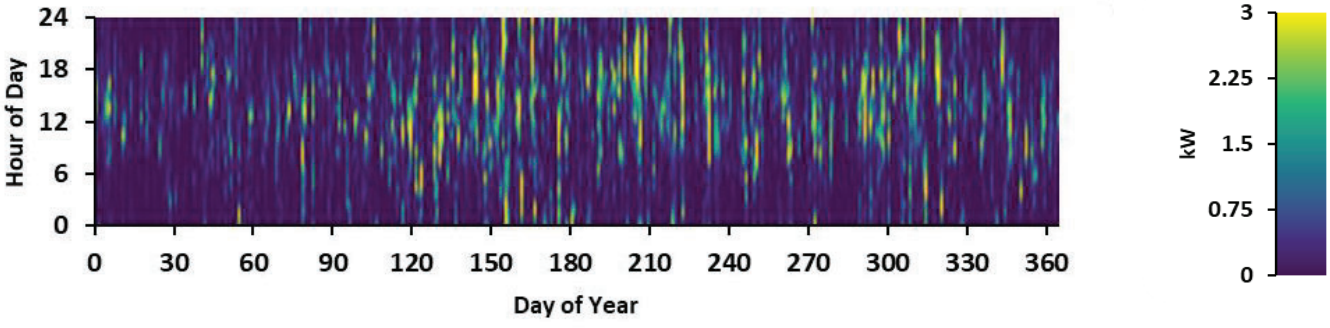

Figure 4- 16: The annual output power of 3-kW WT

4.3.3. Comparison of the optimal on-grid scenario with the off-grid scenario

According to Table 4-3, the hybrid system, which is a combination of BSPV, Wind Turbine and Generator (PV-WT-Ge-B) has NPC around 5 times more than the hybrid system, which is a combination of BSPV, Wind Turbine and Grid (PV-WT-Gr). Also, the LCOE of the off-grid scenario, which is $ 0.784 CAD/kW, is far higher than the on-grid scenario ($ 0.0573 CAD/kW). One reason for the higher LCOE is the higher price of diesel in comparison to buying electricity from the grid. Additionally, the off-grid scenario has 11 more wind turbines and 20 storage batteries which can result in higher NPC. Figures 4-17 and 4-18 depict the share of each of the components of PV-WT-Gr and PV-WT-Ge-B[1] power systems in supplying energy demand. Figures 4-19 and 4-20 show the renewable energy fraction and CO_2 emissions for each of the scenarios. PV-WT-Ge-B has less renewable energy fraction. The energy supplied by the generator is 37,496 kW per year and this amount is less than energy purchased from the grid (55,916 kW/yr.). This result in reduced CO_2 emissions in this scenario.

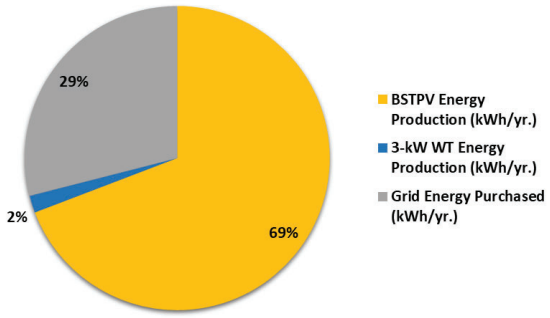

Figure 4- 17: Energy production share of each component of the PV-WT-Gr system

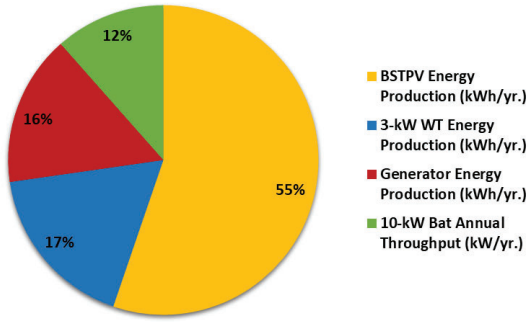

Figure 4- 18: Energy production share of each component of the PV-WT-Ge-B system

[1] 10-kW Bat annual throughput (kW/yr.) was 27,365.

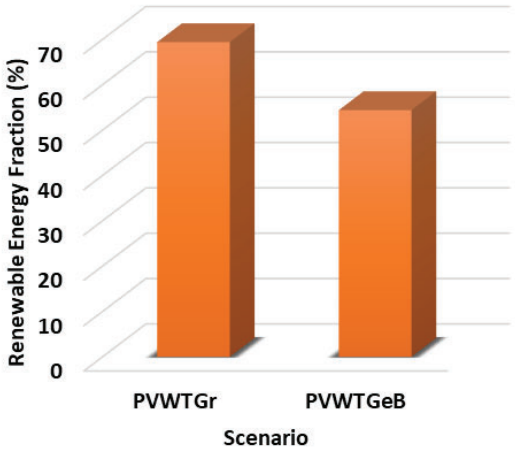

Figure 4- 19: Renewable energy fraction of PV-WT-Gr and PV-WT-Ge-B systems

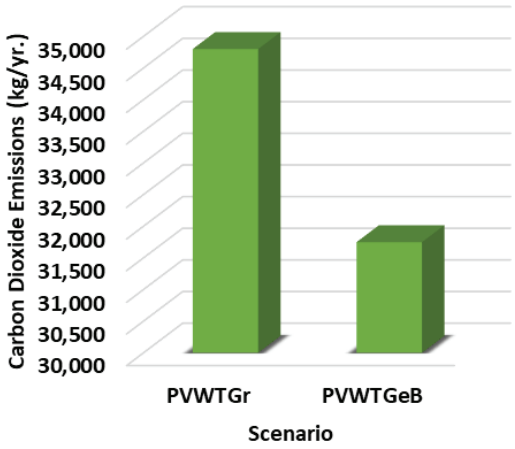

Figure 4- 20: Carbon Dioxide (CO_2) emissions of PV-WT-Gr and PV-WT-Ge-B systems

4.3.4. Sensitivity analysis results

The results of the sensitivity analysis can be seen in Figures 4-21 and 4-22 for the total NPC and Renewable Energy Fraction. As can be seen in both figures, increasing the rate of sellback would result in a lower NPC as well as higher Renewable Energy Fraction. Obviously, increasing the price of purchasing power from the grid would moderate the affect of the higher sellback rate.

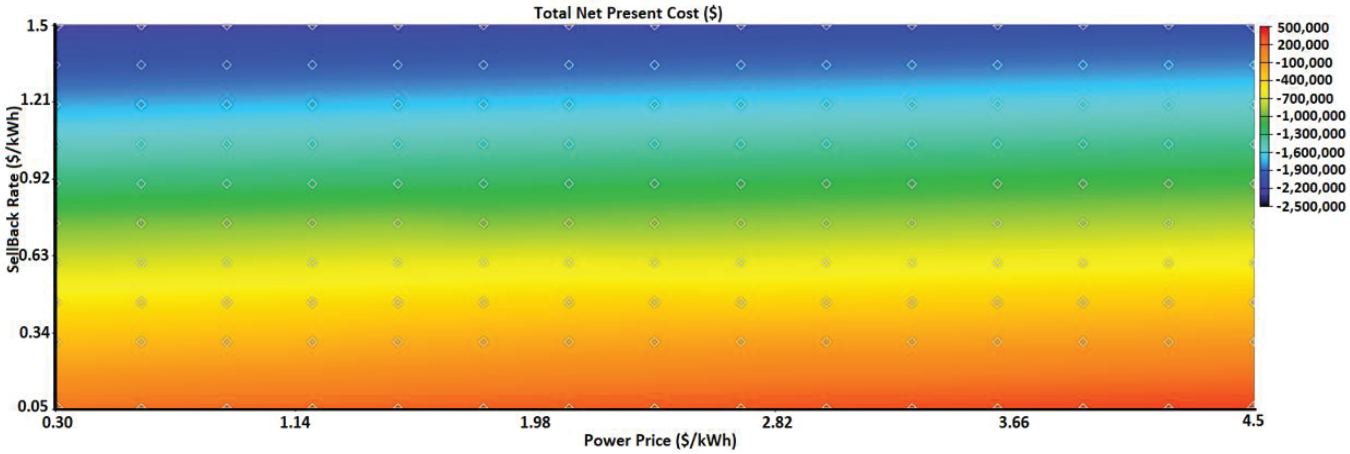

Figure 4- 21: Sensitivity analysis results – Total Net Present Costs (S)

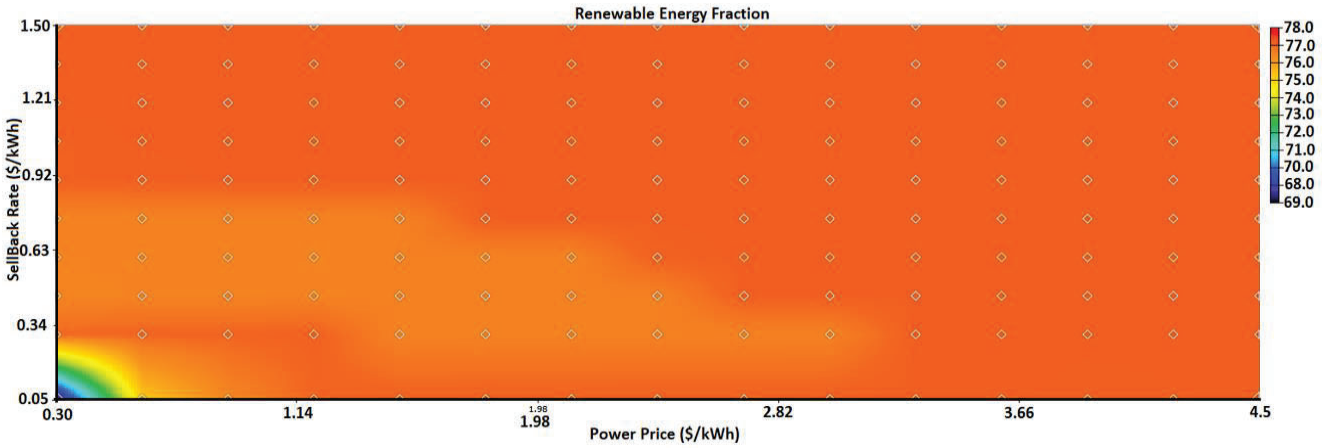

Figure 4- 22: Sensitivity analysis results – Renewable Energy Fraction (%)

4.4. Conclusion

This chapter aims to find an optimal hybrid renewable power system to supply the energy demand of an educational greenhouse. EnergyPlus™ has been used to find the annual energy consumption of the greenhouse in 2020. HOMER has been used to simulate and optimize power systems components. Six on-grid scenarios and one off-grid scenario were defined for the comparison between combinations of different system's components. Components include PV, wind turbine, battery, grid, generator, and converter. To compare the scenarios, consideration was given to minimizing the Net Present Cost (NPC) and Levelized Cost of Energy (LCOE) as economic criteria, maximizing the Renewable Energy Fraction as technical criteria, and minimizing CO_2 emissions as environmental criteria. A sensitivity analysis was conducted to find the effect of changing the cost of grid power and the rate of sellback on NPC and renewable energy fraction of optimum system. The results are as follows:

- Among on-grid scenarios, the minimum NPC is related to the system combining the grid power and 175 panels of PV.
- Among on-grid scenarios, the minimum LCOE and maximum renewable energy fraction are related to the system combining the grid, 175 panels of PV, and one wind turbine.

This system has roughly the minimum CO_2 emissions. Adding one battery to this combination can decrease the amount of CO_2 by about 5 kg per year.

- The off-grid scenario, which is a combination of 175 panels of PV, 12 wind turbines, 20 batteries, and a 230 kW generator, has a lower CO_2 emission than the optimal on-grid combination. The NPC and LCOE are around 5 and 13 times more, respectively.
- The system combining the grid, 175 panels of PV, and one wind turbine meets the defined criteria of the study and is selected as the most optimal on-grid power system.
- According to the results of sensitivity analysis for the optimum system, increasing the price of sellback would result in a better NPC as well as higher Renewable Energy Fraction. Increasing the price of grid power would moderate the effect of increasing sellback rate.
- Future studies should develop a multi-objective optimization algorithm and link it with HOMER to find the best combination of the power system. Other objectives, such as: minimizing CO_2 emissions, LCOE, operation costs, initial costs and maximizing Renewable Energy Fraction affect the sizing process of a power system. These objectives are inter-connected, and their effect should be considered together.
- The approximate cost of components, without considering the installation cost has been considered in this study for the sake of comparison between different energy systems.

References

Ahamed, M. S., Guo, H., & Tanino, K. (2019). Energy saving techniques for reducing the heating cost of conventional greenhouses. *Biosystems Engineering, 178*, 9-33. doi:10.1016/j.biosystemseng.2018.10.017

Bukar, A. L., Tan, C. W., & Lau, K. Y. (2019). Optimal sizing of an autonomous photovoltaic/wind/battery/diesel generator microgrid using grasshopper optimization algorithm. *Solar Energy, 188*, 685-696. doi:https://doi.org/10.1016/j.solener.2019.06.050

Carroquino, J., Roda, V., Mustata, R., Yago, J., Valiño, L., Lozano, A., & Barreras, F. (2018). Combined production of electricity and hydrogen from solar energy and its use in the wine sector. *Renewable Energy, 122*, 251-263. doi: https://doi.org/10.1016/j.renene.2018.01.106

Chen, C., Yu, N., Yang, F., Mahkamov, K., Han, F., Li, Y., & Ling, H. (2019). Theoretical and experimental study on selection of physical dimensions of passive solar greenhouses for enhanced energy performance. *Solar Energy, 191*, 46-56. doi:10.1016/j.solener.2019.07.089

Chisale, S. W., Eliya, S., & Taulo, J. (2023). Optimization and design of hybrid power system using HOMER pro and integrated CRITIC-PROMETHEE II approaches. *Green Technologies and Sustainability, 1*(1). doi:10.1016/j.grets.2022.100005

Crawley, Drury B., Linda K. Lawrie, Frederick C. Winkelmann, W. F. Buhl, Y. Joe Huang, Curtis O. Pedersen, Richard K. Strand*, et al.* 2001. EnergyPlus: Creating a new-generation building energy simulation program. *Energy and Buildings* 33(4): 319-31. doi:https://doi.org/https://doi.org/10.1016/S0378-7788(00)00114-6.

Cristian, H., Bizon, N., & Alexandru, B. (2017, 29 June-1 July 2017). *Design of hybrid power systems using HOMER simulator for different renewable energy sources.* Paper presented at the 2017 9th International Conference on Electronics, Computers and Artificial Intelligence (ECAI).

Cuce, E., Harjunowibowo, D., & Cuce, P. M. (2016). Renewable and sustainable energy saving strategies for greenhouse systems: A comprehensive review. *Renewable and Sustainable Energy Reviews, 64*, 34-59. doi:10.1016/j.rser.2016.05.077

Draxl, C. B. M., Clifton, A., & McCaa, J. (2015a). *Overview and meteorological validation of the wind integration national dataset toolkit* (Technical Report, NREL/TP-5000-61740). Golden, CO: National Renewable Energy Laboratory.

Draxl, C. B. M., Clifton, H. A., & McCaa, J. (2015b). The wind integration national dataset (WIND) toolkit. *Applied Energy* 151: 355366.

Esmaeli, H., & Roshandel, R. (2020). Optimal design for solar greenhouses based on climate conditions. *Renewable Energy, 145*, 1255-1265. doi:10.1016/j.renene.2019.06.090

Hoarcă, I. C., Bizon, N., Șorlei, I. S., & Thounthong, P. (2023). Sizing design for a hybrid renewable power system using HOMER and iHOGA simulators. *Energies, 16*(4). doi:10.3390/en16041926

Homerenergy. HOMER Pro version 3. 13 user manual. Colorado, USA; 2019

Jacobson, M. (2020). 100% Clean, renewable energy and storage for everything. Cambridge: Cambridge University Press. doi:10.1017/9781108786713

King, J., Clifton, A., & Hodge, B. M. (2014). *Validation of power output for the WIND toolkit* (Technical Report, NREL/TP-5D00-61714). Golden, CO: National Renewable Energy Laboratory.

Kıyan, M., Bingöl, E., Melikoğlu, M., & Albostan, A. (2013). Modelling and simulation of a hybrid solar heating system for greenhouse applications using Matlab/Simulink. *Energy Conversion and Management, 72*, 147-155. doi:10.1016/j.enconman.2012.09.036

Lieberman-Cribbin, W., Draxl, C., & Clifton, A. (2014). *Guide to using the WIND toolkit validation code* (Technical Report, NREL/TP-5000-62595). Golden, CO: National Renewable Energy Laboratory.

Ma, Y., Li, X., Fu, Z., & Zhang, L. (2019). Structural design and thermal performance simulation of shade roof of double-slope greenhouse for mushroom-vegetable cultivation. *International Journal of Agricultural and Biological Engineering, 12*(3), 126-133. doi:10.25165/j.ijabe.20191203.4852.

Manonmani, A., Thyagarajan, T., Elango, M., & Sutha, S. (2016). Modelling and control of greenhouse system using neural networks. *Transactions of the Institute of Measurement and Control, 40*(3), 918-929. doi:10.1177/0142331216670235

Mirzamohammadi, S., Jabarzadeh, A., & Shahrabi, M. S. (2020). Long-term planning of supplying energy for greenhouses using renewable resources under uncertainty. *Journal of Cleaner Production, 264*. doi:10.1016/j.jclepro.2020.121611

Mostafavi, S. A., & Rezaei, A. (2019). Energy consumption in greenhouses and selection of an optimized heating system with minimum energy consumption. *Heat Transfer-Asian Research, 48*(7), 3257-3277. doi:10.1002/htj.21540

Mun, S. H., Kang, J., Kwak, Y., Jeong, Y. S., Lee, S.-M., & Huh, J. H. (2020). Limitations of EnergyPlus in analyzing energy performance of semi-transparent photovoltaic modules. *Case Studies in Thermal Engineering, 22*. doi:10.1016/j.csite.2020.100765

EnergyPlus version 9.6.0 Documentation, Engineering Reference, 2021

Ntinas, G. K., Dannehl, D., Schuch, I., Rocksch, T., & Schmidt, U. (2020). Sustainable greenhouse production with minimized carbon footprint by energy export. *Biosystems Engineering, 189*, 164-178. doi:10.1016/j.biosystemseng.2019.11.012

Rasheed, A., Lee, J., & Lee, H. (2018). Development and optimization of a building energy simulation model to study the effect of greenhouse design parameters. *Energies, 11*(8). doi:10.3390/en11082001

Ronay, K., & Dumitru, C.-D. (2015). Hydroponic greenhouse energy supply based on renewable energy sources. *Procedia Technology, 19*, 703-707. doi:10.1016/j.protcy.2015.02.099

Sengupta, M., Y. Xie, A. Lopez, A. Habte, G. Maclaurin, & J. Shelby. (2018). The National Solar Radiation Data Base (NSRDB). *Renewable and Sustainable Energy Reviews* 89 (June): 51-60.

Vourdoubas, J. (2015). Overview of heating greenhouses with renewable energy sources a case study in Crete- Greece. *Journal of Agriculture and Environmental Sciences, 4*(1). doi:10.15640/jaes.v4n1a9

Yang, S. H., Lee, C. G., Lee, W. K., Ashtiani, A. A., Kim, J. Y., Lee, S. D., & Rhee, J. Y. (2012). Heating and cooling system for utilization of surplus air thermal energy in greenhouse and its control logic. *Journal of Biosystems Engineering*, *37*, 19–27.

Zhuang, P., Liang, H., & Pomphrey, M. (2019). Stochastic multi-timescale energy management of greenhouses with renewable energy sources. *IEEE Transactions on Sustainable Energy, 10*(2), 905-917. doi:10.1109/tste.2018.2854662

Chapter 5: Summary and conclusion

The feasibility of designing a year-round energy-efficient greenhouse in Southern Alberta has been investigated in this study. Through comparison of various scenarios, the effect of shape, size, height, orientation, and covering materials on the thermal performance of conventional greenhouses has been assessed. Also, the energy consumption of the most energy-efficient scenarios has been compared with Chinese Style Greenhouses and Plant factories. The components of an optimal hybrid renewable energy system have been found to supply the energy demand of the efficient greenhouse using economical, technical, and environmental criteria. EnergyPlus™ and HOMER have been used and developed for this study.

The results of the study can be summarised as follows:

- The Quonset greenhouse has the minimum contact area with the surrounding environment which results in minimum temperature deviation from the desired temperature range. Even-Span and Gothic are the optimum shapes of the greenhouse after Quonset, respectively.
- For the location of study, when the length of the greenhouse is in the east-west direction, better thermal performance is achieved. Shorter structures, those between 5.5 metres and 7.5 metres of gutter height, results in a more energy-efficient greenhouse. Also, PVC is the best covering material, followed by PC.
- Conventional greenhouses have the highest heating and cooling loads in comparison to Chinese- style greenhouses and plant factories. The heating and cooling loads are lowest for plant factories because of the use of insulated walls and ceilings, as well as the structure being fully enclosed. Plant factories are economical if plants are grown in several vertical layers. If plants are not grown vertically, plant factories are the least

economical greenhouse, as a result of the high electricity usage for lighting and the high upfront costs. Chinese style greenhouses can be considered as the facility that is both energy-efficient and can be economical if using cheap construction materials.

- The system combining the grid, 175 PV panels, and one wind turbine can be considered the most optimal on-grid power system for the OSCC's educational greenhouse as it has minimum Net Present Costs and Levelized Cost of Energy, the lowest CO_2 emissions, and the highest Renewable Energy Fraction. Although the off-grid power system had a lower CO_2 emission, the high Net Present Costs, and Levelized Cost of Energy makes it a sub-optimum system. Also, by increasing the price of sellback to the grid, it is possible to witness an increase in the Renewable Energy Fraction as well as a better NPC for the optimum system.

5.1. Recommendation for future research

The greenhouse footprint for this case study was of limited size and this can affect the economic efficiency of the greenhouse by restricting greenhouse production. According to the results of the study, some of the large commercial greenhouses showed good thermal performance. Having a larger space, leads to a higher yield, and accordingly, larger greenhouses can be considered efficient with higher production profits. Choice of crop produced is a parameter that affects the efficiency of greenhouses and should be considered in the design procedure.

Environmental-control equipment and greenhouse facility frame are the two most important factors that impact the energy load as well as determining the final total cost. Future studies should take into consideration more precise calculations for greenhouse efficiency.

A multi-objective optimization algorithm should be developed and linked with HOMER to find the best combination of the power system in future studies. Objectives such as minimizing CO_2 emissions, LCOE, operation costs, initial costs and maximizing Renewable Energy Fraction affect the sizing process of a power system are inter-connected and their effect needs to be considered together.